NIMBUS-7 CZCS
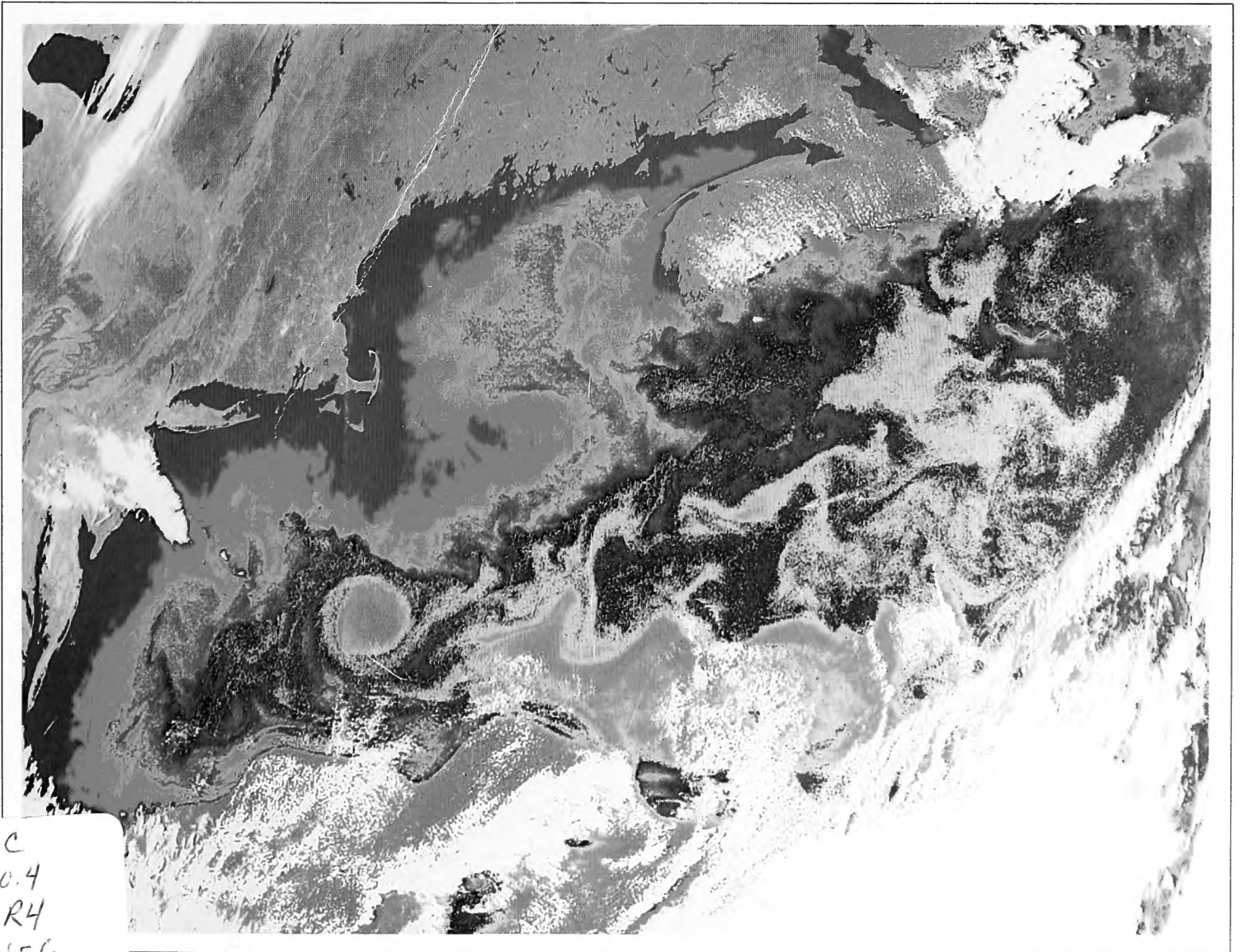## COASTAL ZONE
COLOR SCANNER IMAGERY
for Selected Coastal Regions

anner imagery
a-Europe...
nd Walter A. Boha

Copy 2

RETURNED

JUN 2 9 1988

FEB 1 1 1987

DEMCO

NIMBUS-7 CZCS

COASTAL ZONE
COLOR SCANNER IMAGERY
for Selected Coastal Regions

North America - Europe
South America - Africa - Antarctica

Level II Photographic Product

NASA
Goddard Space Flight Center

Prepared under the direction of

Dr. Warren A. Hovis, Chairman
CZCS, Nimbus Experiment Team

Edmund F. Szajna, Sensor Manager
Space and Earth Sciences Directorate

Walter A. Bohan
The Walter A. Bohan Company

Contents

Foreword

We are presently in an era when new scientific information flows in at a rate that threatens to overwhelm the student in what, for lack of constructive processing, is degraded to useless noise. It is important to assure ourselves from time to time that oceanography retains its rightful place in the forefront of earth science because the ocean is the only readily accessible sample for study of the behavior of an extensive liquid on a whirling globe. To retain its unique place among the welter of spectacular competing discoveries which relate to assemblages of a range of scale from the smallest particles to the immense galaxies of outer space and to their degree of sophistication from mundane to exotic, it will be necessary to provide and nourish a literature that has sufficient substance to stimulate the imagination of the keenest scientific minds.

Perusal of this collection of papers will reassure the thoughtful reader that, at this milestone, oceanography, far from slipping into humdrum obsolescence, remains vital and is still at the cutting edge of scientific revelation of the cosmos around us. By way of examples, one can single out the application of ocean acoustic tomography that realizes a new three-dimensional representation of the deep sea, and remote sensing that effects the synchronous charting of extensive areas of the superficial layers of the ocean from the vantage point of space satellites. This latter ability frees the perception of the student from the constriction inherent in anecdotal point-to-point sampling that in the past has been forged by the narrow field of view available from traditional shipboard observation. Many descriptions in earlier oceanographic texts, because they are derived from observations widely differing in times and methods, result in incongruities. As a result of today's enlarged and refined facilities, small-scale and evanescent events, as well as the interrelations of patterns separated in space and time now emerge so that, little by little, the complexity of the world seas is unfolding. Many areas that until recently belonged to the "mare incognita" are now part of the immediate coherent cognizance of oceanographers. Thanks in part to this integration of perception, the progress of the science is assured. The outlook is indeed promising.

Gifford C. Ewing

Introduction

Global observations from earth-orbiting satellites began in the 1960's with imagers utilizing vidicons for cloud imagery to study the dynamic motions for meteorological purposes. Oceans were observed, but only the brightest features such as river plumes were observable with these early sensors. Even then it was obvious that satellites presented an opportunity to study the vast areas of the oceans in a manner and timeframe impossible with ships or aircraft, since an area of 250,000 square miles could be observed in one minute. Development of improved optical sensors paralleled an increase in interest by oceanographers in studying oceans from space. Ship and aircraft ocean color measurements showed that ocean color could be related to water content in a meaningful way, and that the effects of interference by atmospheric backscatter of sunlight could be overcome. These developments led to an opportunity in the early 1970's where scientific interest, sensor technology, availability of a near-ideal spacecraft, and recognition of the potential benefits by NASA gave birth to the Coastal Zone Color Scanner (CZCS) program.

The CZCS sensor utilizes scanning techniques developed for meteorological and earth resources purposes modified to add a tilt capability to avoid glint, and with spectral bands and dynamic ranges optimized for ocean color. Details of the sensor characteristics are given by Hovis *et al.* (1980). A scheme to remove the interfering effects of the atmosphere, Rayleigh and aerosol backscatter, was developed by members of the CZCS Nimbus Experiment Team (NET) Gordon *et al.* (1980) and Gordon *et al.* (1983). This atmospheric correction scheme is the most unique element of the CZCS program, and makes possible the results shown in this atlas.

The atlas is intended to provide interpretations of CZCS products from the viewpoints of a wide range of oceanographic scientists as an introduction for those not already familiar with the potential of space for such information gathering. Experience has shown that each scientist who examines a CZCS product sees something unique based on his own experience. It is the goal of the atlas and the CZCS NET to introduce these products to the widest possible spectrum of users and assist them in acquiring and interpreting the data. To that end, the data is deposited in a public archive, the Satellite Data Services Division of NOAA, NESDIS, with no restriction on its dissemination except the modest cost of reproduction. A list of the NET members and the address of the archive is found on page xix.

Warren A. Hovis, Chairman
CZCS, Nimbus Experiment Team

References

Gordon, H. R., D. K. Clark, J. L. Mueller, and W. A. Hovis, 1980: Phytoplankton pigments from the Nimbus-7 Coastal Zone Color Scanner: Comparisons with surface measurements. *Science*, **210**, 63–66.

Gordon, H. R., D. K. Clark, J. W. Brown, O. B. Brown, R. H. Evans, and W. W. Broenkow, 1983: Phytoplankton pigment concentrations in the Middle Atlantic Bight: Comparison of ship determinations and CZCS estimates. *Applied Optics*, **22**, 20–36.

Hovis, W. A., D. K. Clark, F. Anderson, R. W. Austin, W. H. Wilson, E. T. Baker, D. Ball, H. R. Gordon, J. L. Mueller, S. Z. El-Sayed, B. Sturm, R. C. Wrigley, and C. S. Yentsch, 1980: Nimbus-7 Coastal Zone Color Scanner: System description and initial imagery. *Science*, **210**, 60–63.

The Nimbus-7 Coastal Zone Color Scanner (CZCS)

The Coastal Zone Color Scanner (CZCS) is the first spacecraft instrument devoted to the measurement of ocean color. Although instruments on other satellites have sensed ocean color, their spectral bands, spatial resolution, and dynamic range were optimized for geographical or meteorological use. In the CZCS, every parameter is optimized for use over water to the exclusion of any other type of sensing. The signal-to-noise ratios in the spectral channels sensing reflected solar radiance are higher than those required in the past. These ratios need to be high because the ocean is such a poor reflecting surface that the majority of the signal seen by the reflected energy channels at spacecraft altitudes is backscattered solar radiation from the atmosphere rather than reflected solar energy from the ocean.

The CZCS is a conventional multi-channel scanning radiometer utilizing a rotating plane mirror at a 45 degree angle to the optic axis of a Cassegrain telescope. The rotating mirror scans 360 degrees, however, only 80 degrees of data centered on the spacecraft nadir is collected for ocean color measurements. During the rest of the scan, the instrument acquires a view of deep space and of internal instrument sources for calibration of the various channels. Spatial resolution, at spacecraft nadir, is 825 × 825 meters with some degradation at the edges of the scan swath. The useful swath width from a spacecraft altitude of 955 km is 1600 km.

The CZCS has six spectral bands, five sensing backscattered solar radiance and one sensing emitted thermal radiance. Table 1 shows the center wavelengths, the spectral bandwidths, and the minimum signal-to-noise ratio specified for the instrument at the most sensitive gain setting; that is, the gain setting that would be used for the darkest targets. The first four channels were selected to cover specific absorption bands and the so-called hinge point. These channels are meant to look at water only and saturate when the field of view is over land surfaces and clouds. The spectral response of Channels 1 through 5 is illustrated in Figure 1.

Table 1. CZCS Performance Parameters.

Performance Parameters	Channels					
	1	2	3	4	5	6
Scientific Observation	Chlorophyll Absorption	Chlorophyll Correlation	Yellow Stuff	Chlorophyll Absorption	Surface Vegetation	Surface Temperature
Center Wavelength λ Micrometers	0.443 (blue)	0.520 (green)	0 550 (yellow)	0 670 (red)	0.750 (far red)	11.5 (infrared)
Spectral Bandwidth Δλ Micrometers	0.433 – 0.453	0.510 – 0 530	0.540 – 0.560	0.660 – 0.680	0.700 – 0.800	10 5 – 12.5
Instantaneous Field of View (IFOV)	0.865 x 0 865 Milliradians (0.825 x 0.825 km at sea level)					
Co-registration at NADIR	<0.15 Milliradians					
Accuracy of Viewing Position Information at NADIR	<2 0 Milliradians					
Signal to Noise Ratio (min.) at Radiance Input $N < (mW/cm^2 \cdot STER \cdot \mu m)$	>150 at 5.41	>140 at 3.50	>125 at 2.86	>100 at 1.34	>100 at 10.8	NETD of 0.220°K at 270°K
Consecutive Scan Overlap	25%					
Modulation Transfer Function (MTF)	1 at 150 km target size, 0.35 min. at 0.825 km target size					

Figure 1. CZCS Spectral Response for Channels 1–5.
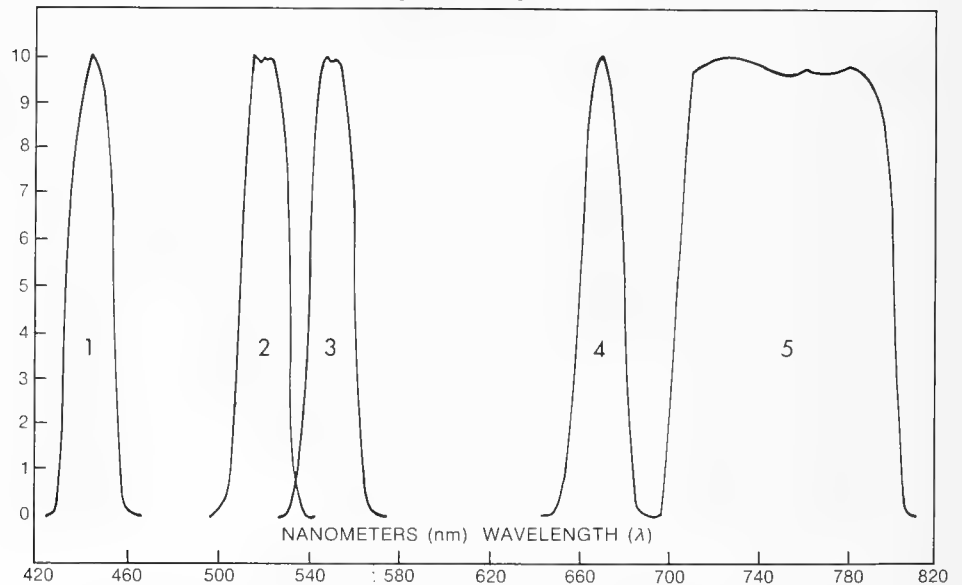
Channel 5 has the same spectral response as Channel 6 of the Landsat multi-spectral scanner series. The gain of Channel 5 is fixed and set to produce the same percentage of maximum signal over land targets as the Landsat Channel 6. However, the actual radiance for saturation is higher since the Nimbus-7 spacecraft crosses the Equator at high noon whereas Landsat crosses the Equator at 9:30 a.m. local time.

The CZCS Channel 6 (10.5 to 12.5 μm) measures equivalent blackbody temperature as seen by the sensor with a moist equivalent temperature difference of less than 0.35° K at 270° K. Atmospheric interference with this channel, principally from weak water vapor absorption in the 10.5 to

12.5 μm region, can produce measurement errors of several degrees. Temperature gradients, however, should be seen quite well because of the extremely low moist equivalent temperature difference of this sensor. Channel 6 senses equivalent blackbody temperature with the same spatial resolution as the other channels and is co-registered with those channels. All channels of the CZCS instrument operate simultaneously. During daytime operations all six channels provide useful information. If the sensor operates at night, only data from Channel 6 is usable.

The CZCS has considerable flexibility built-in to accommodate a wide range of conditions. The first four spectral bands, for instance, have four separate gains that change, on command, to accommodate the range of sun angles observed during the complete orbit and throughout the various seasons. The gains are changed to utilize the best dynamic range possible without saturating over-water targets. Normally, the gain used in the first four channels is determined by the solar elevation angle of the target to be acquired. When a special circumstance is expected, such as a particularly bright material in the water, the gain can be changed to accommodate the special circumstances.

In addition to gain change, the CZCS scan mirror can be tilted from nadir to look either forward or behind the spacecraft line of flight. It can tilt in two degree increments, up to twenty degrees in either direction. This feature was built into the instrument to avoid the glint caused by capillary waves on the ocean that would obscure any scattering from below the surface. The angle of tilt of the scan mirror is determined by the solar elevation angle. It is normally tilted to avoid sunglint and would only be commanded to look into the glint for a special sunglint study.

Since Nimbus-7 orbits from south to north in daylight, the scan mirror is positioned to look behind the satellite when the spacecraft is south of the subsolar point and ahead of the spacecraft when it is north of the subsolar point. Tilt and gain setting information is transmitted with the CZCS data and is part of the data product records.

To improve the instrument response to ocean color, a DC offset can be inserted into the on-board processing of the radiance measured in the first four bands. In the DC offset mode, the entire digital capability of the on-board digitizer is utilized to cover approximately the top 30 percent of the signal which contains modulation due to change in ocean color. Since the knowledge of the exact amount of the offset eliminated in the on-board processing is always known, it can be reinserted where needed for processing on the ground.

The sensor is turned on in sufficient time prior to collection of data to allow for instrument warm-up and for the sensor to stabilize. Since all channels are calibrated continuously during flight, any effect of turn-on transient should be noticed immediately.

The most important aspect to be understood about the CZCS operation is that data acquisition is limited, due to spacecraft power constraints, to approximately two hours per day. Because of this operational limit, data must be taken in carefully preselected locations. Minimum on-off data taking time is a two-minute segment. Frequently, longer segments are taken—up to a maximum of ten minutes of continuous data.

The CZCS data is transmitted from the spacecraft to ground receiving stations at a rate of 800 kb either in real time or in playback of the tape recorder. Whenever possible the data is recorded in real time. However, when a satellite is out of the range of tracking stations, the data is recorded on an on-board tape recorder. These tapes contain both radiometric information from the imagery and CZCS housekeeping information.

The Coastal Zone Color Scanner Atmospheric Correction Algorithm

Warren A. Hovis, Chairman
CZCS Nimbus Experiment Team

Structure that can be clearly seen in the water in the Level II data product from the Coastal Zone Color Scanner (CZCS) is quite frequently not obvious in the Level I data product where only an approximate Rayleigh correction for the atmosphere is carried out to increase contrast. A scene from 10 June 1979, off the East Coast, is shown in both the Level I and Level II products (pages xiv and xv), illustrating the power of the atmospheric correction algorithm. The difficulty in estimating what the final product will look like before applying the complete atmospheric correction technique is obvious.
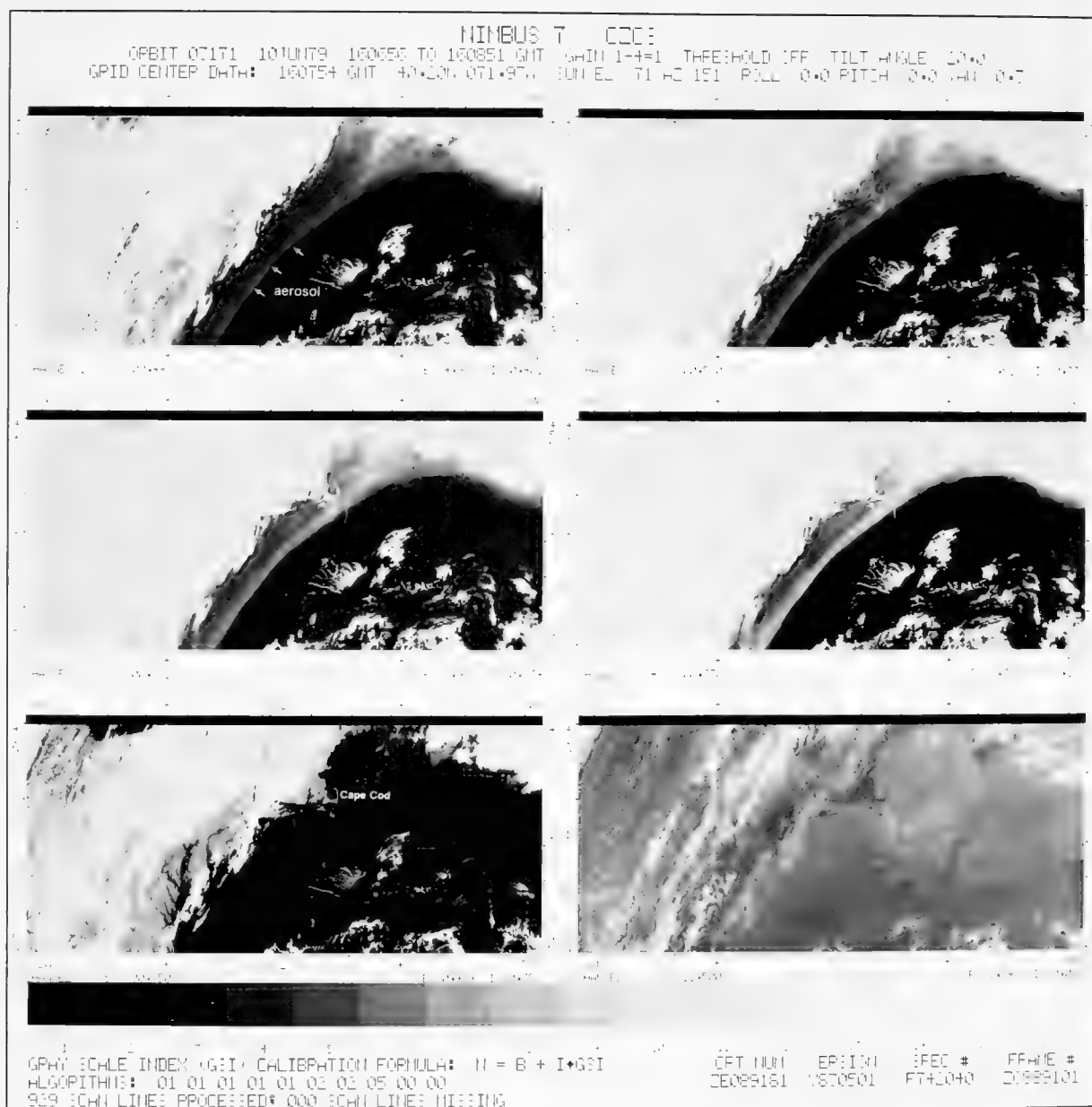
An Example of the Coastal Zone Color Scanner Atmospheric Correction Algorithm Capability

A number of observers utilizing CZCS data have been confused by the fact that structure in the water that can be seen quite clearly on one day, may not be so clearly identifiable on images taken on successive days. One problem is that when the area in question is directly, or nearly directly, below the subsatellite track, the sensor is viewing the area through the minimum atmosphere. The same area may be visible several days after, but the atmospheric attenuation will increase as the path length increases since the scanner can scan out to 40 degrees either side of the spacecraft nadir. In some cases, scenes are not selected for Level II processing because of an apparent lack of information in the Level I data. The Level I image on this page is the only Level I image shown in this atlas; however, Level I images constitute the major archive from which scenes are selected for Level II processing. Potential investigators should understand the characteristics of the Level I data.

The technique for processing the Level I data to remove the atmospheric effect has been described extensively by Gordon (1978 and 1981a), and Gordon *et al.* (1979), and is used by NASA in the production of all of the Level II imagery. The Level I image shown on this page appears to contain very little ocean content information along the East Coast, which is obscured by a light aerosol band extending from the area of the mouth of Chesapeake Bay, over Cape Cod, and into the Gulf of Maine. This scene would probably have not been selected for Level II processing except that there was a ship operating in the area outside of the light aerosol bank along the East Coast during the validation phase of the CZCS program, and it was desirable to produce the Level II for that area of the image that appeared to be clear. The Level II image (opposite page), presented in the conventional Level II format, shows the amount of detail that can be extracted from the Level I data after application of the atmospheric algorithm. Very little evidence of the light aerosol bank is seen at all, and considerable structures are seen in the water in both pigment and diffuse attenuation coefficient imagery. This case should be kept in mind before rejecting any of the Level I imagery for conversion to Level II when the scene is of great interest and yet appears to show little detail in Level I. Unless the Level I data is saturated, in which case no correction will be successful, there is the potential of extracting information such as that shown in this remarkable case.

References

Gordon, H. R., 1978: Removal of atmospheric effects from satellite imagery of the oceans. *Applied Optics*, **17**, 1631–1636.

———, 1981a: A preliminary assessment of the Nimbus-7 CZCS atmospheric correction algorithm in a horizontally inhomogeneous atmosphere. In *Oceanography from Space*, edited by J. F. R. Gower, Plenum Press, New York, 257–266.

Gordon, H. R., J. L. Mueller, and R. C. Wrigley, 1979: Atmospheric correction of Nimbus-7 Coastal Zone Color Scanner imagery, Presented at IFAORS Workshop on *Interpretation of Remotely Sensed Data*, Williamsburg, VA, May 23–25 (also in *Remote Sensing of Oceans and Atmospheres*, edited by A. Deepak, Academic Press, New York, 1980).

Nimbus-7. Orbit 3171. 10 June 1979. CZCS Level I Images.

Nimbus-7. Orbit 3171. 10 June 1979. CZCS Level II Images.

List of Contributors

Mark R. Abbott
Jet Propulsion Laboratory
California Institute of Technology
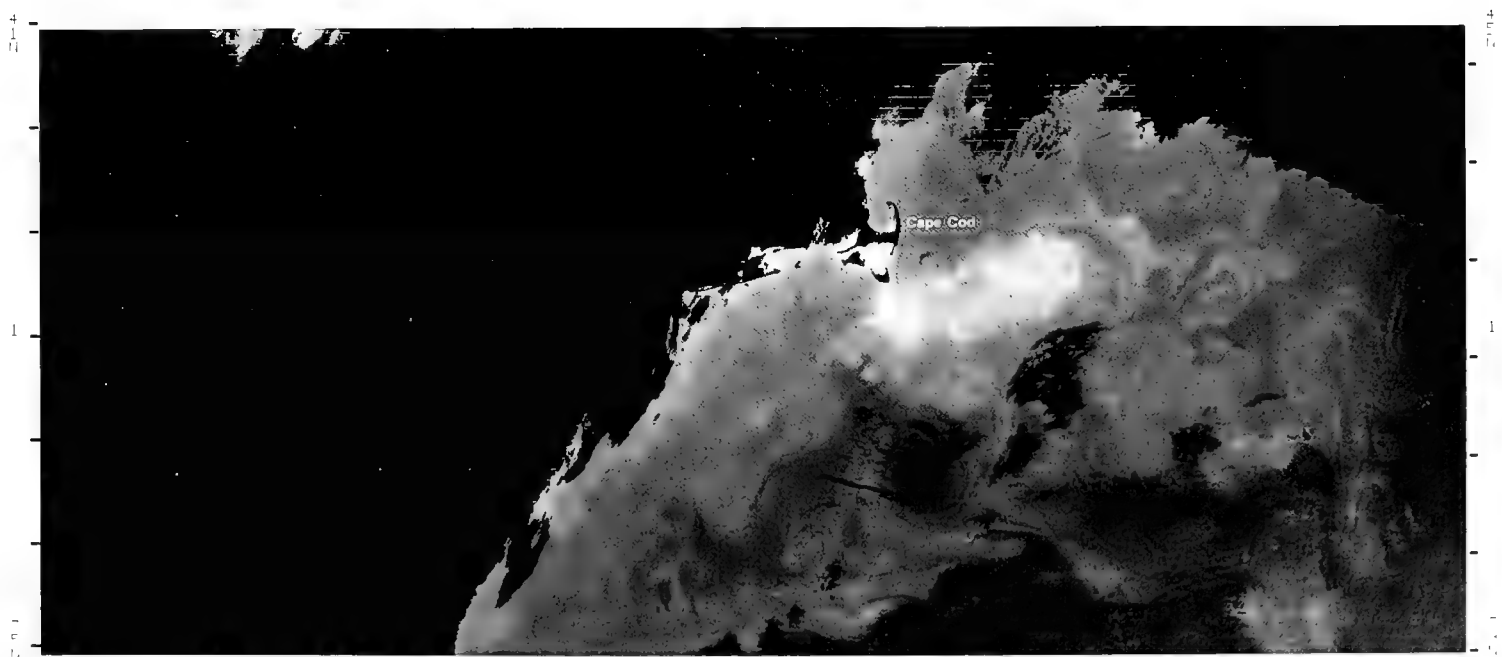4800 Oak Grove Drive
Pasadena, CA 91106
and
Scripps Institution of Oceanography
University of California, San Diego
La Jolla, CA 92093

Frank P. Anderson
National Research Institute for Oceanology
Council for Scientific and Industrial Research
P.O. Box 320
Stellenbosch 7600
South Africa

Edward T. Baker
Pacific Marine Environmental Laboratory/NOAA
7600 Sand Point Way, N.E.
Seattle, WA 98115

Robert L. Bernstein
Scripps Institution of Oceanography
University of California, San Diego
La Jolla, CA 92093

William W. Broenkow
Moss Landing Marine Laboratory
P.O. Box 223
Moss Landing, CA 95039

Ken L. Denman
Institute of Ocean Sciences
P.O. Box 6000
9860 West Saanich Road
Sidney, B.C. V8L 4B2
Canada

Sayed Z. El-Sayed
Department of Oceanography
Texas A&M University
College Station, TX 77843

James F. R. Gower
Institute of Ocean Sciences
P.O. Box 6000
9860 West Saanich Road
Sidney, B.C. V8L 4B2
Canada

Eileen E. Hofmann
Department of Oceanography
Texas A&M University
College Station, TX 77843

Patrick M. Holligan
Marine Biological Association
Citadel Hill
Plymouth PL1 2PB
United Kingdom

Takashi Ichiye
Department of Oceanography
Texas A&M University
College Station, TX 77843

Donald B. Olson
Rosenstiel School of Marine and
    Atmospheric Science
University of Miami
4600 Rickenbacker Causeway
Miami, FL 33149

Thomas C. Royer
Institute of Marine Science
University of Alaska
Fairbanks, AK 99701

Eckart H. Schumann
Department of Oceanography
University of Port Elizabeth
P.O. Box 1600
Port Elizabeth 6000
South Africa

L. Vere Shannon
Sea Fisheries Research Institute
Private Bag X2
Rogge Bay 8012
Cape Town
South Africa

Charles C. Trees
Department of Oceanography
Texas A&M University
College Station, TX 77843

Michel Viollier
Station d'Océanologie et de Biologie Marine
Place Georges Teissier
F-29211 Roscoff
France

Robert C. Wrigley
Ames Research Center/NASA
Mail Stop 242-4
Moffett Field, CA 94035

Charles S. Yentsch
Bigelow Laboratory of Ocean Sciences
McKown Point
West Boothbay Harbor, ME 04574

Members of the Nimbus Experiment Team (NET) for the Coastal Zone Color Scanner (CZCS)

Dr. Warren A. Hovis, Chairman
CZCS, Nimbus Experiment Team

Dr. Frank P. Anderson
National Research Institute for Oceanology
Council for Scientific & Industrial Research
P.O. Box 320, Stellenbosch 7600
South Africa
202–362–8805 (South African Embassy
in Washington, D.C.)

Dr. John Apel
Applied Physics Laboratory
The Johns Hopkins University
Laurel, MD 20707
301–953–5038

Mr. Roswell W. Austin
Visibility Laboratory P003
Scripps Institution of Oceanography
University of California, San Diego
La Jolla, CA 92093
619–294–3680

Dr. Edward T. Baker
Pacific Marine Environmental Laboratory/NOAA
NOAA Building Number 32
7600 Sand Point Way, N.E.
Seattle, WA 98115
FTS8–446–6251

Mr. Dennis K. Clark
NOAA/NESDIS
Oceanic Sciences Branch
Suitland Professional Center
Room 310
Washington, D.C. 20233
301–763–4244

Dr. Sayed Z. El-Sayed
Texas A&M University
Department of Oceanography
College Station, TX 77843
409–845–2134

Dr. Howard R. Gordon
Physics Department
University of Miami
P.O. Box 248046
Coral Gables, FL 33124
305–284–2323

Dr. James L. Mueller
U.S. Naval Post Graduate School
Department of Oceanography
Monterey, CA 93940
408–646–3266

Dr. Boris Sturm
Commisione delle Comunita Europee
2102 Centro Euratom di Ispra
Ispra, Italy
(0332) 780131/780271

Mr. Robert C. Wrigley
Ames Research Center/NASA
Mail Stop 242-4
Moffett Field, CA 94035
415–694–6060

Mr. Charles S. Yentsch
Director of Research
Bigelow Laboratory of Ocean Sciences
McKown Point
West Boothbay Harbor, ME 04574
207–633–2173

CZCS Archive

Mr. Carroll A. Hood
NOAA/NESDIS
Satellite Data Services Division
World Weather Building
Room 100
Washington, D.C. 20233
301–763–8111

Section 1
Gulf of Alaska/Aleutian Islands/Bering Sea

1

1A   Gulf of Alaska/Aleutian Islands

James F. R. Gower
Institute of Ocean Sciences
Sidney, B.C., Canada
and
Thomas C. Royer
Institute of Marine Science
University of Alaska
Fairbanks, Alaska

The relatively fresh surface water of the Gulf of Alaska converges into the Alaska Current and then flows out into the Pacific via the Alaskan Stream, a narrow boundary current that follows the continental slope along the southeast side of the Aleutian Island chain.

The following two CZCS images present rare glimpses of the flow pattern in the Gulf of Alaska. They show the convergent flow of water into the Alaska Current and Alaskan Stream; the movement of the stream along the continental shelf breakoff, the Alaska Peninsula, and the Aleutian Island arc; and the onset of eddy formation south of Unalaska Island.

Areas of high productivity are shown by the high pigment concentrations on the continental shelf near Kodiak Island. Flow features close to the coast, in and to the east of Cook Inlet, are traced out by patterns of river and glacial silt introduced by the high run-off characteristic of the region.

5-1. Locator Map for 5-2.

5-2. Nimbus-7. Orbit 4390. 6 September 1979. CZCS Pigment Image. (**M**–Middleton Is., **K**–Kayak Is.)

The resulting high productivity supports the valuable fisheries of the area. The patchiness illustrated here is, in general, similar to the variations in benthic marine populations.

Patterns resulting from flow of water from these areas into the westward Alaska Current along the shelf break can also be identified in the image. Off Kodiak Island, the flow is converging from a broader eastern boundary current into the swift (speeds >1 m s^{-1}), narrow, western boundary current of the Alaskan Stream (Royer, 1981). Further convergence is apparent as the flow continues to the southwest.

Because of the high coastal runoff to the east of Kodiak Island, gray tones in the image near this coast will be affected by river and glacial silt as well as by phytoplankton pigment concentrations. Features of the nearshore circulation are thus made visible on the image.

The narrow Alaska Coastal Current (<20 km wide) can be seen adjacent to Kayak Island as a lighter tone due to large silt loads from glaciers (Malaspina Glacier and others). At the southwest tip of the island the flow bifurcates. A portion joins the Alaska Current, flowing westward along the shelf break, while the rest flows into a cyclonic pattern behind the island (arrows, 5-1). This nearshore flow is joined by the silt-laden Copper River water (white) and flows westward into Prince William Sound where additional, less silty water enters to cover the Copper River water. This nearshore circulation has been identified by satellite-tracked drifting buoys (Royer et al., 1979). The nearshore water of the Alaska Coastal Current leaves Prince William Sound and brings nutrient-rich water to the shelf fisheries east of Kodiak Island. From the image, it can be seen that part of the coastal current enters Cook Inlet through the Kennedy Entrance. Within Cook Inlet, light tones are caused by the high silt concentrations from the Susitna and Mastanuska Rivers. There is little evidence of the Alaska Coastal Current to the west of Kodiak Island since the fresh water influx is small.
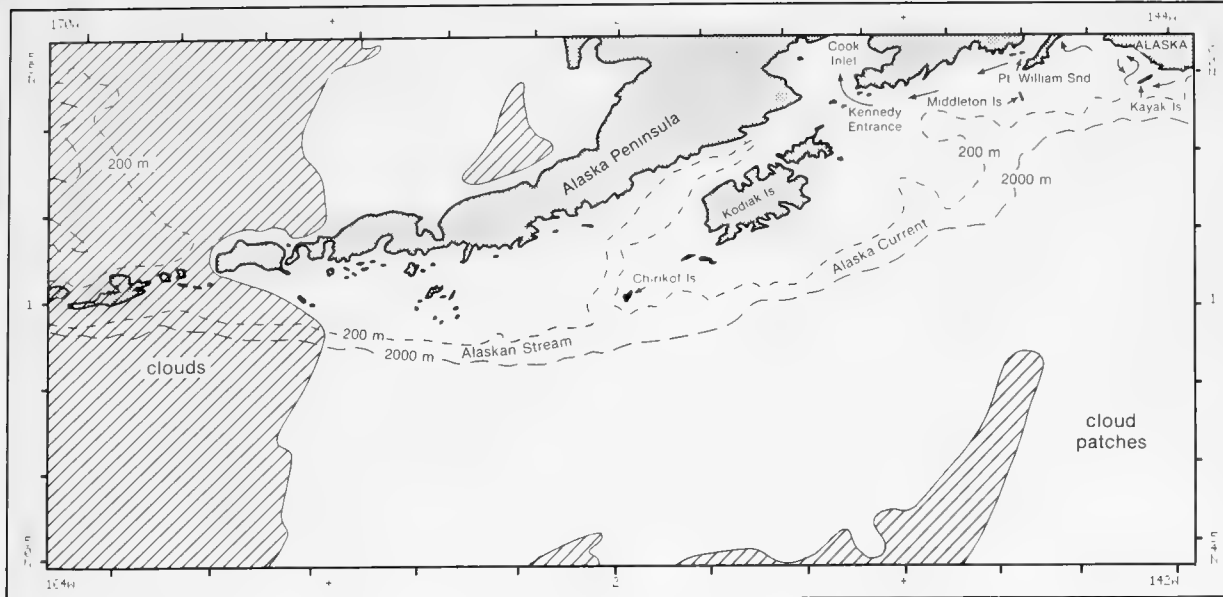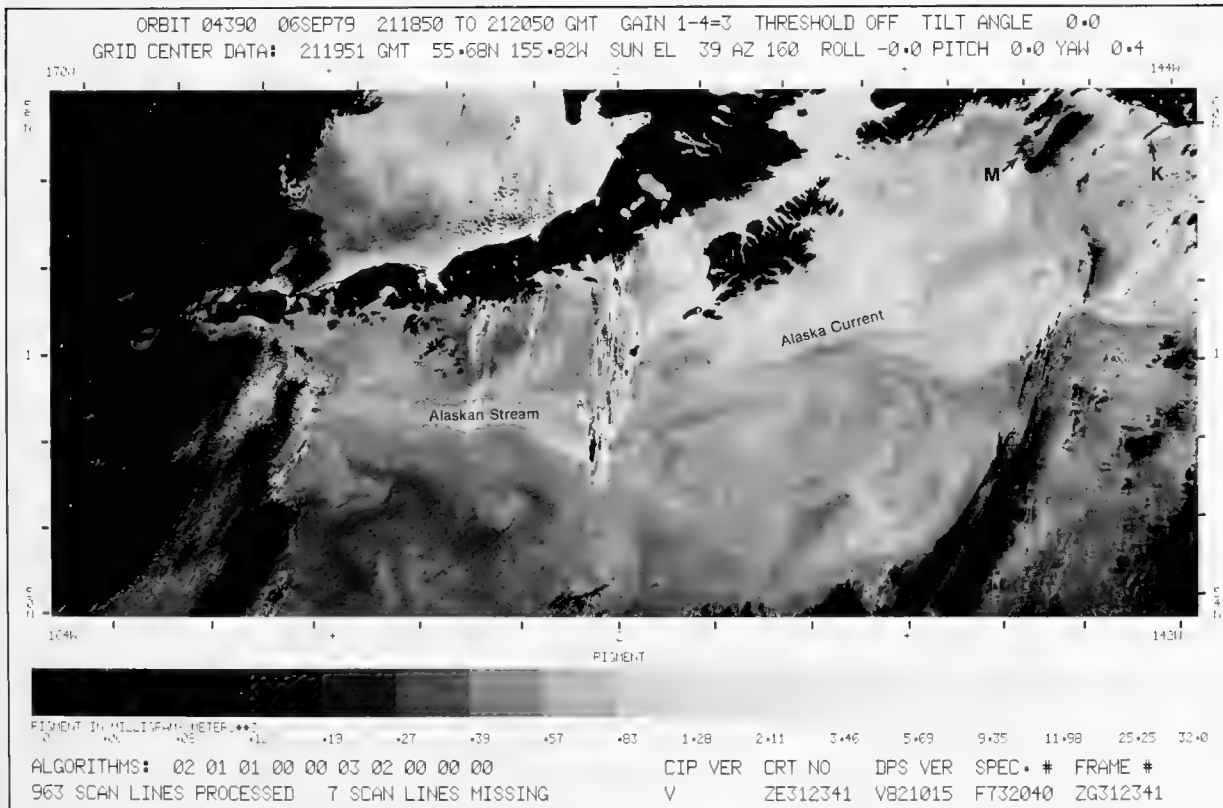
References
Royer, T. C., 1981: Baroclinic transport in the Gulf of Alaska. Parts I and II. *J. Marine Res.*, **39**, 239–266.
Royer, T. C., D. V. Hansen, and D. J. Pashinski, 1979: Coastal flow in the northern Gulf of Alaska as observed by dynamic topography and satellite-tracked drogued drift buoys. *J. Phys. Oceanogr.*, **9**, 785–801.
Thomson, R. E., 1972: On the Alaskan Stream. *J. Phys. Oceanogr.*, **2**, 363–371.
Wright, C., 1981: Observations of the Alaskan Stream during 1980. NOAA Technical Memorandum ERL PMEL-23

The Alaskan Stream and Gulf of Alaska Circulation
July and September 1979

The waters of the northern Gulf of Alaska contain very large across-shelf gradients of salinity caused by the high influx of fresh water along the British Columbia and Alaska coasts. This influx alters the vertical density gradients, resulting in contrast in surface temperature and phytoplankton concentration. Near the coasts the suspended sediments brought in by the fresh water also result in strong but smaller scale ocean color differences.

Persistent cloud cover in this area makes successful satellite imaging a rare event. For thermal infrared images the horizontal temperature contrasts are low, usually covering a range of 1° to 2° C, making it difficult to trace ocean features. The CZCS ocean color (pigment) images, by contrast, show dramatic flow features traced by the varying phytoplankton concentrations in the stratified Gulf of Alaska water.

The CZCS pigment image on 10 July (4-2) covers a small strip of the northeast Pacific Ocean along the southern edge of the Aleutian Island chain (4-1). The image shows the surface ocean color structure associated with the Alaskan Stream in terms of pigment level variations in the range of 0.4 to 1.0 mg m^{-3}. Some of the Aleutian Islands appear as black areas in the image; others are covered by clouds and cannot be identified. However, most of the southeastern coasts of the Aleutian Island chain in the right half of the image are cloud-free.

The Alaskan Stream is the major current by which water leaves the Gulf of Alaska. It flows westward as a narrow jet along the continental slope, between 200 m and 2,000 m (4-1). The stream structure visible in the image (4-2) confirms the narrow (60 km) width deduced by Royer (1981) from hydrographic observations, and shows the start of a recirculating eddy near the bottom center of the image, south of Unalaska Island. Such recirculation, in which Gulf of Alaska water mixes into the Pacific Ocean, has been deduced to occur within a range of longitudes as discussed by Thomson (1972). The position of this eddy is at the start of this range and near the position for the start of recirculation reported by Wright (1981), for March 1980. Eddies of this type are of great interest and were, for example, the subject of a 30-day cruise in 1981. Such images, if taken immediately before and during such a cruise, would be very valuable both for the planning of the cruise and for the subsequent data analysis.

The CZCS pigment image on 6 September (5-2), shows turbulent patterns traced out by varying phytoplankton pigment concentrations over a large area of the Gulf of Alaska. The patterns are distorted by the convergent flow of the surface water into the Alaska Current. It is this current which moves across the middle of the image from right to left following the 2,000-m contour on the shelf break (5-1), and converges into the Alaskan Stream to the west. The indicated pigment levels and the flow pattern on the left side of the image are very similar to those in 4-2, which shows the same area two months earlier.

A solid cloud layer covers the far left side of the image, and there are cloud bands and cloud lines across the right side (compare with 5-1). Patches of clouds confuse the coastline, especially near the upper right corner. Streaks of thinner clouds are not perfectly masked to black north of the Alaska Peninsula in this example, and some of the more linear light features in the center of the image are of atmospheric origin.

Light tones in the upper right area of image 5-2 indicate the areas of high chlorophyll content on the continental shelf southwest and northeast of Kodiak Island and near Middleton Island. Shoals in those areas cause vertical mixing, allowing nutrient-rich water to be brought to the surface.
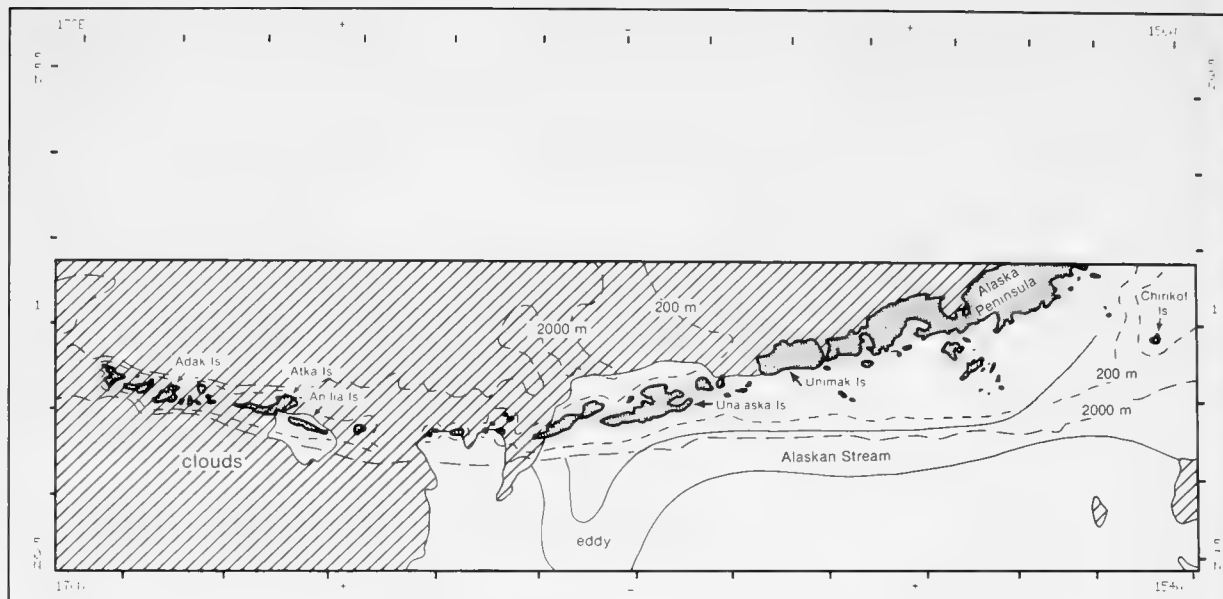
4-1. Locator Map for 4-2.
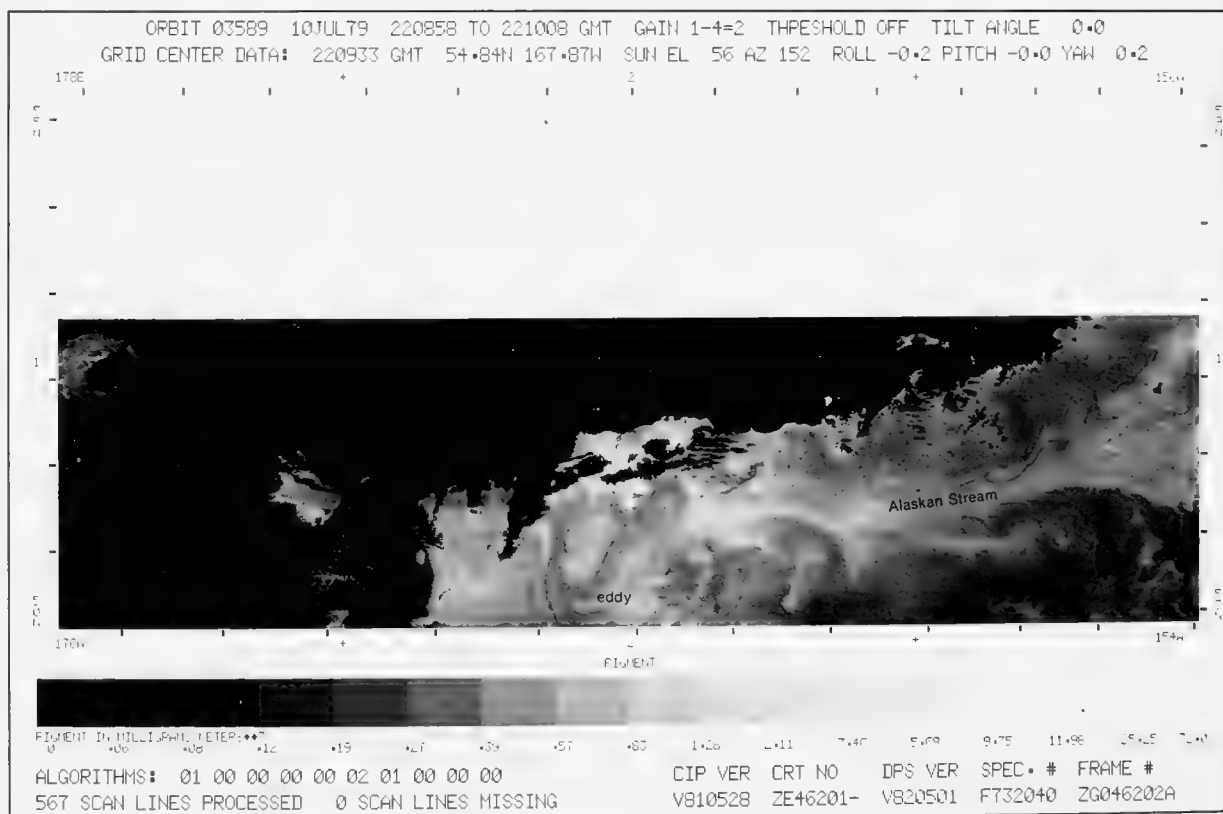
4-2. Nimbus-7. Orbit 3589. 10 July 1979. CZCS Pigment Image.

1B   Gulf of Alaska/Southeast Bering Sea

Edward T. Baker

Pacific Marine Environmental Laboratory/NOAA
Seattle, Washington

Circulation in the northeast Gulf of Alaska is dominated by the eastern and northern limbs of the North Pacific subarctic gyre. The broad and sluggish eastern limb narrows, deepens, and accelerates near the head of the gulf, turning westward to flow south of Kodiak Island and the Alaska Peninsula as the Alaskan Stream.

In the southeastern Bering Sea, circulation patterns and hydrographic domains are bathymetrically controlled. A hydrographic front approximately coincident with the 50-m isobath separates well-mixed and turbid inshore water from stratified, less turbid offshore water.

Sea Surface Turbidity
September 1979

The northeastern Gulf of Alaska is bordered by mountainous coastline containing numerous glaciers, rivers, and streams which deliver large quantities of suspended material to the gulf during the summer when maximum discharge occurs. A CZCS image of the diffuse attenuation coefficient of the area from late summer (9-2) illustrates various processes that transport this coastally derived material offshore. (The diffuse attenuation coefficient image is used instead of the pigment image due to the preponderance of inorganic material in Alaskan coastal waters.) The image also illustrates what appear to be streamlines of the Alaska Current, the northern portion of the subarctic gyre that sweeps through the gulf with peak surface speeds of 100 cm s^{-1}.

Inspection of the CZCS image of the Alaskan coast in the region around Kayak Island (see locator map 9-1) reveals a prominent plume of turbid coastal water deflected offshore in an anticyclonic gyre created by impingement of the Alaska Current on Kayak Island. Similar offshore transport of suspended particles occurs on the south side of Montague Island, although in this image clouds obscure much of that area. These coastal processes provide large quantities of material to the Alaska Current for westward transport.

West of Montague Island, the continental shelf widens and forces the northern border of the Alaska Current southward. West of Kodiak Island, the broad sweep of the Alaska Current in the eastern gulf coalesces into a relatively narrow, fast-flowing current, with sharply defined borders, called the Alaskan Stream. Although no synchronous hydrographic data is available for this image, historical observations suggest that the sharp ocean color gradient (dashed line-**G**) may indicate the southern limit of the Alaska Current/Alaskan Stream.

The CZCS image of the westward flowing Alaska Current/Alaskan Stream presents markedly different flow characteristics than eastward flowing boundary currents such as the Gulf Stream or the Kuroshio. Streamlines of the Alaskan currents (not shown) are relatively organized and show little indication of the multiple meanders and extensive eddy formation observed in the Gulf Stream. Theoretical considerations based on vorticity conservation predict multiple wavelike features in the flow pattern of prograde flows (depth decreases to the left looking downstream) such as the Gulf Stream but not in retrograde flows (depth decreases to the right looking downstream) such as the Alaskan currents; CZCS imagery of these two current systems support those predictions.

In the southeastern Bering Sea, a change in the degree of vertical mixing, occurring at roughly the 50-m isobath (9-1), controls the areal distribution of both hydrographic properties and suspended particles. Inshore of the 50-m isobath, the water column is typically well-mixed and alongshore distribution of local sediment sources produces high turbidity levels and sharp offshore gradients. In the CZCS image, the diffuse attenuation coefficient decreases abruptly seaward of this frontal zone, particularly along the Alaska Peninsula. Unlike the coast of the Gulf of Alaska, water flow on the north shore of the Alaska Peninsula is tidally dominated and mean flow is very weak. Offshore transport of suspended particles by advection rarely occurs. Loss of suspended particles from the nearshore zone is largely by seaward diffusion; therefore, offshore gradients are steep.
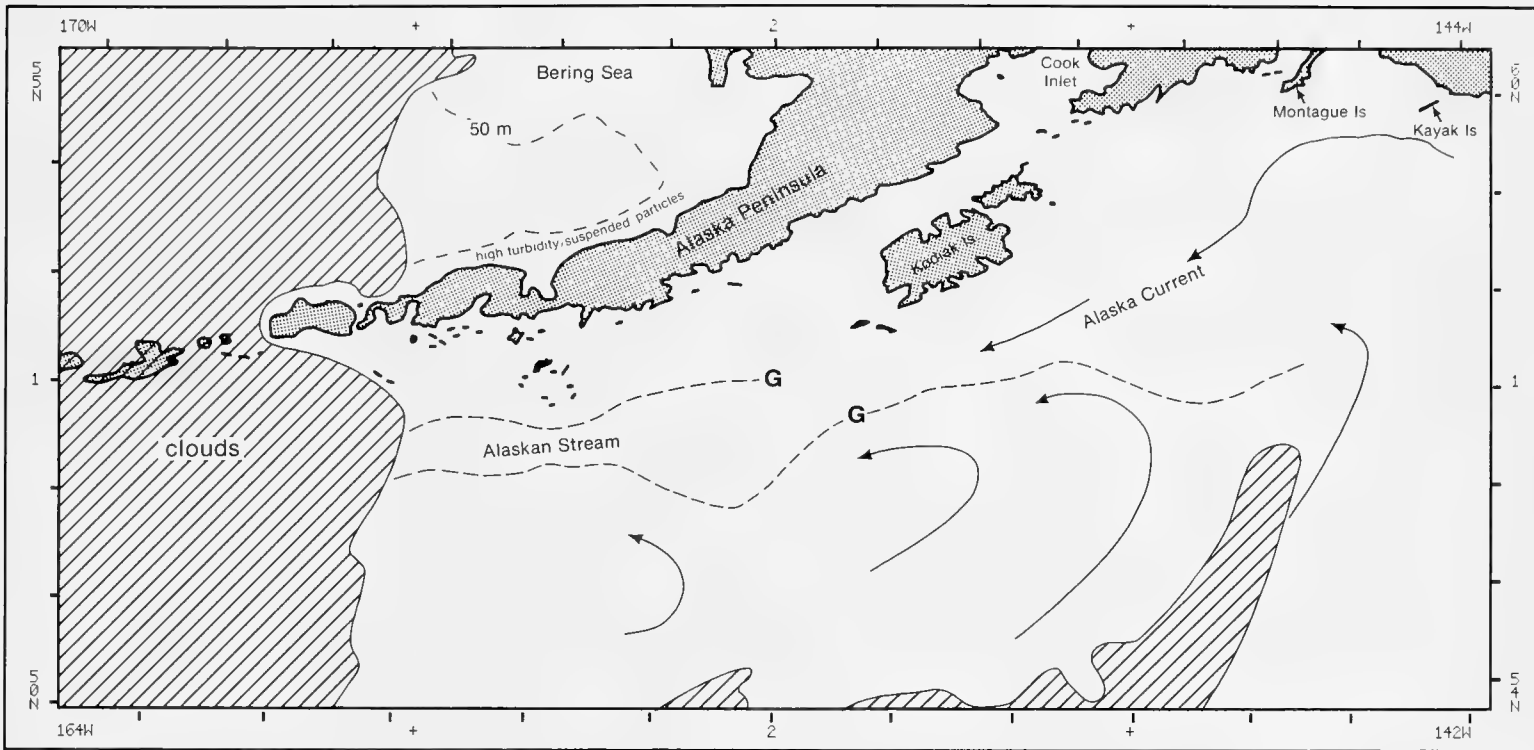
9-1. Locator Map for 9-2.
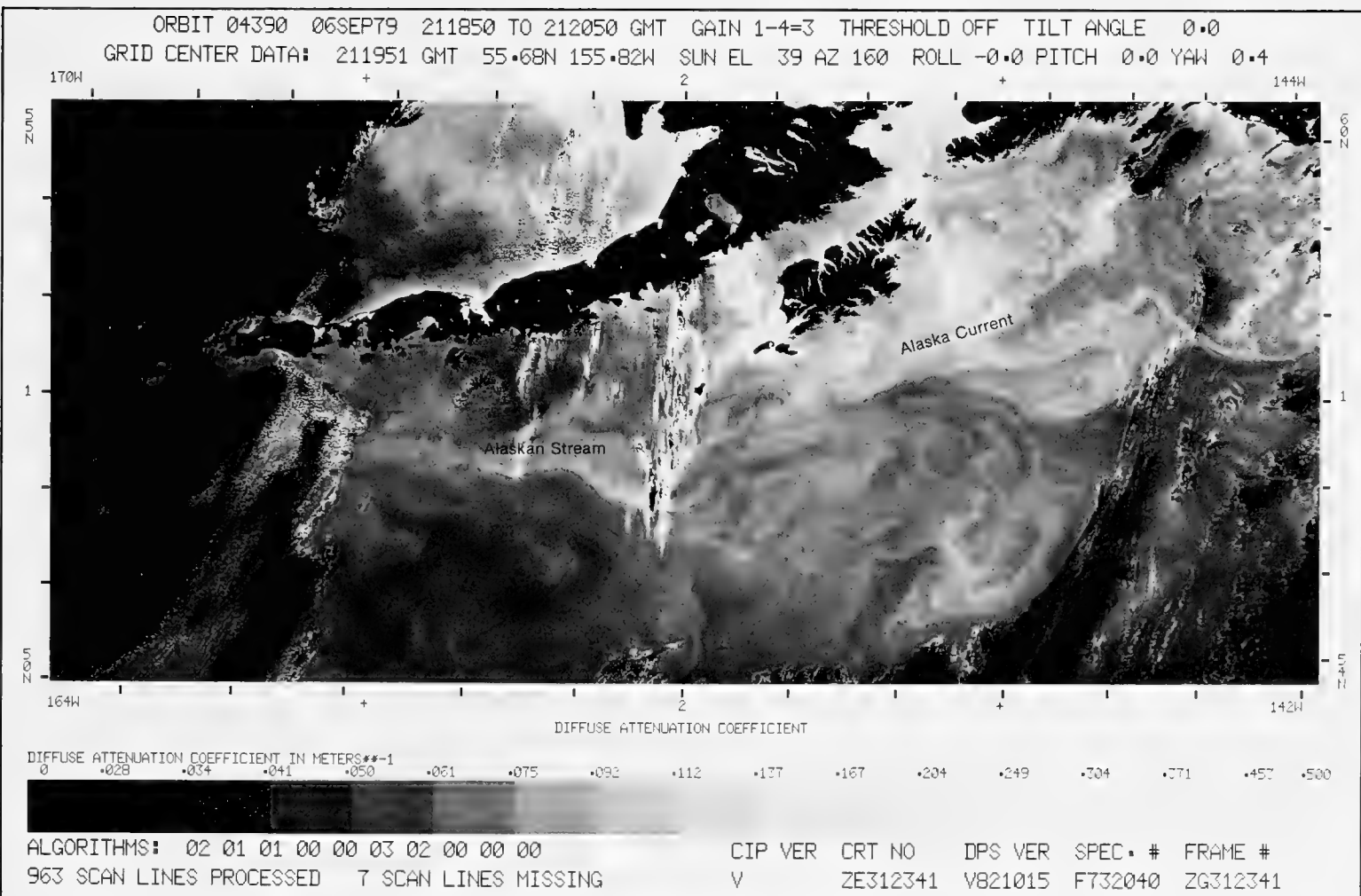
9-2. Nimbus-7. Orbit 4390. 6 September 1979. CZCS Diffuse Attenuation Coefficient Image.

Section 2
Pacific North American Coast

2A North America West Coast

Robert L. Bernstein
Scripps Institution of Oceanography
University of California, San Diego
La Jolla, California

When coastal winds change from wintertime westerly or southwesterly to summertime northerly along the North American west coast, surface water is driven southward and offshore. Cooler, nutrient-rich waters underneath are brought to the surface, creating conditions favorable for phytoplankton growth. Thus during summer, cool, green water (high chlorophyll pigment levels) is clearly detected by sensors operating in the blue-green and thermal infrared portions of the spectrum. The earliest seasonal development of upwelling occurs in the spring along Baja California, and peaks later as one proceeds north toward Vancouver Island. The process usually reaches its maximum amplitude in July along the central and northern California coast.

Seasonal Development of Coastal Upwelling
March–July 1979

The seasonal development of coastal upwelling is clearly indicated by the following sequence of images, which show chlorophyll pigment levels derived from CZCS data. Along the Pacific Coast of Baja California, on 17 March (14-1), only modest development is observed, compared with subsequent images 15-1 and 15-2, one and two months later, respectively. Also observed is the persistent cyclonic rotation just off Punta Eugenia which is well-known from numerous hydrographic surveys. Cyclonic eddies tend to spin-up there, eventually detaching and drifting westward at a rate of about 4 to 5 km day^{-1}. The isolated patch of high pigment about 300 km west of Punta Eugenia (15-2), may be the indication of an eddy apparently having been spun-up along the coast two months earlier. Also in the image several other southwestward-directed jets of high pigment water (light tones) are observed which exhibit cyclonic turning. Such jets and eddies are a recurring phenomenon all along the west coast during the upwelling period. They tend to appear in the same locations, in association with configurations of the coastline, offshore bathymetry, and wind which combine to favor intense upwelling.

Proceeding north to southern California, a comparison of images 16-1, 16-2, and 17-1 shows the steady development of upwelling (light tones, high pigment levels) between early April and July of 1979. Note that by July (17-1), Point Conception has become a center for strong persistent upwelling. Even more dramatic is the shift from winter to summer conditions along northern California (18-1 and 18-2). The CZCS image for July (18-2) shows the development of offshore jets, and a cyclonic eddy is observed between Cape Mendocino and Point Arena. Such eddies occur regularly at this location during the summer, from where they translate southward at a rate of 5 to 10 km day^{-1}.

Further north along the Oregon, Washington, and Vancouver Island coastlines (19-1 and 19-2), similar upwelling development is observed between March and July 1979. Of interest in the March image (19-1) is the small amount of upwelling-induced, high-pigment water close to the coast, probably induced quite temporarily by north or northeasterly winds which created the cloud-free conditions to permit a view of the surface. The upwelled water acts as a tracer, allowing visualization of the northward current along the coastal region. This northward flow, known as the Davidson Current, appears at the surface only during winter, but is actually present at greater depths throughout the year.
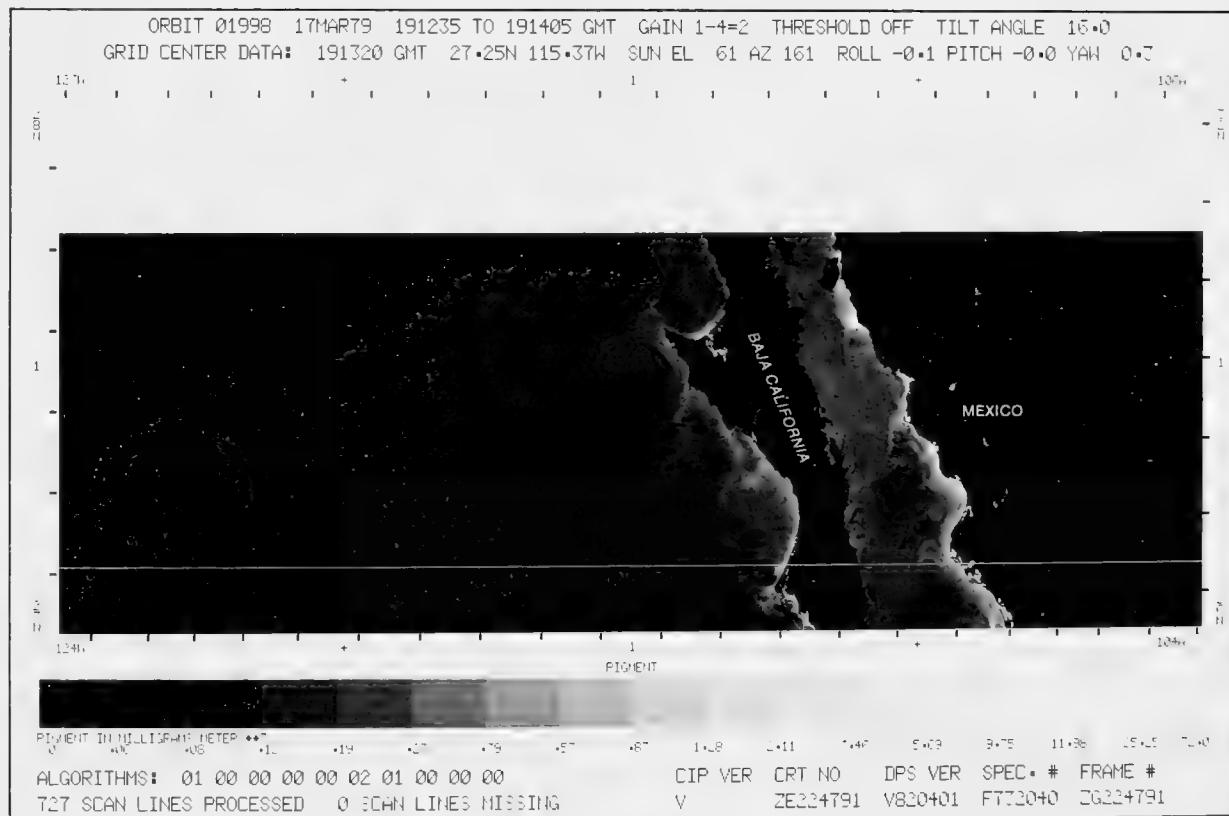
14-1. Nimbus-7. Orbit 1998. 17 March 1979. CZCS Pigment Image.
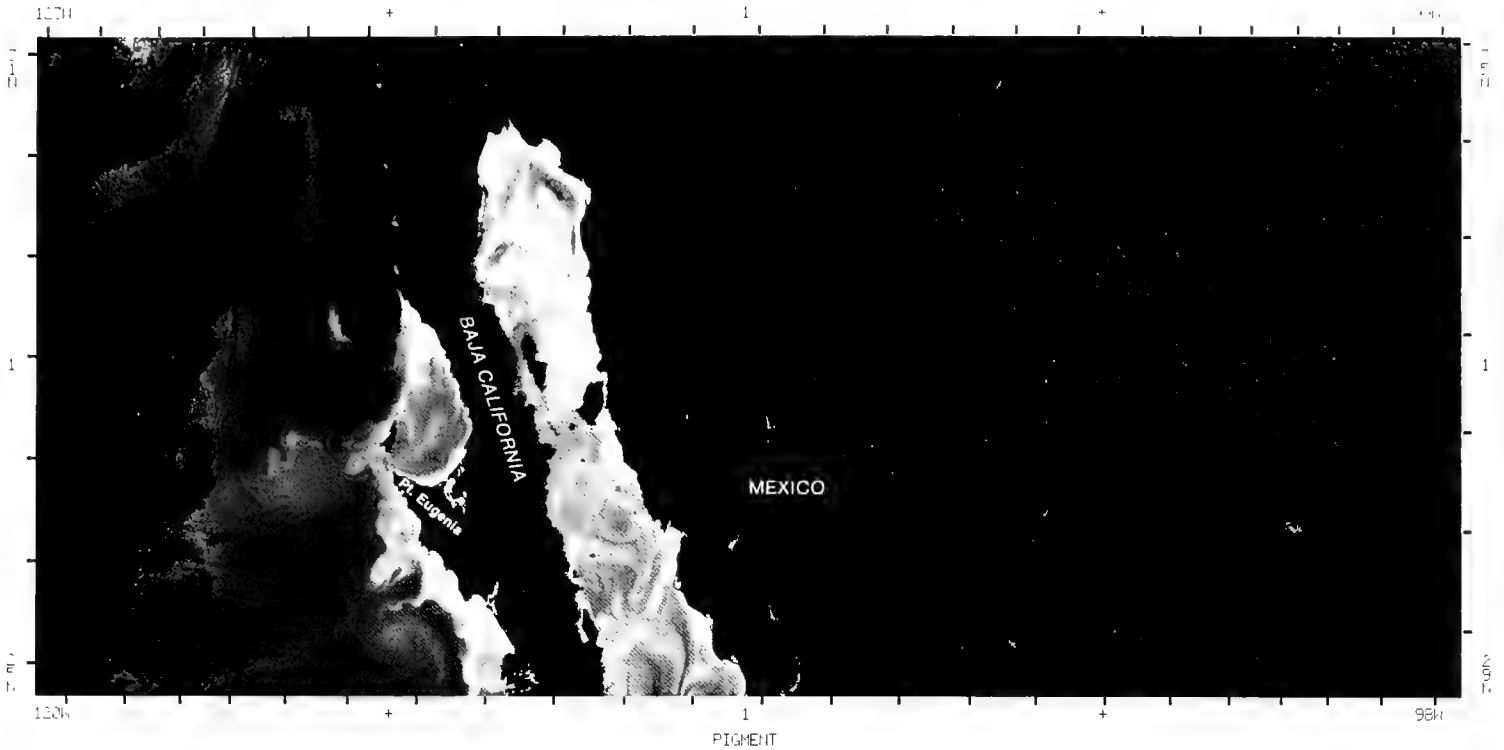
15-1. Nimbus-7. Orbit 2371. 13 April 1979. CZCS Pigment Image.

15-2. Nimbus-7. Orbit 2772. 12 May 1979. CZCS Pigment Image.

ORBIT 02247   04APR79   193211 TO 193411 GMT   GAIN 1-4=1   THRESHOLD OFF   TILT ANGLE   20·0
GRID CENTER DATA: 193312 GMT   31·43N 121·13W   SUN EL   63 AZ 161   ROLL -0·1 PITCH -0·2 YAW   0·3
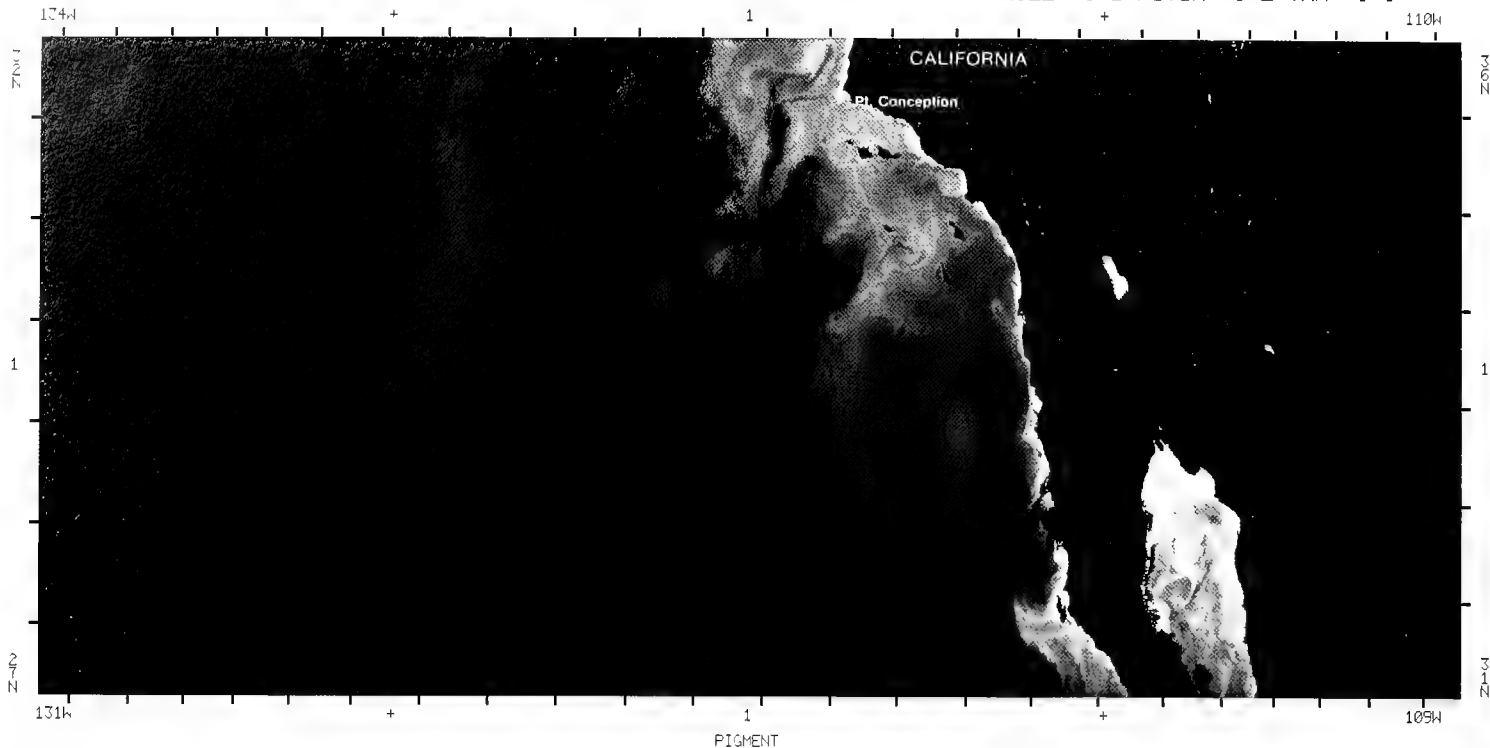
CALIFORNIA

Pt. Conception

PIGMENT

ALGORITHMS: 01 00 00 00 00 02 01 00 00 00

970 SCAN LINES PROCESSED   0 SCAN LINES MISSING

CIP VER   CRT NO   DPS VER   SPEC· #   FRAME #
V800710   ZE05501-   V820501   F732040   ZG005502

16-1. Nimbus-7. Orbit 2247. 4 April 1979. CZCS Pigment Image.

ORBIT 02772   12MAY79   190940 TO 191140 GMT   GAIN 1-4=1   THRESHOLD OFF   TILT ANGLE   20·0
GRID CENTER DATA: 191041 GMT   33·84N 116·01W   SUN EL   73 AZ 155   ROLL -0·1 PITCH -0·0 YAW   0·4

CALIFORNIA

Pt. Conception

PIGMENT

MILLIGRAME METER·**2   ·05   ·13   ·19   ·27   ·39   ·57   ·83   1·28   2·11   3·46   5·69   9·35   11·98   25·25   32·0

ALGORITHMS: 01 00 00 00 00 02 01 00 00 00

970 SCAN LINES PROCESSED   0 SCAN LINES MISSING

CIP VER   CRT NO   DPS VER   SPEC· #   FRAME #
V   ZE76891-   V820401   F732040   ZG976803

16-2. Nimbus-7. Orbit 2772. 12 May 1979. CZCS Pigment Image.

ORBIT 03560 08JUL79 193953 TO 194153 GMT GAIN 1-4=1 THRESHOLD OFF TILT ANGLE 20·0
GRID CENTER DATA: 194053 GMT 33·85N 123·54W SUN EL 76 AZ 141 ROLL -0·2 PITCH 0·2 YAW 0·3

PIGMENT

PIGMENT IN MILLIGRAMS METERS**3
0   ·06   ·08   ·12   ·19   ·27   ·39   ·57   ·83   1·28 2·11 3·46 5·69 9·35 11·98 25·25 72·0

ALGORITHMS: 01 00 00 00 00 02 01 00 00 00   CIP VER   CRT NO   DPS VER   SPEC· #   FRAME #
970 SCAN LINES PROCESSED   0 SCAN LINES MISSING   V800710   ZE45101- V820501   F732040   ZG045101

17-1. Nimbus-7. Orbit 3560. 8 July 1979. CZCS Pigment Image.

ORBIT 02081 23MAR79 192229 TO 192429 GMT GAIN 1-4=1 THRESHOLD OFF TILT ANGLE 18·0
GRID CENTER DATA: 192329 GMT 41·00N 121·13W SUN EL 49 AZ 162 ROLL -0·1 PITCH -0·0 YAW 0·3
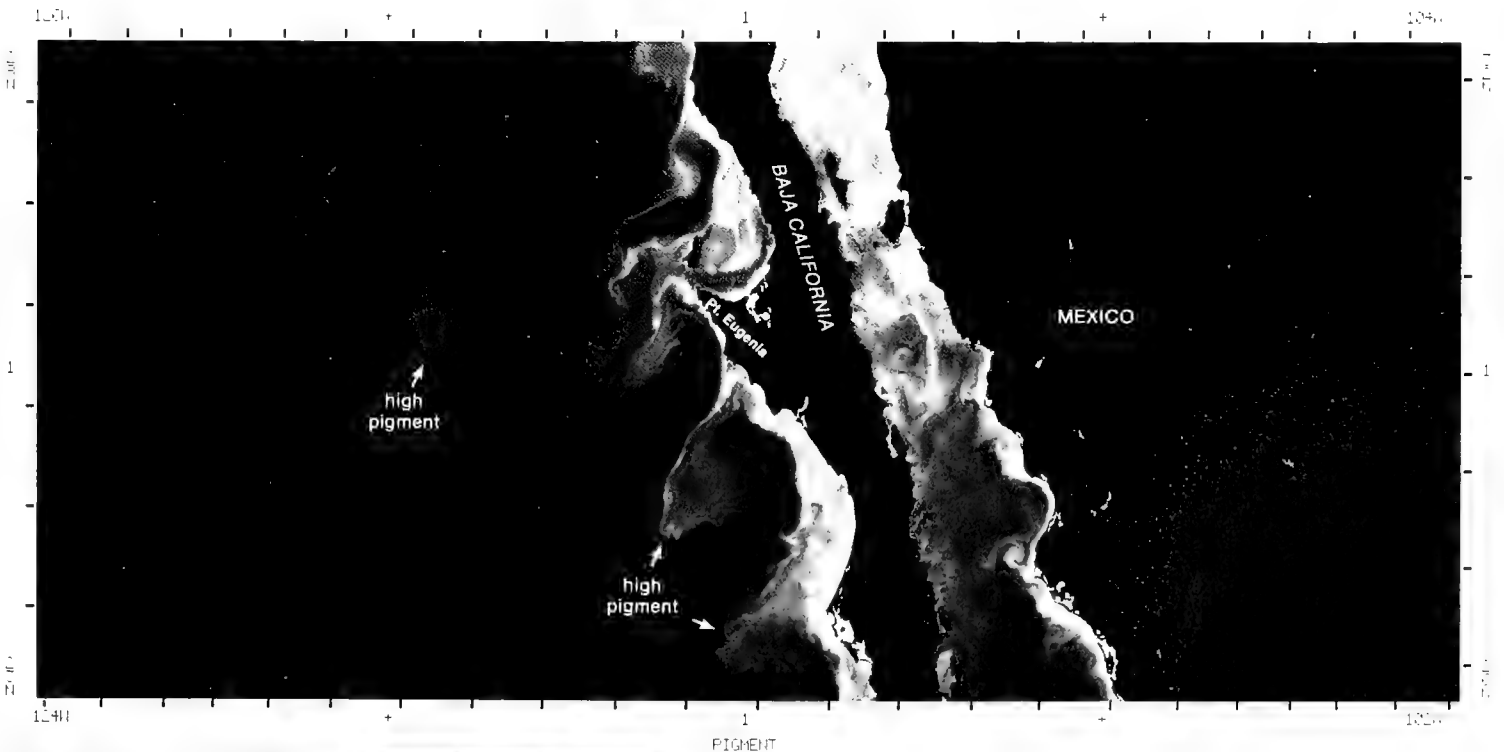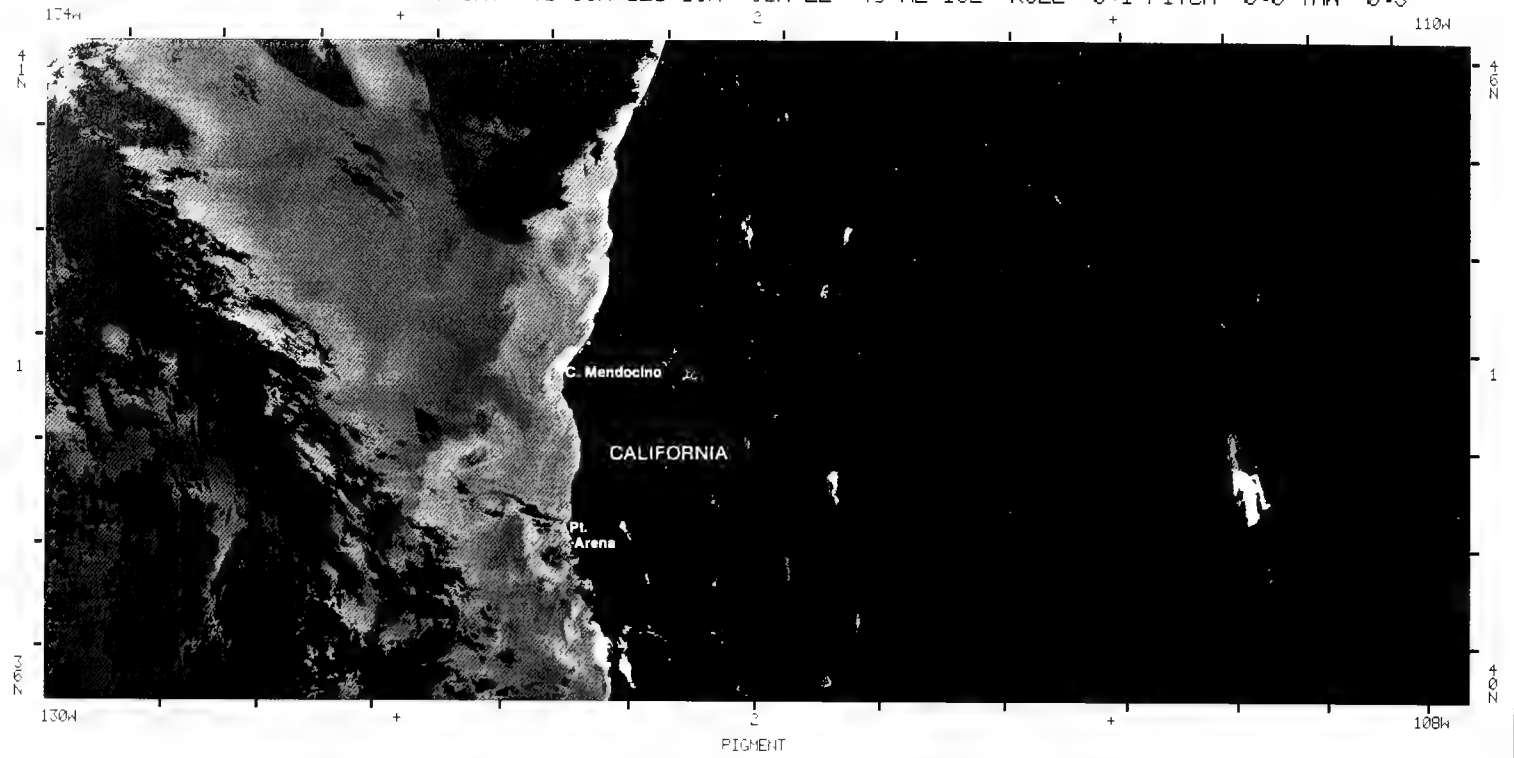
PIGMENT

ALGORITHMS: 01 00 00 00 00 02 01 00 00 00
970 SCAN LINES PROCESSED *** SCAN LINES MISSING

CIP VER   CRT NO   DPS VER   SPEC· #   FRAME #
V810421   ZE49482-   V820208   F732040   ZG849404

18-1. Nimbus-7. Orbit 2081. 23 March 1979. CZCS Pigment Image.

ORBIT 03629 13JUL79 193103 TO 193303 GMT GAIN 1-4=1 THRESHOLD OFF TILT ANGLE 20·0
GRID CENTER DATA: 193203 GMT 3T·52N 122·26W SUN EL 72 AZ 147 ROLL 0·0 PITCH 0·2 YAW 0·3
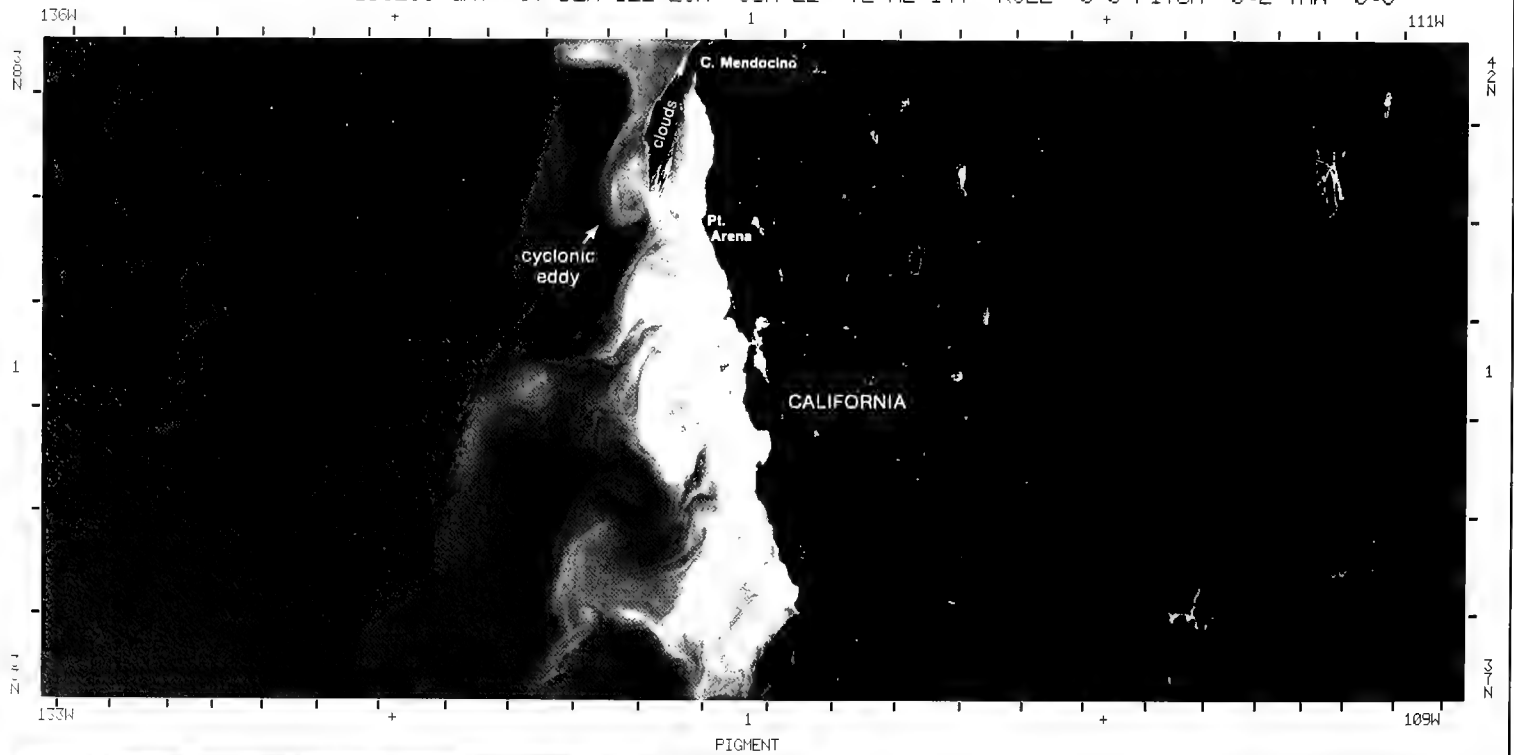
PIGMENT

PIGMENT IN MILLIGRAMS METERS**3
0   ·06   ·09   ·12   ·19   ·27   ·39   ·57   ·83   1·28   2·11   3·46   5·69   9·35   11·98   25·25   32·0
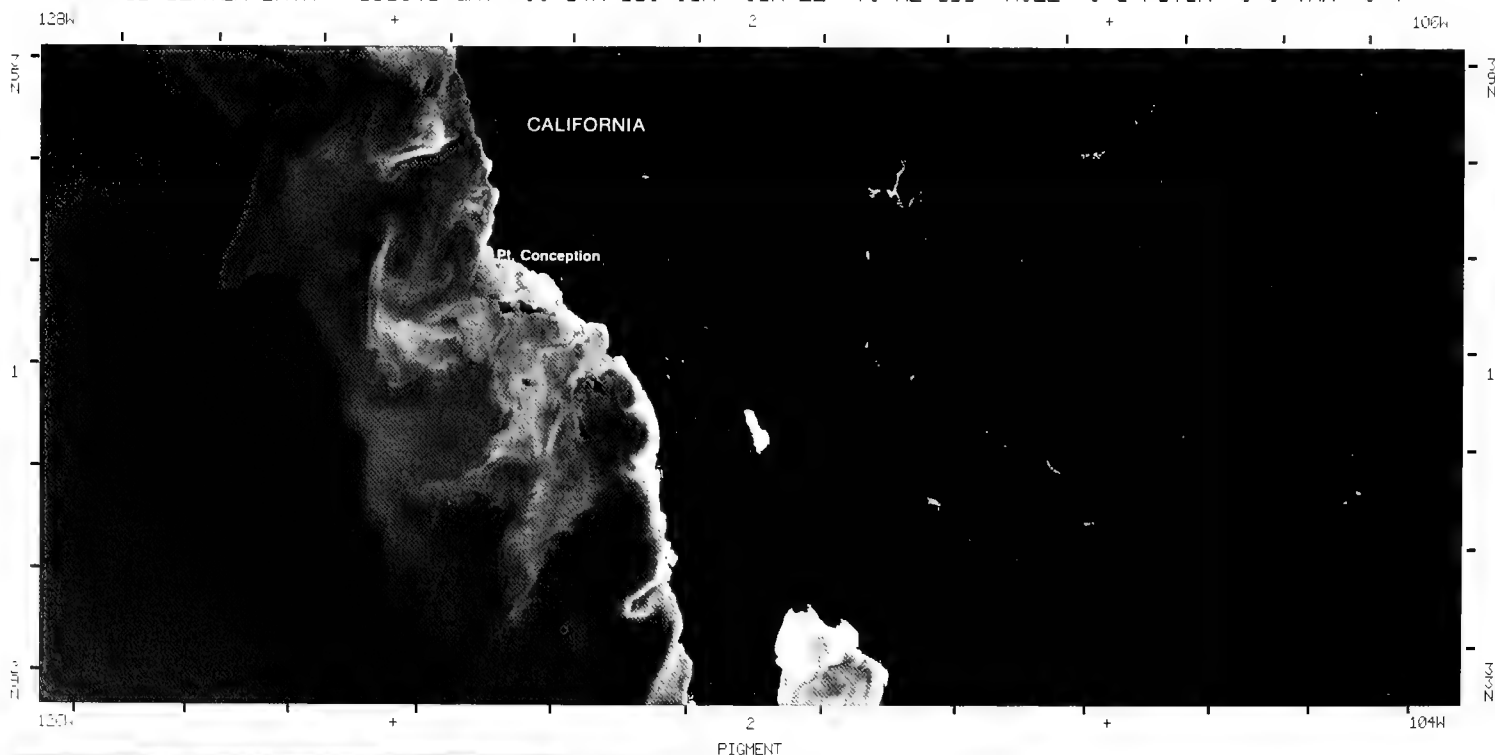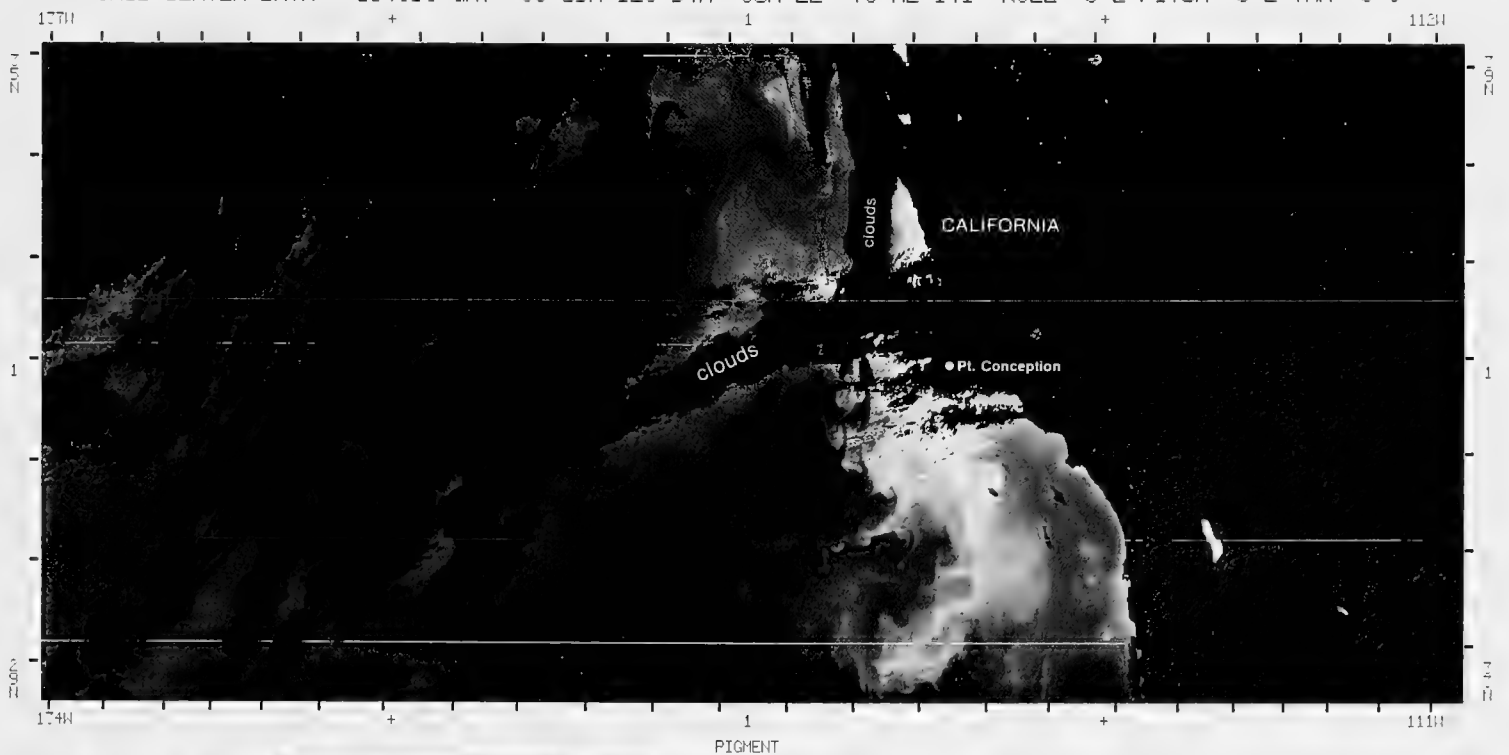
ALGORITHMS: 01 00 00 00 00 02 01 00 00 00
870 SCAN LINES PROCESSED   0 SCAN LINES MISSING

CIP VER   CRT NO   DPS VER   SPEC· #   FRAME #
V800710   ZE18801-   V820501   F732040   ZG018802A

18-2. Nimbus-7. Orbit 3629. 13 July 1979. CZCS Pigment Image.

ORBIT 02026   19MART9   195535 TO 195725 GMT   GAIN 1-4=2   THRESHOLD OFF   TILT ANGLE   0.0
GRID CENTER DATA: 195535 GMT   45.64N 170.88W   SUN EL   42 AZ 151   ROLL   0.0 PITCH -0.1 YAW 0.4
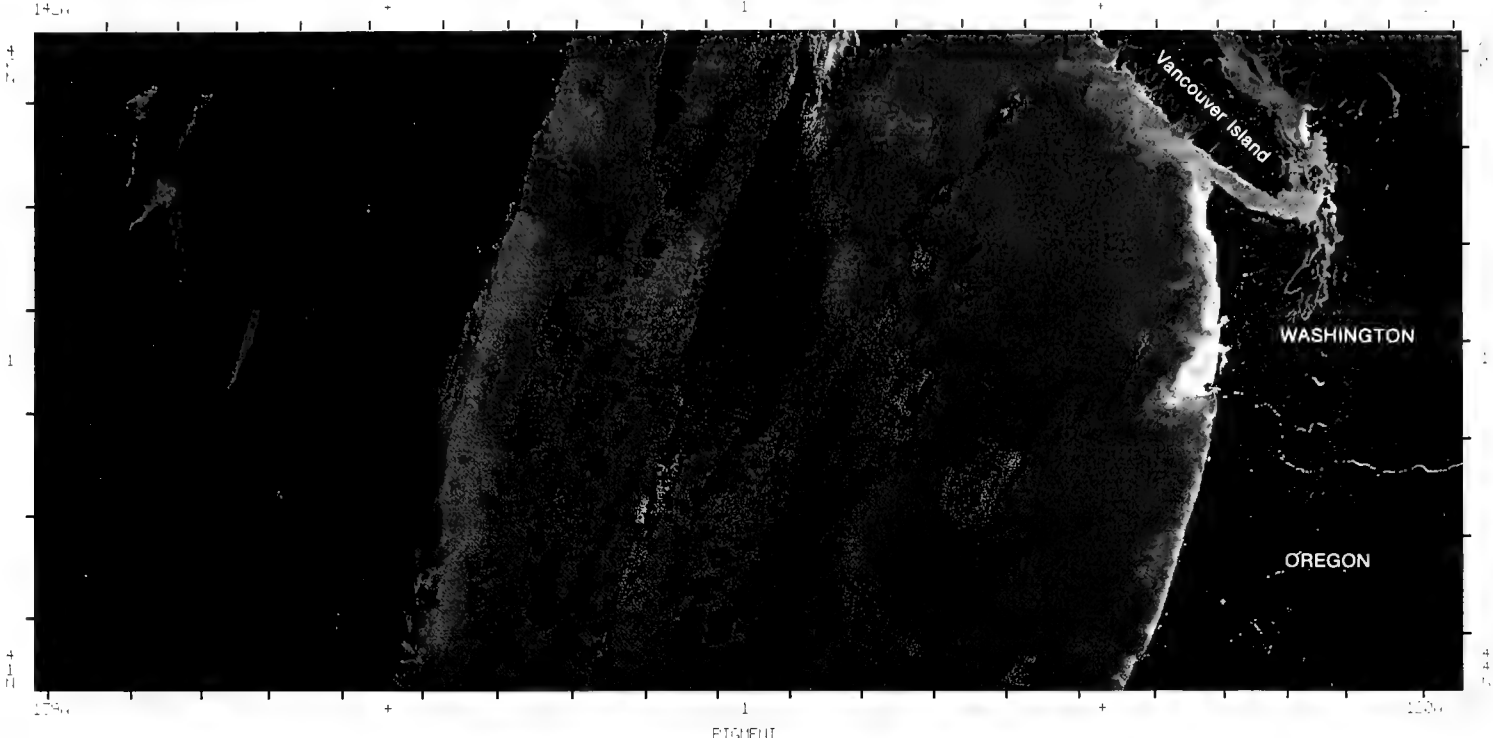
ALGORITHMS: 01 00 00 00 00 00 02 01 00 00 00   CIP VER   CPT NO   DPS VER   SPEC. #   FRAME #
970 SCAN LINES PROCESSED   0 SCAN LINES MISSING   V810538   2E47481-   V820308   F772040   2G847407

19-1. Nimbus-7. Orbit 2026. 19 March 1979. CZCS Pigment Image.

ORBIT 03643   14JULT9   195717 TO 195513 GMT   GAIN 1-4=1   THRESHOLD OFF   TILT ANGLE   20.0
GRID CENTER DATA: 195417 GMT   48.65N 171.33W   SUN EL   61 AZ 153   ROLL -0.3 PITCH 0.1 YAW 0.7
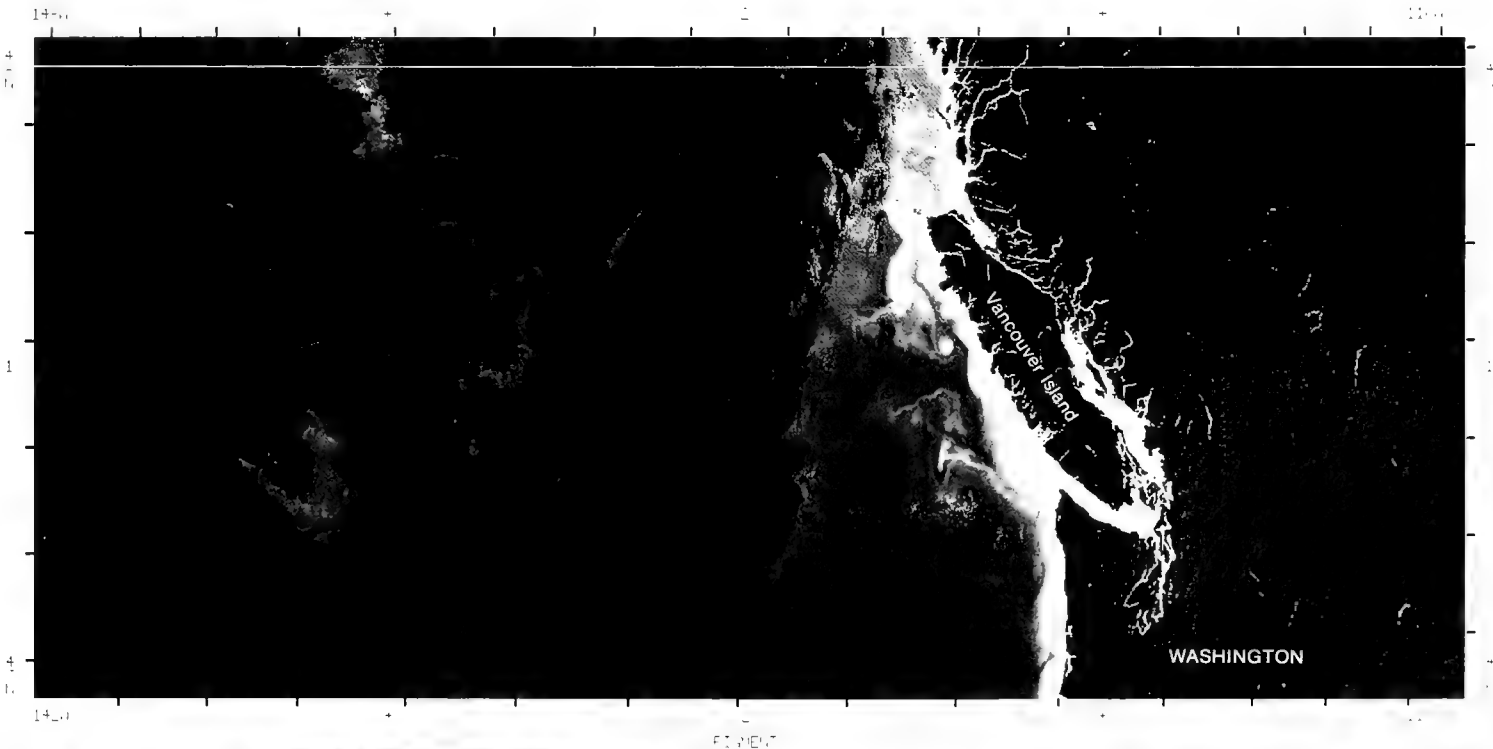
PIGMENT IN MILLIGRAM-METER-**3

ALGORITHMS: 01 00 00 00 00 00 02 01 00 00 00   CIP VER   CPT NO   DPS VER   SPEC. #   FRAME #
969 SCAN LINES PROCESSED   0 SCAN LINES MISSING   V   2E334808   V810501   F772040   2G334804

19-2. Nimbus-7. Orbit 3643. 14 July 1979. CZCS Pigment Image.

19

2B   Vancouver Island

James F. R. Gower

and

Ken L. Denman

Institute of Ocean Sciences
Sidney, B.C., Canada

The prevailing northwest wind that blows along the Canadian west coast in the summer months causes upwelling of nutrient-rich water onto the continental shelf off Vancouver Island. The resulting primary production leads to high chlorophyll pigment levels in surface water near the coast. This productivity is important to the local fisheries, especially the commercially valuable salmon industry. The pigment-rich water also traces out dynamic patterns of surface flow, particularly those that result in movement of shelf water offshore to deeper water.

Persistent cloud cover seriously hinders regular monitoring of the Vancouver Island region, but occasional cloud-free images show the variety of features that occur. The CZCS image on 14 July (22-2) shows the waters around Vancouver Island, B.C., Canada, on a clear day during the summer period when coastal upwelling leads to high productivity on the continental shelf. This image is remarkable in the clarity with which the resulting pigmented water has traced out interesting features of the coastal dynamics. The locator map (22-1) provides ocean features and bottom contours at 200- and 2,000-m depths for comparison. It should be noted that most of the features visible in the image have very low temperature contrast with the surrounding water, so that thermal infrared images will often not record them.

The waters on the continental shelf and in the straits of Georgia and Juan de Fuca show high pigment levels (>5 mg m^{-3}), although apparent values in the image will be increased by silt from coastal runoff. This increase is especially evident at the mouth of the Fraser River (see enlargement, 23-1), whose plume can be faintly seen in the image. Isolated brighter areas in Queen Charlotte Sound, north of Vancouver Island, correspond roughly to the positions of shoals **S**. The fresher surface water from this sound flows southward **F** down the west coast of Vancouver Island where it is entrained in the cyclonic eddy **E1**. CZCS imagery for the next two days (not shown) indicate that the eddy remained stationary (<3 km translational motion per day) while rotational velocities of 20 km day^{-1} (20 cm s^{-1}) are implied by displacement of surface features. The apparent center of the eddy is located at 49°32'±1' N and 127°33'±2' W. The diameter of the eddy is about 20 km, but counterclockwise rotation can be seen over an area at least twice this large. Thomson (1984) has studied an eddy at this same location that was observed in September 1980 in hydrographic data, but which was not present in July of that year. He suggests that the position of the eddy is ultimately related to bottom topography, and that its formation is triggered by baroclinic instability due to the vertical shear between the opposing southward surface flow and the northward subsurface flow in the California Undercurrent along the continental slope. In the present case, the eddy may have formed from the horizontal shear between the temporary northward flow of shelf water, caused by the strong wind reversal that occurred a few days earlier, and the southward flow further offshore.

The increasing width of the band of pigmented water (>2 mg m^{-3}) to the southeast of this eddy corresponds to the widening continental shelf (see 200-m contour, 23-1). Presence of a second eddy **E2** (23-1), on the shelf off the mouth of the Strait of Juan de Fuca, can be traced by the motion of features between successive days. This eddy appears to be a regular feature of the summer circulation (Freeland and Denman, 1982). At its center, water is brought up to the surface from the California Undercurrent through a branch of the Juan de Fuca Canyon.

A clearly visible hammerhead feature **H** is moving to the west at about 20 km day^{-1}. The length of the head of this feature is increasing at a rate that, on 14 July, implies an age of about five days. Its starting location, at the edge of the continental shelf near the boundary of the eddy **E2**, has a similar pigment concentration. The narrow trail of high-pigment water to the east of this feature appears to trace out its path over this time period, although rotation of the eddy **E2** has moved this trail to the south and lengthened it.

The starting date of 9 July deduced for the feature **H** corresponds to a
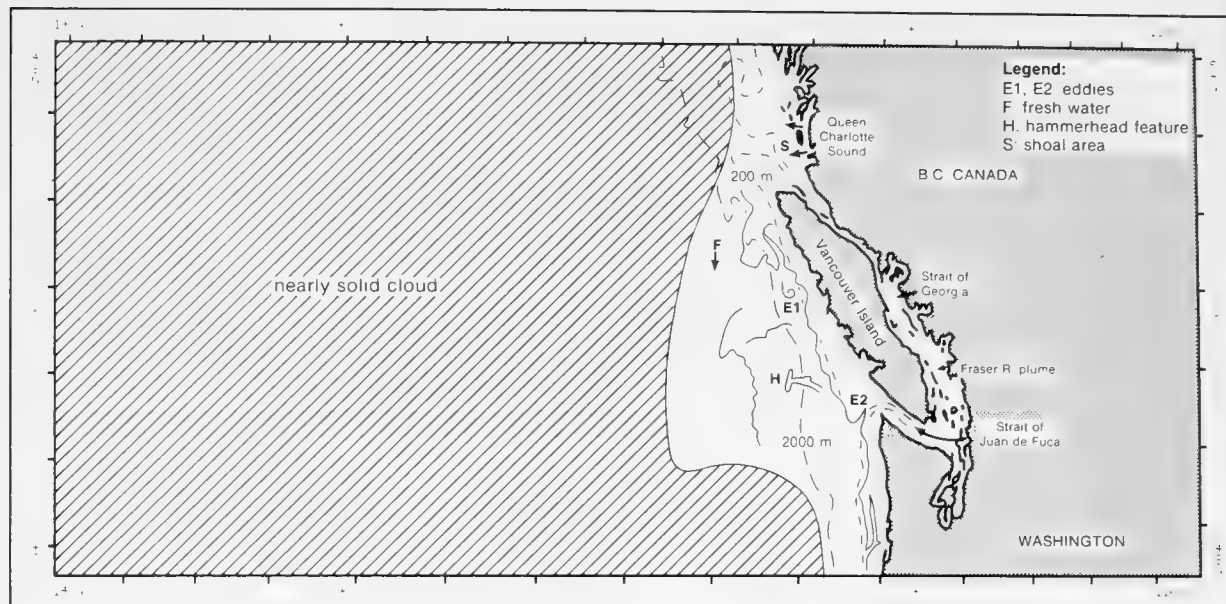
22-1. Locator Map for 22-2 and 23-1.
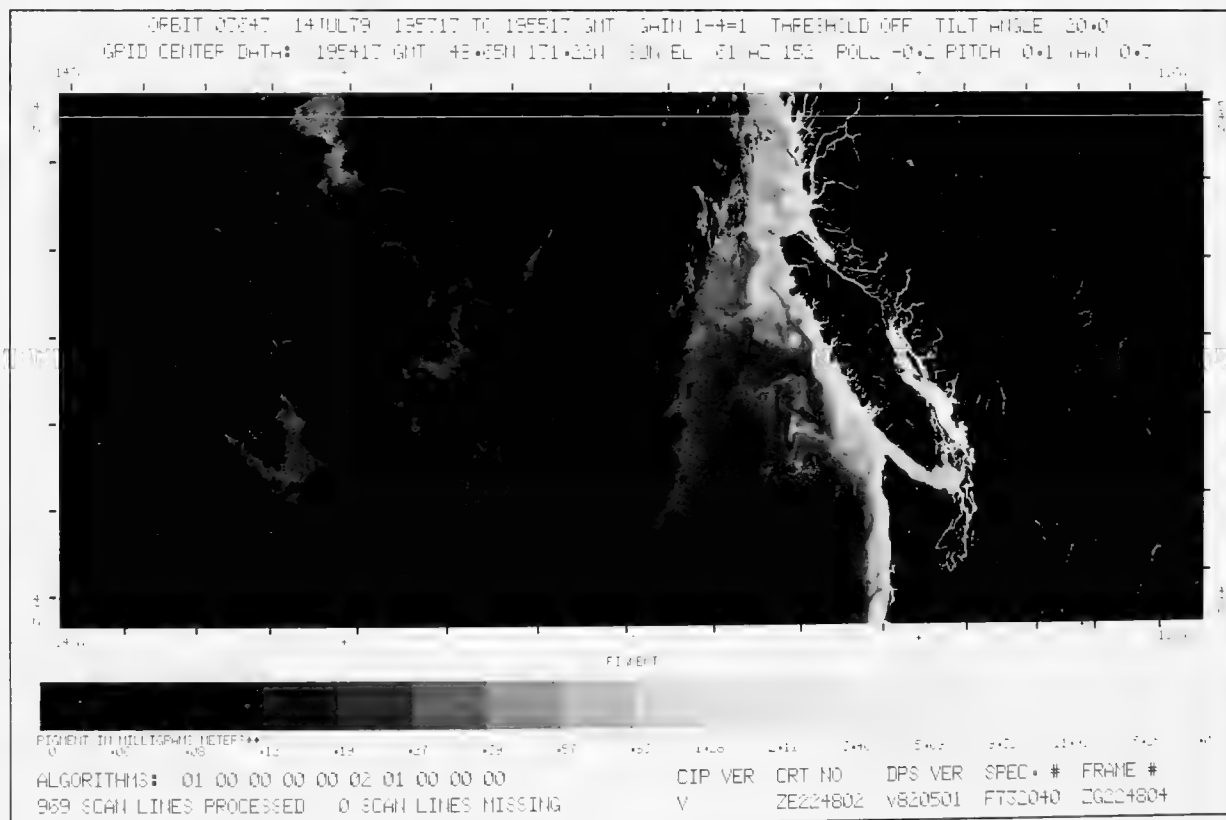
22-2. Nimbus-7. Orbit 3643. 14 July 1979. CZCS Pigment Image.

strong break in the northwest wind regime in which the coastal upwelling, which had continued since April, was briefly replaced by downwelling. It seems probable that the launch of this feature to the west may be related to this wind event.

Other fainter features are visible further offshore in the clearer, less pigmented water. Velocities here are 8–10 km day^{-1} to the southwest.

The areas of high chlorophyll pigments (light tones in 23-1) indicate areas of high summer planktonic production which imply potential food sources for young salmon. These salmon are known to feed in the area during summer months on their journey to the open ocean where they spend their adult life. The areas adjacent to the eddy **E2** also support a large adult salmon fishing industry. The information on surface dynamics is extremely valuable in showing the water movements which cause and modify the distribution of these food sources. This example demonstrates how the CZCS imagery can provide this information where the absence of strong temperature contrasts makes infrared imagery of little value.

References
Freeland, H. J., and K. L. Denman, 1982: A topographically-controlled upwelling center off Vancouver Island. *J. Marine Res.*, **40**, 1069–1093.
Thomson, R. E., 1984: A cyclonic eddy over the continental margin of Vancouver Island: Evidence for dynamic instability. Submitted to the *J. Phys. Oceanogr*.
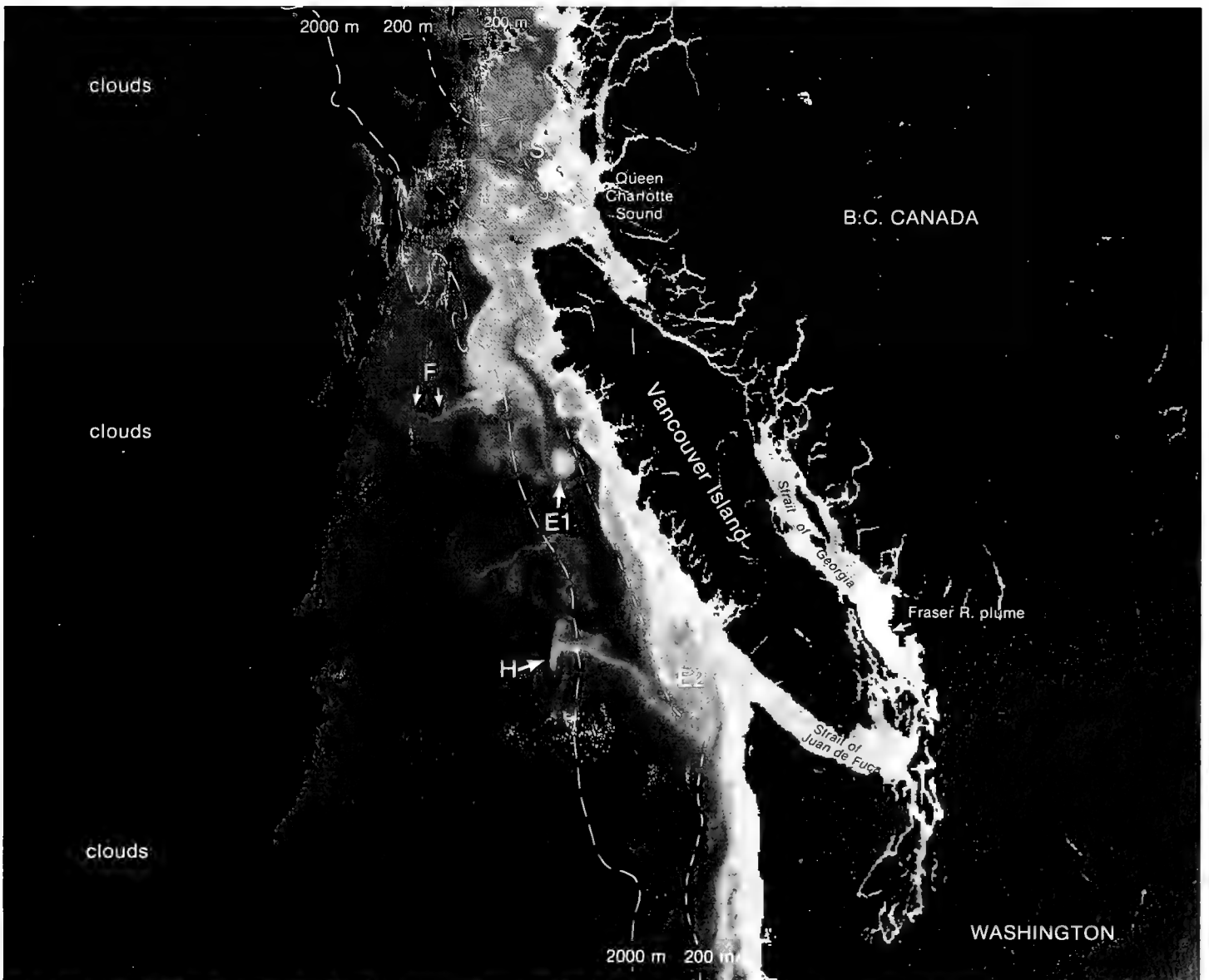
23-1. Enlarged View. Nimbus-7. Orbit 3643. 14 July 1979. CZCS Pigment Image with depth contours.

2C Northern California/Cape Mendocino

Mark R. Abbott

Jet Propulsion Laboratory
California Institute of Technology
Pasadena, California
and
Scripps Institution of Oceanography
University of California, San Diego
La Jolla, California

The California Current System was originally thought to be a broad, slow-moving, southward current. However, it is apparent from CZCS imagery that this idea is far too simple. Rather, the California Current is more like a series of eddies and jets with a net southward drift. The jets themselves are interesting features in that they are associated with the larger promontories in the coastline. Velocities in these jets range from 50 to 100 cm s^{-1}, and they often extend several hundred kilometers away from the coast. Thus, the jets could be an efficient mechanism for the exchange of high chlorophyll productive nearshore waters with poorer productive offshore waters.

The California Current—
A Comparison of False-Color CZCS Pigment
and Thermal Infrared Imagery
July 1981

The CZCS image (27-1) and AVHRR image (27-2) were obtained on 7 July and 8 July, respectively. These images of the West Coast were made during the presence of an unusually strong high pressure center in the Pacific Northwest coupled with a low pressure center off the coast of southern California. The result was strong northerly winds along the coast with sustained speeds of 15 m s^{-1} near Cape Mendocino.

The images reveal several features typical of eastern boundary currents. Such currents are typically areas of high productivity and, hence, high biomass. They are also areas of upwelling, although there is some question as to whether this is classic wind-driven coastal upwelling or a larger scale process forced by the curl of the wind stress.

The near-time coincidence of these images reveals significant large-scale similarities between near-surface pigment (27-1) and sea surface temperature distributions (27-2). In general, colder water is associated with higher pigment concentrations, although one can detect numerous areas that differ from this. For example, a comparison of the two images indicates that the upwelling areas near Cape Mendocino have very low temperatures and low pigment concentrations. This is consistent with the combination of upwelling of very deep, clear water to the surface and the delay time in the phytoplankton response to this nutrient-rich water.

Finally, the CZCS pigment image (27-1) shows some of the limitations of the current CZCS algorithms. In particular, some of the high pigment concentrations near San Francisco Bay and near the mouth of the Columbia River are a result of high sediment concentrations, not phytoplankton concentrations.

NIMBUS-7 CZCS PIGMENT CONCENTRATION
07 JULY 1981 1927 GMT

VANCOUVER
SEATTLE
COLUMBIA R.
PORTLAND
C. BLANCO
C. MENDOCINO
PT. ARENA
SAN FRANCISCO
MONTEREY
PT. CONCEPTION
L.A.
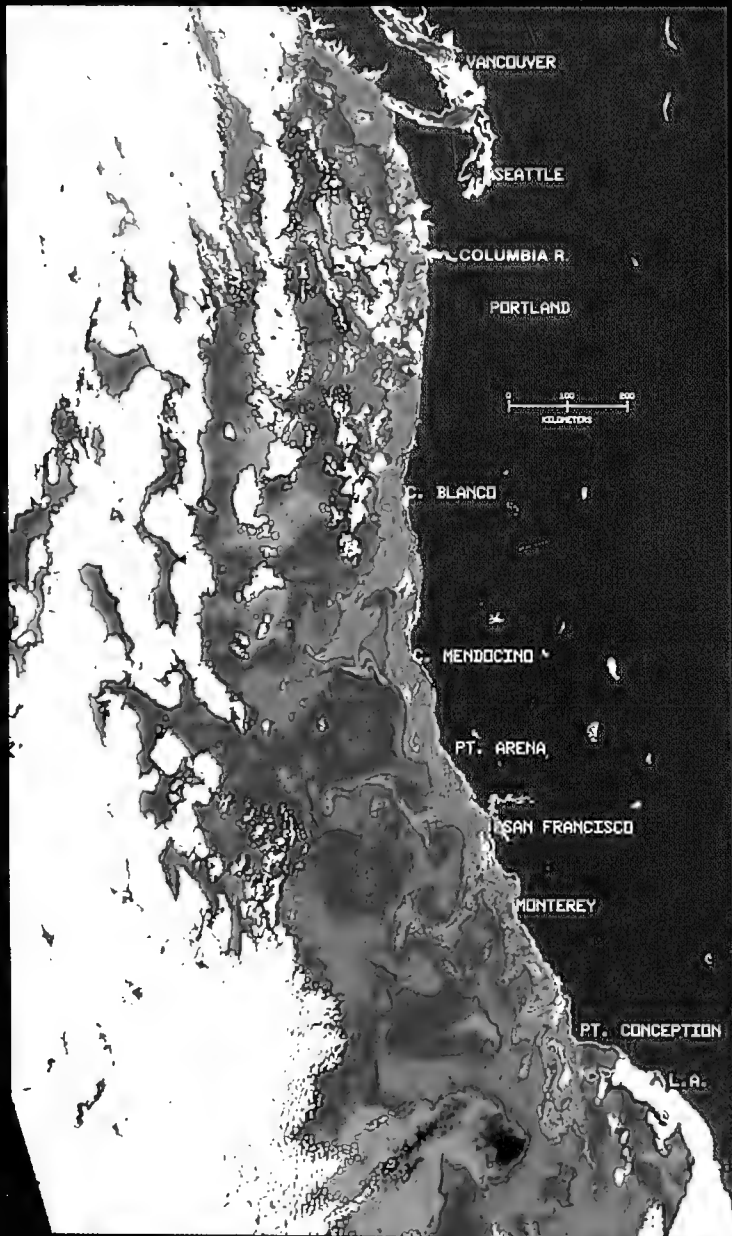
LOG₁₀ PIGMENT (MG/M3)

-1.0   -0.5   0.0   0.5   1.0

27-1. Nimbus-7. Orbit 1348. 7 July 1981.
CZCS False-Color Pigment Image.

NOAA-6 AVHRR SEA SURFACE TEMPERATURE
08 JULY 1981 0316 GMT

SEATTLE
COLUMBIA R.
PORTLAND
C. BLANCO
C. MENDOCINO
PT. ARENA
SAN FRANCISCO
MONTEREY
PT. CONCEPTION
L.A.
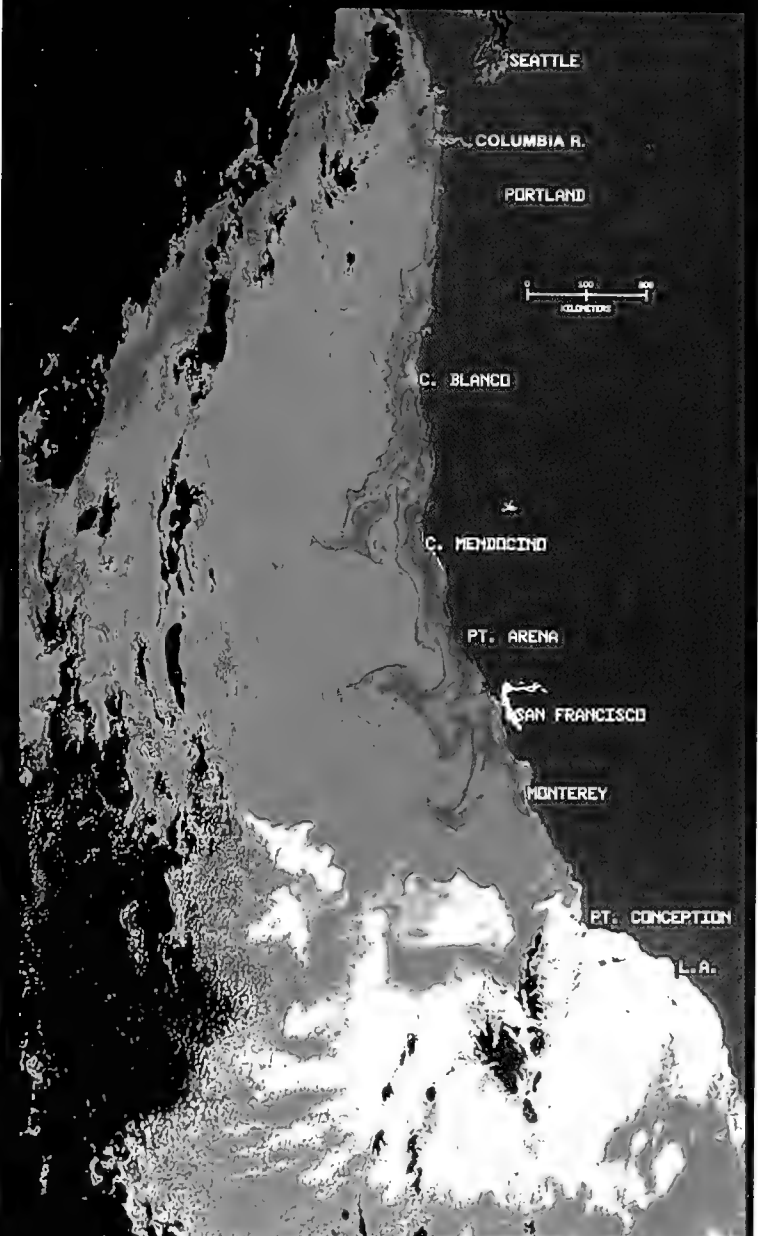
SEA SURFACE TEMPERATURE (°C)

7.5   9.0   10.5   12.0   13.5   15.0

27-2. NOAA-6. AVHRR. 8 July 1981.
False-Color Sea Surface Temperature Image.

27

2D Central California/Monterey Bay

Robert C. Wrigley
Ames Research Center/NASA
Moffett Field, California
and
William W. Broenkow
Moss Landing Marine Laboratory
Moss Landing, California

The California Current is an eastern boundary current characterized by half-knot southerly drift, punctuated by mesoscale eddies and coastal jets. Coastal upwelling occurs along the central California coast, usually during the spring and summer (March through July) due to Ekman divergence caused by persistent northwesterly winds. A transition period (August through October) of weaker winds marks the end of the strongest coastal upwelling. Between November and February the occurrence of periodic southerly winds causes a surface convergence along the coast and promotes northerly surface flow within 50 km of shore (the Davidson Current or California Countercurrent).

The California Current Upwelling System
May, July, and September 1979

Three CZCS pigment images (30-1, 31-1, and 31-2) are shown for the California Current System between Cape Mendocino and San Diego. All three images show that highest pigment concentrations are confined to within 200 km of shore (about the distance from Pt. Reyes to Pt. Sur). This agrees with the observation that the main axis of the California Current lies about 300 km offshore along central California (Hickey, 1979). Although many of the eddies and meanders shown in these images are transient features of the California Current, a persistent cyclonic geostrophic eddy (E, 31-1) has been observed south of San Francisco (Broenkow and Smethie, 1978; Hickey, 1979). Apparent shoreward flow of lower pigment waters (L, streaks of darker tones) from the "San Francisco Eddy" is shown in the 13 July (31-1) and 6 September (31-2) images, and some indication of lower pigment waters (L, faint dark tones) intruding into Monterey Bay are shown in the 13 May image (30-1). The location of this eddy is apparently due to local change in the wind stress curl (Hickey, 1979) and perhaps to the abrupt bathymetric break at Monterey Bay (Broenkow and Smethie, 1978).

Coastal jets extending normal to the coastline are frequently observed in the California Current. A prominent jet (CJ1) in the 13 May image (30-1) may have resulted from counterrotating eddies as suggested by Mooers and Robinson (1984). A similar, but larger such feature (CJ2) is shown in the 6 September image (31-2) at about the same latitude, but further offshore. High pigment levels along the coast south of Pt. Conception in the 13 May image (30-1) seem to spawn several small (50 km) filaments (arrows) between Santa Cruz Island and San Diego. In addition, the large arcuate feature 150 km west of Pt. Conception in the image showed high radiances in the 443, 520, and 550 nm bands relative to surrounding waters. Viewed in false-color CZCS imagery (not shown) this feature appeared white, suggesting it was not caused entirely by phytoplankton absorption. Since the feature was not sampled from ships, its origin remains something of a mystery, but it is suspected to be due to Coccolithophorids, which are algae with calcium carbonate shells.
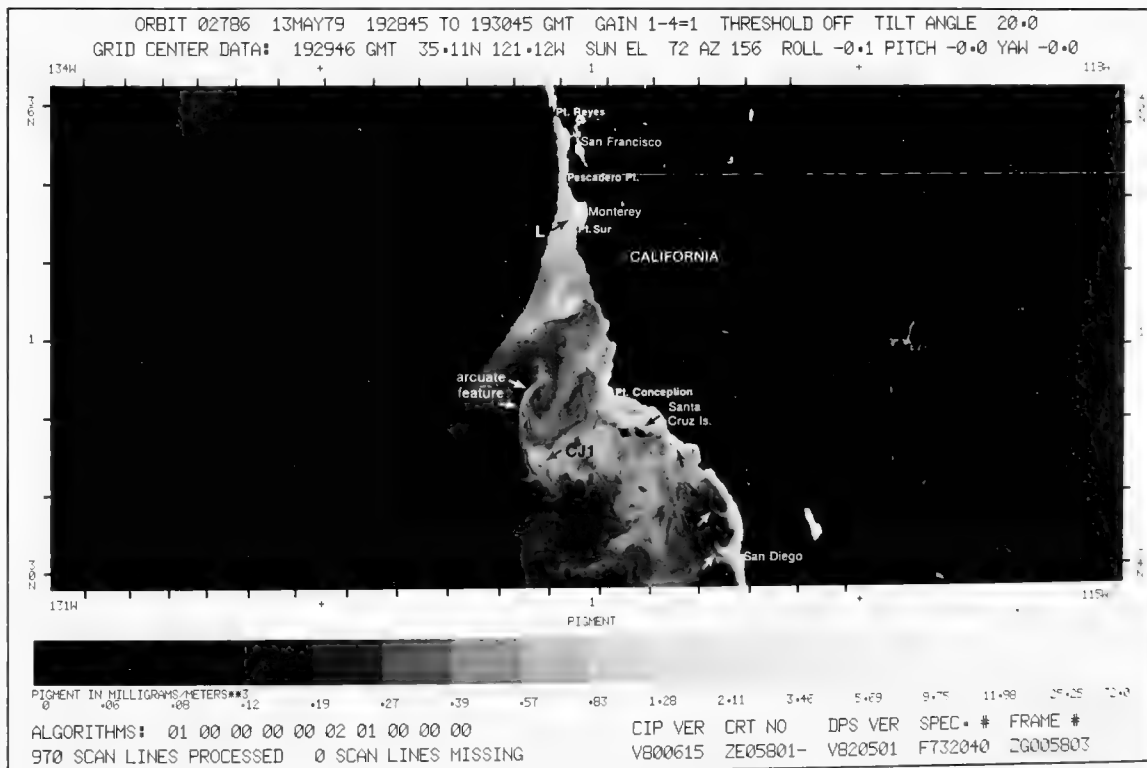
Several upwelling loci are found along the central California coast: the area from Cape Mendocino to Pt. Reyes, from Pescadero Pt. to Monterey Bay, and from the Big Sur coast south of Monterey Bay to Pt. Conception. The 13 May image (30-1) shows high pigment levels in coastal waters just north of Pt. Conception, an apparent lack of high-pigment waters along the Big Sur coast, and higher levels in and north of Monterey Bay. A ship station in the center of Monterey Bay on this date showed a chlorophyll concentration of 8.7 mg m^{-3}; a 2.5 mg m^{-3} chlorophyll concentration was measured in the pigment-poor tongue extending into the Bay. The 3×3 pixel averages of CZCS data at these locations showed 2.1 and 1.1 mg m^{-3}, respectively. The 13 July image (31-1) is partially obscured by clouds trailing southwest from Cape Mendocino where thermal infrared imagery (not shown) indicated coolest surface waters and intense upwelling. It is interesting that the CZCS data indicate that highest pigment concentrations were located 50 to 100 km offshore except along the Pt. Sur upwelling area. Incipient upwelling may occur with a rapid offshore transport of plankton-rich coastal waters which are replaced by cool, low-chlorophyll waters. As phytoplankton production proceeds, the waters warm and become colored.

Ship data at two stations in Monterey Bay just before satellite overpass on 13 July (31-1) indicated chlorophyll concentrations of 6.9 and 11.7 mg m^{-3}, respectively, both of which are indicative of highly productive water. CZCS data at these locations gave values of 2.4 and 4.5 mg m^{-3}, respectively. Wrigley and Klooster (1983) compared surface truth data

obtained by Moss Landing Marine Laboratories with the CZCS data and found that the CZCS values consistently underestimate pigment concentrations in the areas where pigment levels are greater than 3 mg m^{-3}. They attribute the discrepancy to excessive atmospheric correction caused by phytoplankton reflectance in the 670-nm band. The small black areas between San Francisco and Monterey Bays (31-1) and south of Big Sur (31-2) are image processing artifacts where the water-leaving radiances at 443, 520, and 550 nm were reduced to zero by the atmospheric correction algorithm. The condition, caused by pigment levels beyond the limits of the normal CZCS correction scheme, often occurs in images along the central California coast in the 443-nm band, but is rarely found in all three bands.

References

Broenkow, W. W., and W. M. Smethie, Jr., 1978: Surface circulation and replacement of water in Monterey Bay. *Estuarine and Coastal Marine Science*, 6, 583-603

Hickey, B. M., 1979: California Current System: Hypotheses and Facts. *Progress in Oceanography*, 8, 191-279

Mooers, C. N. K., and A. R. Robinson, 1984: Turbulent jets and eddies in the California Current and inferred cross-shore transport. *Science*, 223, 51-53

Wrigley, R. C., and S. A. Klooster, 1983: Coastal Zone Color Scanner data of rich coastal waters. In: Digest, International Geoscience and Remote Sensing Symposium, 31 August-2 September 1983, San Francisco, CA

30-1. Nimbus-7. Orbit 2786. 13 May 1979. CZCS Pigment Image.

2D Central California/Monterey Bay

Robert C. Wrigley
Ames Research Center/NASA
Moffett Field, California
and
William W. Broenkow
Moss Landing Marine Laboratory
Moss Landing, California

The California Current is an eastern boundary current characterized by half-knot southerly drift, punctuated by mesoscale eddies and coastal jets. Coastal upwelling occurs along the central California coast, usually during the spring and summer (March through July) due to Ekman divergence caused by persistent northwesterly winds. A transition period (August through October) of weaker winds marks the end of the strongest coastal upwelling. Between November and February the occurrence of periodic southerly winds causes a surface convergence along the coast and promotes northerly surface flow within 50 km of shore (the Davidson Current or California Countercurrent).

The California Current Upwelling System
May, July, and September 1979

Three CZCS pigment images (30-1, 31-1, and 31-2) are shown for the California Current System between Cape Mendocino and San Diego. All three images show that highest pigment concentrations are confined to within 200 km of shore (about the distance from Pt. Reyes to Pt. Sur). This agrees with the observation that the main axis of the California Current lies about 300 km offshore along central California (Hickey, 1979). Although many of the eddies and meanders shown in these images are transient features of the California Current, a persistent cyclonic geostrophic eddy (**E**, 31-1) has been observed south of San Francisco (Broenkow and Smethie, 1978; Hickey, 1979). Apparent shoreward flow of lower pigment waters (**L**, streaks of darker tones) from the "San Francisco Eddy" is shown in the 13 July (31-1) and 6 September (31-2) images, and some indication of lower pigment waters (**L**, faint dark tones) intruding into Monterey Bay are shown in the 13 May image (30-1). The location of this eddy is apparently due to local change in the wind stress curl (Hickey, 1979) and perhaps to the abrupt bathymetric break at Monterey Bay (Broenkow and Smethie, 1978).

Coastal jets extending normal to the coastline are frequently observed in the California Current. A prominent jet (**CJ1**) in the 13 May image (30-1) may have resulted from counterrotating eddies as suggested by Mooers and Robinson (1984). A similar, but larger such feature (**CJ2**) is shown in the 6 September image (31-2) at about the same latitude, but further offshore. High pigment levels along the coast south of Pt. Conception in the 13 May image (30-1) seem to spawn several small (50 km) filaments (arrows) between Santa Cruz Island and San Diego. In addition, the large arcuate feature 150 km west of Pt. Conception in the image showed high radiances in the 443, 520, and 550 nm bands relative to surrounding waters. Viewed in false-color CZCS imagery (not shown) this feature appeared white, suggesting it was not caused entirely by phytoplankton absorption. Since the feature was not sampled from ships, its origin remains something of a mystery, but it is suspected to be due to Coccolithophorids, which are algae with calcium carbonate shells.
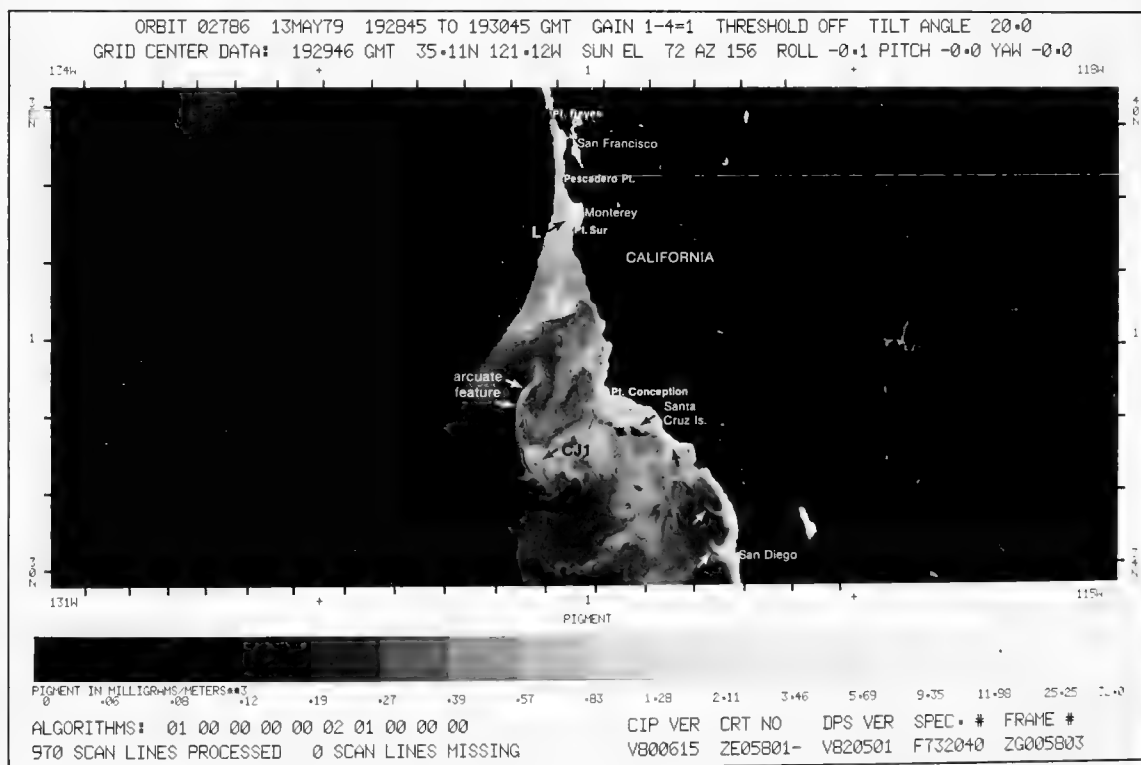
Several upwelling loci are found along the central California coast: the area from Cape Mendocino to Pt. Reyes, from Pescadero Pt. to Monterey Bay, and from the Big Sur coast south of Monterey Bay to Pt. Conception. The 13 May image (30-1) shows high pigment levels in coastal waters just north of Pt. Conception, an apparent lack of high-pigment waters along the Big Sur coast, and higher levels in and north of Monterey Bay. A ship station in the center of Monterey Bay on this date showed a chlorophyll concentration of 8.7 mg m^{-3}; a 2.5 mg m^{-3} chlorophyll concentration was measured in the pigment-poor tongue extending into the Bay. The 3×3 pixel averages of CZCS data at these locations showed 2.1 and 1.1 mg m^{-3}, respectively. The 13 July image (31-1) is partially obscured by clouds trailing southwest from Cape Mendocino where thermal infrared imagery (not shown) indicated coolest surface waters and intense upwelling. It is interesting that the CZCS data indicate that highest pigment concentrations were located 50 to 100 km offshore except along the Pt. Sur upwelling area. Incipient upwelling may occur with a rapid offshore transport of plankton-rich coastal waters which are replaced by cool, low-chlorophyll waters. As phytoplankton production proceeds, the waters warm and become colored.

Ship data at two stations in Monterey Bay just before satellite overpass on 13 July (31-1) indicated chlorophyll concentrations of 6.9 and 11.7 mg m^{-3}, respectively, both of which are indicative of highly productive water. CZCS data at these locations gave values of 2.4 and 4.5 mg m^{-3}, respectively. Wrigley and Klooster (1983) compared surface truth data

obtained by Moss Landing Marine Laboratories with the CZCS data and found that the CZCS values consistently underestimate pigment concentrations in the areas where pigment levels are greater than 3 mg m^{-3}. They attribute the discrepancy to excessive atmospheric correction caused by phytoplankton reflectance in the 670-nm band. The small black areas between San Francisco and Monterey Bays (31-1) and south of Big Sur (31-2) are image processing artifacts where the water-leaving radiances at 443, 520, and 550 nm were reduced to zero by the atmospheric correction algorithm. The condition, caused by pigment levels beyond the limits of the normal CZCS correction scheme, often occurs in images along the central California coast in the 443-nm band, but is rarely found in all three bands.

References

Broenkow, W. W., and W. M. Smethie, Jr., 1978: Surface circulation and replacement of water in Monterey Bay. *Estuarine and Coastal Marine Science*, **6**, 583–603.

Hickey, B. M., 1979: California Current System: Hypotheses and Facts. *Progress in Oceanography*, **8**, 191–279.

Mooers, C. N. K., and A. R. Robinson, 1984: Turbulent jets and eddies in the California Current and inferred cross-shore transport. *Science*, **223**, 51–53

Wrigley, R. C., and S. A. Klooster, 1983: Coastal Zone Color Scanner data of rich coastal waters. In: Digest, International Geoscience and Remote Sensing Symposium, 31 August–2 September 1983, San Francisco, CA

30-1. Nimbus-7. Orbit 2786. 13 May 1979. CZCS Pigment Image.

ORBIT 03629 13JUL79 193103 TO 193303 GMT GAIN 1-4=1 THRESHOLD OFF TILT ANGLE 20.0
GRID CENTER DATA: 193303 GMT 37.52N 122.26W SUN EL 72 AZ 147 ROLL 0.0 PITCH 0.2 YAW 0.3

ALGORITHMS: 01 00 00 00 00 02 01 00 00 00
970 SCAN LINES PROCESSED   0 SCAN LINES MISSING

CIP VER   CRT NO   DPS VER   SPEC. #   FRAME #
V800710   ZE18801- V820501   F732040   ZG018802A

31-1. Nimbus-7. Orbit 3629. 13 July 1979. CZCS Pigment Image.

ORBIT 04389 06SEP79 192805 TO 193005 GMT GAIN 1-4=1 THRESHOLD OFF TILT ANGLE 14.0
GRID CENTER DATA: 192906 GMT 35.80N 121.09W SUN EL 60 AZ 167 ROLL -0.0 PITCH 0.1 YAW 0.7
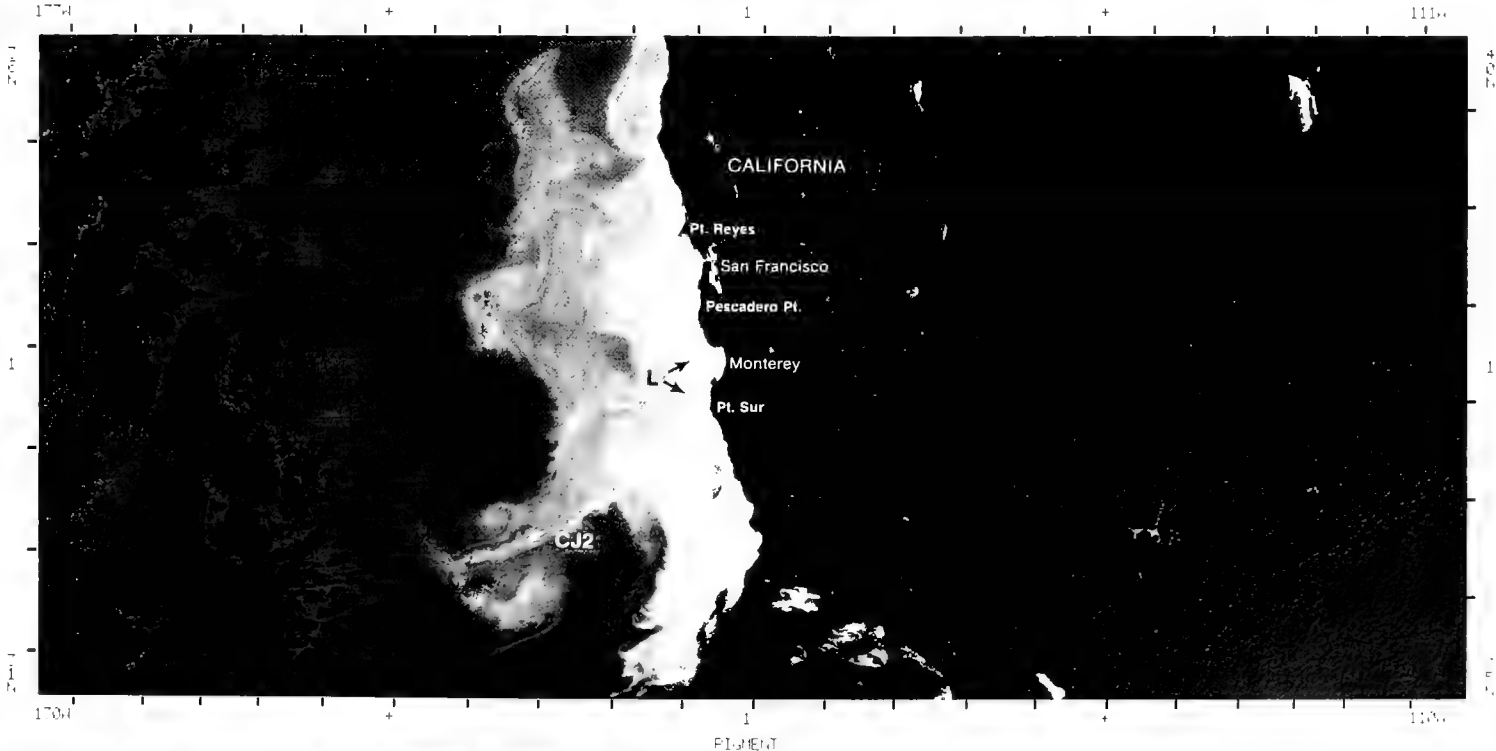
PIGMENT IN MILLIGRAM METERS**3

ALGORITHMS: 02 01 01 00 00 07 03 00 00 00
970 SCAN LINES PROCESSED   0 SCAN LINES MISSING

CIP VER   CPT NO   DPS VER   SPEC. #   FRAME #
V800710   ZE18901- V820821   F732040   ZG018903

31-2. Nimbus-7. Orbit 4389. 6 September 1979. CZCS Pigment Image.

Section 3

Atlantic North American Coast

3A   Carolina Capes/Sargasso Sea

Donald B. Olson

Rosenstiel School of Marine and Atmospheric Science
University of Miami
Miami, Florida

Five CZCS pigment images of the northwestern Sargasso Sea and the North American slope and shelf are described. The pigment field shows the rapid change in optical characteristics across the Gulf Stream. Mesoscale features dominate the interior of the major water mass provinces. A large warm-core ring appears as a low-pigment feature in the slope water, and a number of cold-core rings can be seen in the Sargasso Sea. These are regions with elevated pigment and are the centers of large-scale advective features. Portions of the shelf region are low in pigment in these particular images, in contrast to normal conditions. This, in comparison with other years, implies large interannual variability in the phytoplankton standing crops in these regions. Subscale plumes associated with capes are also seen along the Carolina coast.

The CZCS images cover the area from the Carolina capes out to the region between the Sargasso Sea and Scotian Shelf in a two-week period in the mid to late spring of 1979. Since many of the features in the pigment distributions are found in several of the images, the discussions included with each of the images are relevant to the others. A mercator projection depiction (35-1) identifies important features in the images in relation to various landmarks. The reader is encouraged to compare the images in order to obtain a better feeling for the temporal changes in the regions covered.
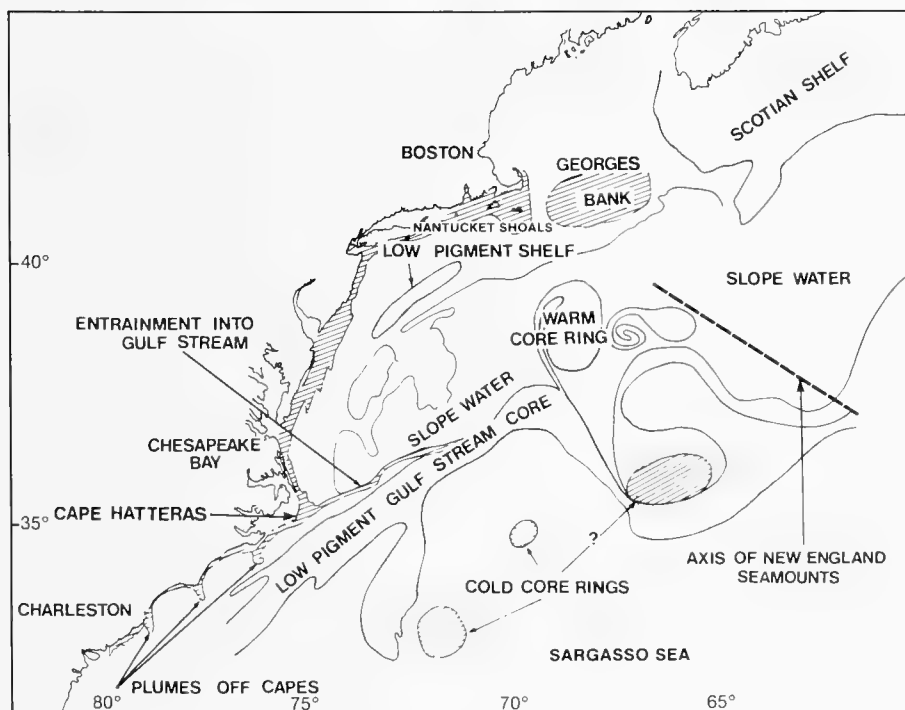
35-1. Mercator Projection Depiction. North Atlantic Coast Waters.

21 April

The CZCS pigment image (36-1) reveals a complex set of plumes (light tones nearly perpendicular to coastline) associated with the Carolina capes. These are superimposed upon a generally enhanced pigment concentration within 10 to 30 km of the coast. This concentration is the result of higher primary productivity caused by the introduction of nutrients by river runoff and vertical mixing due to tidal stresses in the shallow waters. The winds are also conducive to upwelling along this coast although this is probably of minor significance, except in summer and fall. The plumes associated with the capes might be explained as a combination of simple offshore advection of high pigment water and an upwelling response as the flow rounds the capes. Similar plumes are observed in many regions of the world in relation to equatorward flow around capes (Arthur, 1965; Brink *et al.*, 1983). The image also shows an entrainment of a filament (narrow, white-tone band) of inshore high-pigment water into the Gulf Stream at Cape Hatteras. This feature is about 10 km in width suggesting low cross-scale mixing along its nearly 300-km length. Entrainment of shelf water into the northern edge of the stream seems to be a common occurrence at Cape Hatteras. Features similar to this filament are reported by Ford and Miller (1952), and Fisher (1972), based on the presence of low salinity shelf water along the edge of the stream.

In addition, the image also contains a cold-core, cyclonic ring which seems to be advecting a streamer of low-chlorophyll fluid out of the Gulf Stream. The ring is manifest as a high-pigment region in the Sargasso Sea. The lowest pigment concentrations are not associated with the Sargasso waters around the ring in the image, but rather with the Gulf Stream core. A patch of this low-chlorophyll fluid appears to the west of the ring and may indicate the advection of waters by the cyclonic ring out of the stream core and into the Sargasso Sea.

2 May

The CZCS pigment image off the East Coast (37-1) gives a reasonable coverage of the Gulf Stream between Cape Hatteras and the New England Seamounts. In this image, the Gulf Stream appears as an abrupt reduction in pigment concentration (**A–B**) as one proceeds from north to south. As in the 21 April image (36-1), the stream core exhibits consistently lower values of pigment concentration compared to the slope water to the north and the Sargasso Sea to the south.

To the south, in the northern Sargasso Sea (37-1), there is an approximately 30-km area of high pigment. This small, nearly circular feature is probably associated with the core of a cyclonic ring. High chlorophyll concentrations in cold-core ring centers in fall and spring are described by Wiebe *et al.* (1976). They found carbon-14 measured productivity in a ring during spring to be nearly double that in the surrounding Sargasso Sea. This is attributed to enhanced nutrient levels as compared to the Sargasso Sea and higher light penetration than that found in the slope waters. The scale of the feature in this image is somewhat less than the radius of the velocity maximum in a typical cyclonic ring, suggesting that the high-pigment zone is associated with increased productivity in a small region near the ring center or on the edge of the ring in response to some asymmetry forced on the ring.

The structure of the meanders in the Gulf Stream and the warm-core rings in the North American slope water is discussed below in relationship to the images (37-2, 38-1, and 38-2). Structures of interest in this set of images include the complicated patterns present in the slope water as manifest north of the Gulf Stream meander, just downstream of Cape Hatteras (37-1). Further east there is a large, warm-core ring and a large (nearly 200 km), elongated filament of high-pigment water that appears to the south of the eddy in each of the images.

3 May

This East Coast CZCS pigment image (37-2) shows features similar to those along the Carolina capes (36-1) and Gulf Stream extension (37-1, 38-1, and 38-2). The higher pigment values associated with the capes (37-2) are apparent. Note that the large-scale meander pattern in the Gulf Stream is essentially the same as in the other images in this set. The details of the pattern to the east of the warm-core ring are worth further comment in relation to the time of this image and those on 7 and 8 May (38-1 and 38-2).

To the east of the warm-core ring (37-2) is a cyclonic (counterclockwise) hook or streamer of low-pigment water. This feature and its time evolution (38-1 and 38-2) suggest a cyclonic circulation of scale comparable to the ring. Features such as these may imply a pairing of vortices which may be of considerable importance to the dynamics of regions, which are characterized by strong non-linear eddies such as western boundary current extensions.

continued
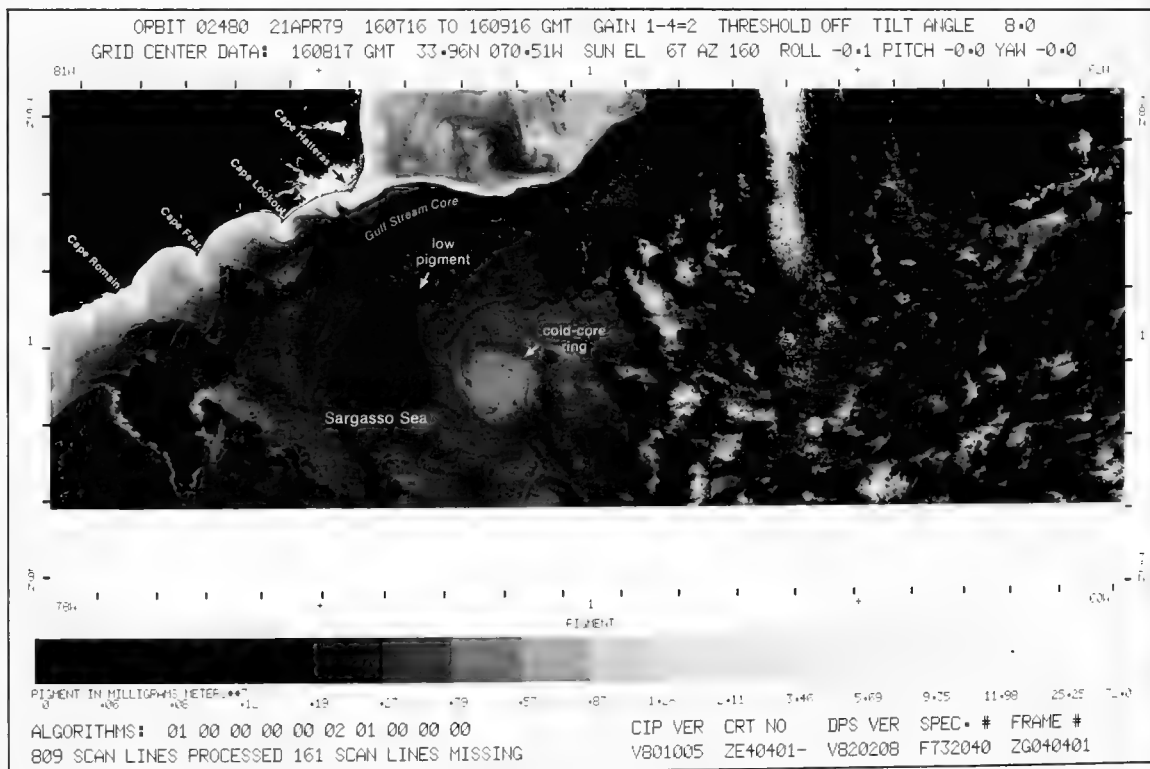
36-1. Nimbus-7. Orbit 2480. 21 April 1979. CZCS Pigment Image.

ORBIT 02632 02MAY79 160343 TO 160543 GMT GAIN 1-4=1 THRESHOLD OFF TILT ANGLE 18·0
GRID CENTER DATA: 160443 GMT 36·18N 070·13W SUN EL 68 AZ 159 ROLL 0·0 PITCH 0·1 YAW 0·5
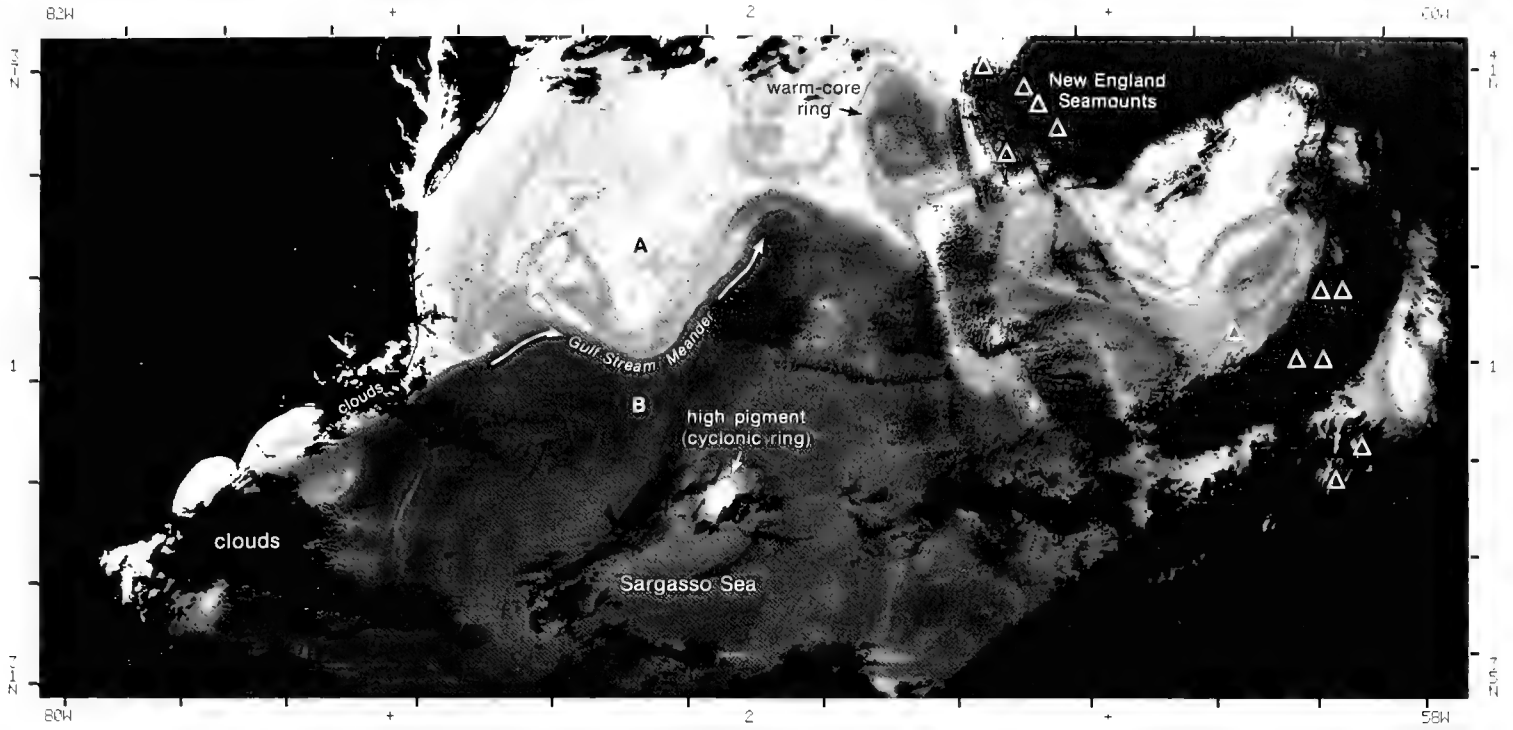
ALGORITHMS: 01 00 00 00 00 02 01 00 00 00
970 SCAN LINES PROCESSED   0 SCAN LINES MISSING

CIP VER CRT NO   DPS VER   SPEC· # FRAME #
V   ZE205971 V820401   F732040 ZG205971

37-1. Nimbus-7. Orbit 2632. 2 May 1979. CZCS Pigment Image.

ORBIT 02646 03MAY79 162242 TO 162442 GMT GAIN 1-4=1 THRESHOLD OFF TILT ANGLE 20·0
GRID CENTER DATA: 162342 GMT 37·65N 075·27W SUN EL 67 AZ 159 ROLL 0·1 PITCH -0·1 YAW 0·3

PIGMENT IN MILLIGRAMS/METERS**3
0   ·06   ·08   ·12   ·19   ·27   ·39   ·57   ·83   1·28   2·11   3·46   5·69   9·35   11·98   25·25
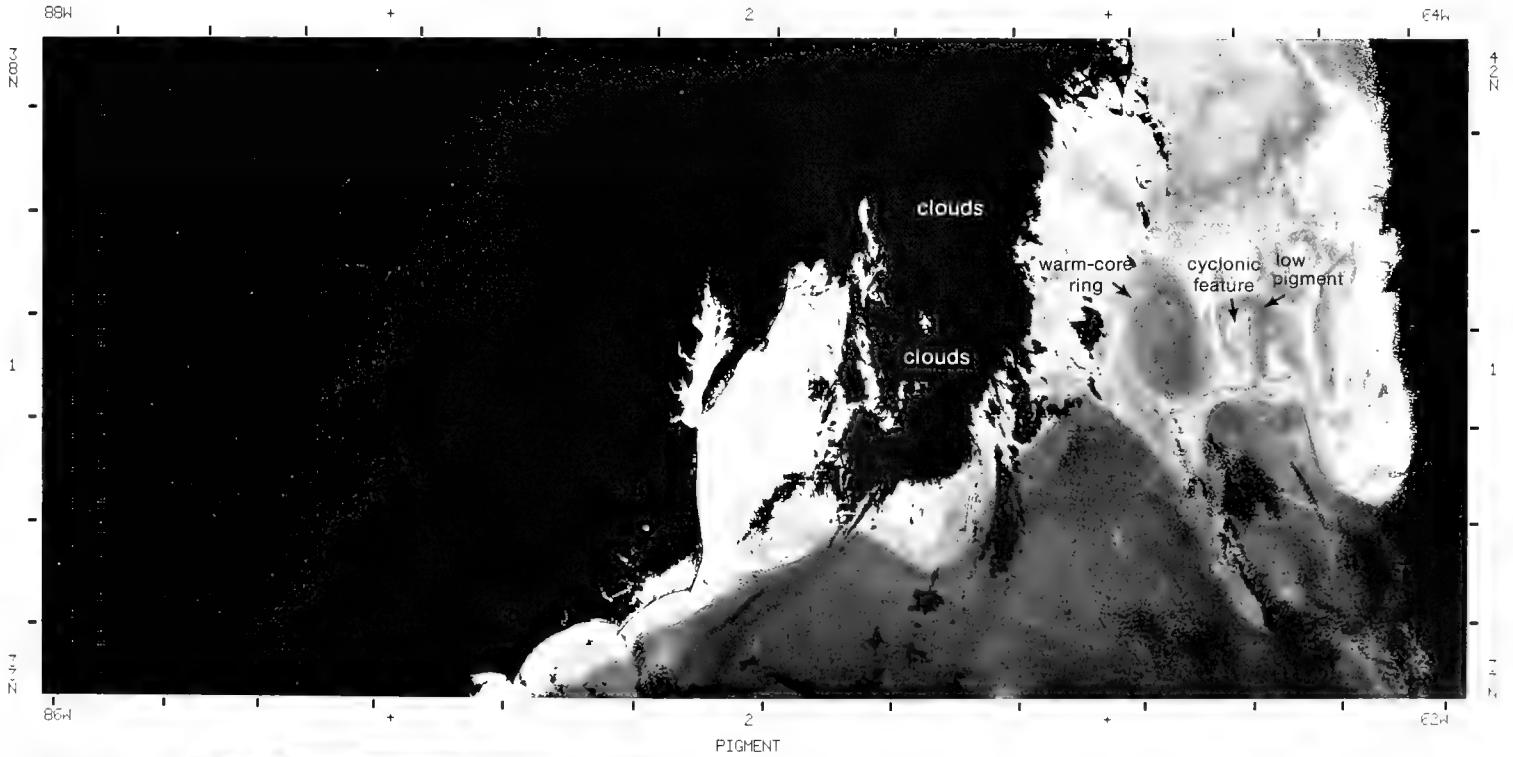
ALGORITHMS: 01 00 00 00 00 02 01 00 00 00
970 SCAN LINES PROCESSED   0 SCAN LINES MISSING

CIP VER CRT NO   DPS VER   SPEC· # FRAME #
V   ZE205981 V820401   F732040 ZG205981

37-2. Nimbus-7. Orbit 2646. 3 May 1979. CZCS Pigment Image.

7 May

The CZCS pigment image (38-1) shows the entire zonal extent of the North American slope water and the frontal zones which border it, between Cape Hatteras and Scotian Shelf. The slope water is the site of the largest horizontal pigment variability in the image, in keeping with the nature of transition zones. The contrast between the slope water and the Sargasso Sea is clearly visible. Meanders and rings viewed in the other images are also evident in this scene. The shelf front separating the slope water and the water on the continental shelf can be traced here as a sharp decrease in pigment as one proceeds into shallow water (depths <200 m).

Low pigment concentrations on the outer shelf in comparison to the slope waters are somewhat unexpected. The spring bloom on the mid to outer shelf in the Mid Atlantic Bight typically occurs in late March to early April (Walsh, 1983), while the inner shelf bloom is later, with the mean euphotic-zone chlorophyll peaking in mid-May. In the time period in question, the shelf should have a uniform pigment distribution from Walsh's (1983) curves. This is, in fact, the case for April and May 1982 (Evans, 1985). By June 1979, the shelf has nearly uniform pigments (not shown) as viewed from space (Gordon et al., 1982). The slope water also has lower pigment concentrations in these later images in 1979.

The appearance of low, near-surface pigment concentrations on the outer shelf (38-1) in comparison to the normal conditions (Walsh, 1983) suggests that there are strong interannual variations in the phytoplankton community on the North American shelf. This anomaly may just reflect a deeper or better mixed distribution of pigments in the vertical in 1979. It might also be a result of different offshore Ekman transports (Walsh, 1983) or perhaps an earlier reduction in phytoplankton by grazing.

The Scotian Shelf also shows very low pigment concentrations in this image. This may be a more common situation set up by the seasonal decrease in surface salinities in this region tied to the spring melt and increased fresh water output from the Gulf of St. Lawrence. Both Georges Bank and Nantucket Shoals appear as high-pigment areas. This is a consequence of tidal mixing in the shallow waters which leads these areas to have more than double the annual primary production of the upwelling zone off Oregon or at the Mid Atlantic Bight (Walsh, 1981).

The temporal variations in the area covered are largest in the slope water, which typically contains streamers of extremely low pigment fluid drawn in from the Sargasso Sea and high-chlorophyll waters from the shelf. In the image (38-1), the shelf is an apparent source of the low-pigment waters in the slope region, with the highest chlorophyll concentrations appearing in the slope water south of the Scotian Shelf. In contrast, a month and a half later in the June imagery (not shown), Gordon et al. (1982), show that this region has very low pigments, suggestive of a large flux of Sargasso Sea waters across the Gulf Stream downstream of the New England Seamounts between May and June. Much of this sort of entrainment of fluid into the slope water is tied to the presence of warm-core rings in the slope and large-amplitude meanders in the stream. These are discussed in relationship to the CZCS pigment image of 8 May.

8 May

The last CZCS pigment image in this group (38-2) covers the eastern portion of the slope water and gives the best coverage of the meandering of the Gulf Stream. A comparison of all the images shows that the large meanders in the stream evolve on a longer time scale than the two weeks covered here. In addition, a careful inspection of the images reveals small changes in the northern edge of the stream in connection with small-amplitude features over the period, but no major changes in the large
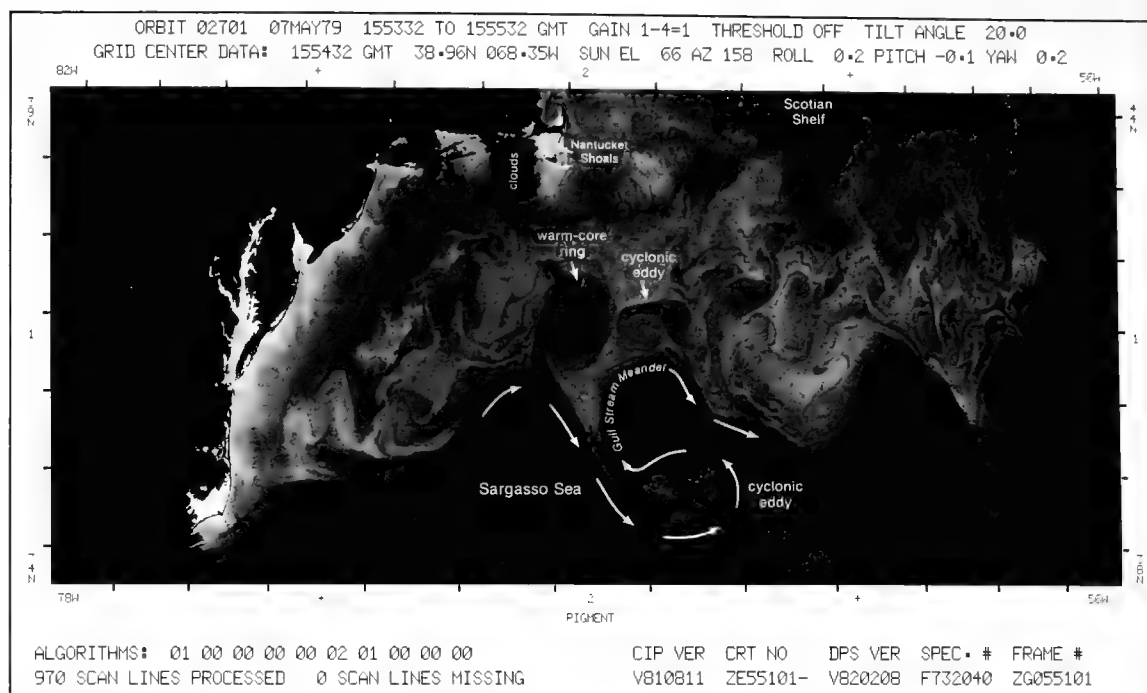
38-1. Nimbus-7. Orbit 2701. 7 May 1979. CZCS Pigment Image.
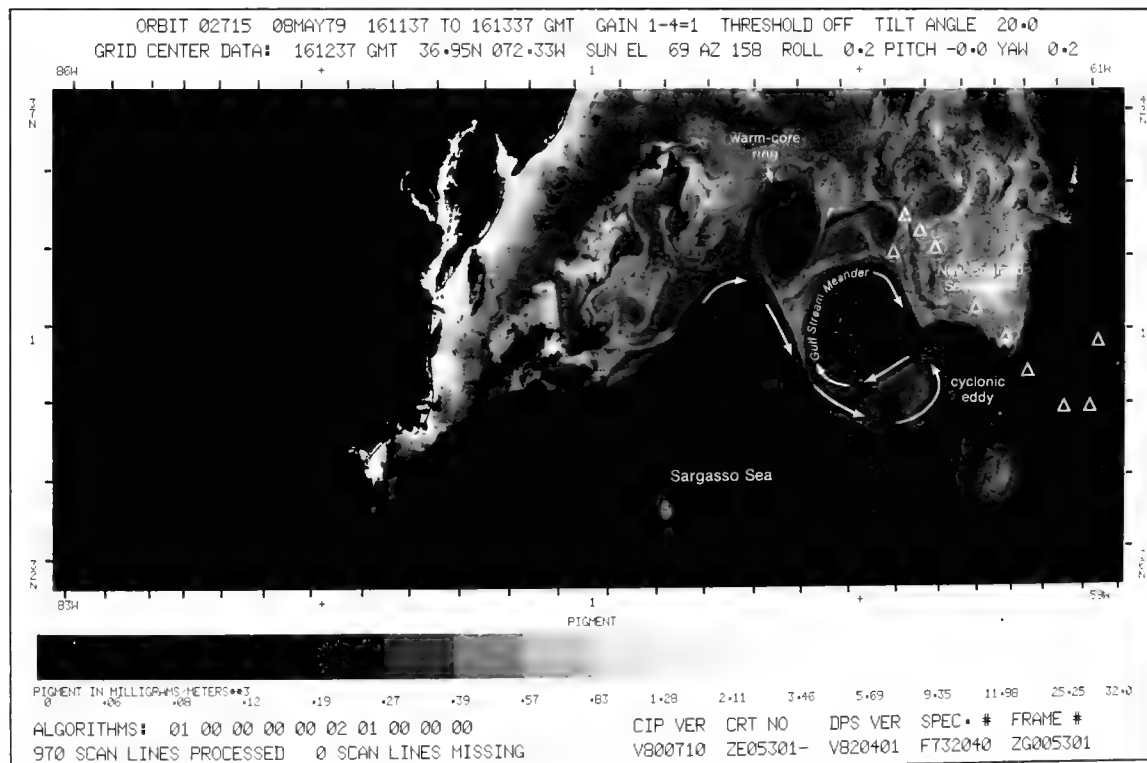
38-2. Nimbus-7. Orbit 2715. 8 May 1979. CZCS Pigment Image.

meander pattern centered around 69° W. In combination, the warm-core ring and the large cyclonic, meander/ring form a perturbation in the stream path of over 300 km. This pattern, with a high pressure cell (warm-core ring) to the poleward side of a mean jet and a cyclonic cell (cyclonic eddy) to the equatorward side of the jet, is similar to blocking patterns which are common in the atmospheric jet stream. These large, long-lived perturbations to the path of the Gulf Stream are just upstream of the New England Seamounts (open triangles). Again this is reminiscent of the atmospheric case in which blocking situations are often tied closely to topographic features. The presence of large meanders and flow down the axis of the seamounts, depicted in the schematic (35-1), is fairly common in the Gulf Stream (Richardson, 1981).

The meander pattern observed on this day (38-2) eventually broke down. The warm-core ring proceeded on to the west and was found at 69° W in June (Gordon *et al.*, 1982). It is not known whether or not the cyclonic portion of the pattern separated from the stream to form a ring. A full description of the events which took place in the slope water during 1979, based on thermal infrared data, can be found in Fitzgerald and Chamberlin (1981).

References
Arthur, R. S., 1965: On the calculation of vertical motion in eastern boundary currents from determinations of horizontal motion. *J. Geophys. Res.*, **70**, 2799–2803.

Brink, K. H., D. W. Stuart, and J. C. Van Leer, 1983: Observations of the coastal upwelling region near 34°30′ N off California: Spring 1981. Submitted to *J. Phys. Oceanogr.*

Evans, R. E., 1985: Personal Communication.

Fisher, A., Jr., 1972: Entrainment of shelf water by the Gulf Stream northeast of Cape Hatteras. *J. Geophys. Res.*, **77**, 3248–3255.

Fitzgerald, J., and J. L. Chamberlin, 1981: Anticyclonic warm-core Gulf Stream eddies off the northeastern United States during 1979. *Annales Biologiques*, **36**, 44–51.

Ford, W. L., and A. R. Miller, 1952: The surface layer of the Gulf Stream and adjacent waters, *J. Marine Res.*, **11**, 267–280.

Gordon, H. R., D. K. Clark, J. W. Brown, and R. E. Evans, 1982: Satellite measurement of the phytoplankton pigment concentration in the surface waters of a warm-core Gulf Stream ring. *J. Marine Res.*, **40**, 491–502.

Richardson, P. L., 1981: Gulf Stream trajectories measured with free-drifting buoys. *J. Phys. Oceanogr.*, **11**, 999–1010.

Walsh, J. J., 1981: Shelf-sea ecosystems. In *Analysis of Marine Ecosystems*, edited by A. R. Longhurst, Academic Press, New York, 159–196.

———, 1983: Death in the sea: Enigmatic phytoplankton losses. *Prog. Oceanogr.*, **12**, 1–86.

Wiebe, P. H., E. M. Hulburt, E. J. Carpenter, A. E. Jahn, G. P. Knapp III, S. H. Boyd, P. B. Ortner, and J. L. Cox, 1976: Gulf Stream cold-core rings: Large-scale interaction sites for open-ocean plankton communities. *Deep-Sea Res.*, **23**, 695–710.

3B   Cape Hatteras/Cape Cod

Charles S. Yentsch
Bigelow Laboratory of Ocean Sciences
West Boothbay Harbor, Maine

Mesoscale eddies are common features of the Gulf Stream System, especially in the region north of Cape Hatteras. These eddies or Gulf Stream rings, as they are often called, form from extensive meanders of the Gulf Stream System as a whole. Such meanders at times close, pinching off portions of the water masses on either side of the stream. The eddies approach being in geostrophic balance and continue to rotate in a manner not unlike the parent flow of the Gulf Stream. Eddies that become entrained in the slope waters contain a warm core of Sargasso Sea water and are referred to as warm-core rings, while eddies that reside in the Sargasso Sea contain a cold core of slope water and are designated cold-core rings.

Gulf Stream Eddies—Circulation Features
April 1979 and April 1982

CZCS pigment images for 21 April 1979 (42-1), and 24 April 1982 (42-2), show that both warm- and cold-core rings are defined in terms of ocean color which is traceable to the gradients in measured phytoplankton pigment (Gordon *et al.*, 1983). The gradients of pigment observed in these eddies is due to the fact that they are rotating, which influences the density field within the eddy. Nutrient-rich water is vertically mixed along the sloping isopycnals of the eddies. In the anticyclonic mode, the sea surface level, due to geostrophy, domes-up around the axis of a warm-core ring; while in a cyclonic mode, it is depressed around a cold-core ring. Therefore, in an anticyclonic eddy (warm-core ring) lighter, nutrient-poor water will accumulate at its center and heavier, nutrient-rich water will be swept to its rim. This distribution of nutrient-rich and -poor water dictates the pattern of phytoplankton distribution observed in the eddies. In the case of the warm-core ring (42-2) the higher concentrations of phytoplankton will be found at the outer rim of the eddy, whereas in the cold-core ring (42-1), the reverse will be true, with the central region containing most of the phytoplankton-rich water. The false-color CZCS pigment image (43-1) of the warm-core ring example (42-2), illustrates how dramatically these differences can be displayed by the color presentation.

In summary, the explanation for the observed distribution of phytoplankton pigments in rings argues that geostrophic principles apply to these rings. Associated with this is the idea that these are the forces of enrichment, thus the rotary motion induces nutrient transport along isopycnals and phytoplankton production occurs when these isopycnals intersect the euphotic layers of the ring water masses.
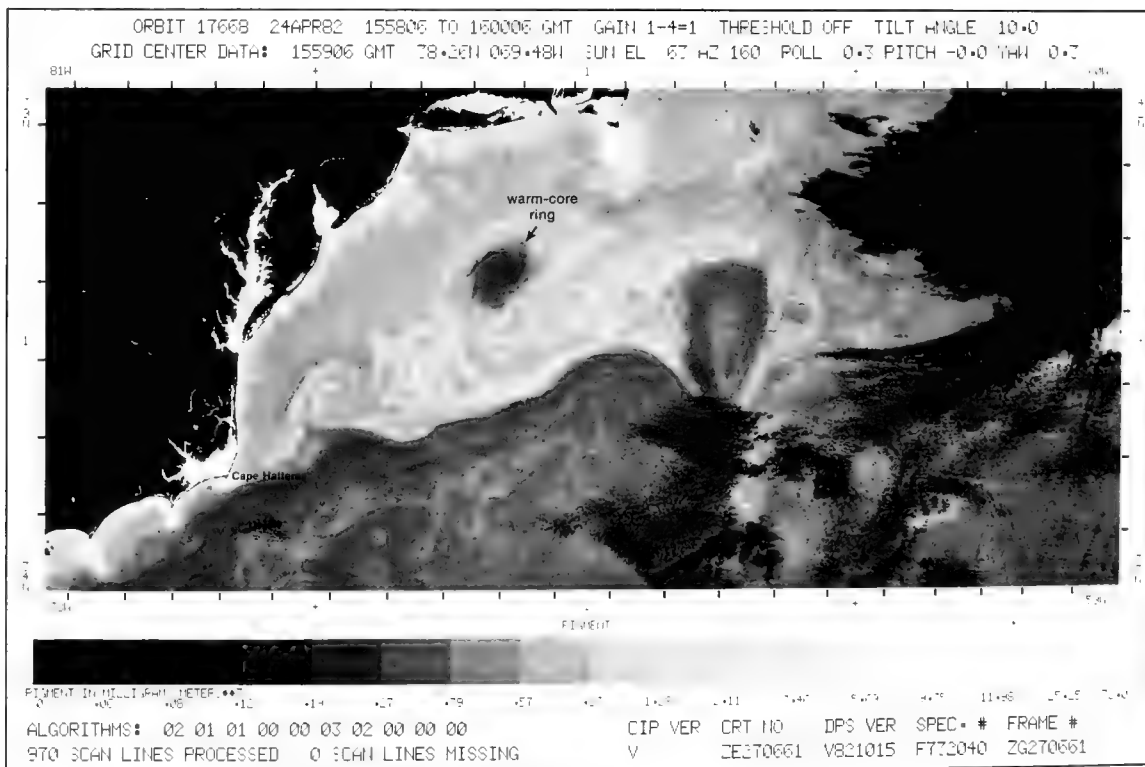
Reference
Gordon, H. R., D. K. Clark, J. W. Brown, O. B. Brown, R. H. Evans, and W. W Broenkow. 1983: Phytoplankton pigment concentrations in the Middle Atlantic Bight: Comparison of ship determinations and CZCS estimates. *Applied Optics*, **22**, 20-36.

42-1. Nimbus-7. Orbit 2480. 21 April 1979. CZCS Pigment Image.

42-2. Nimbus-7. Orbit 17668. 24 April 1982. CZCS Pigment Image.
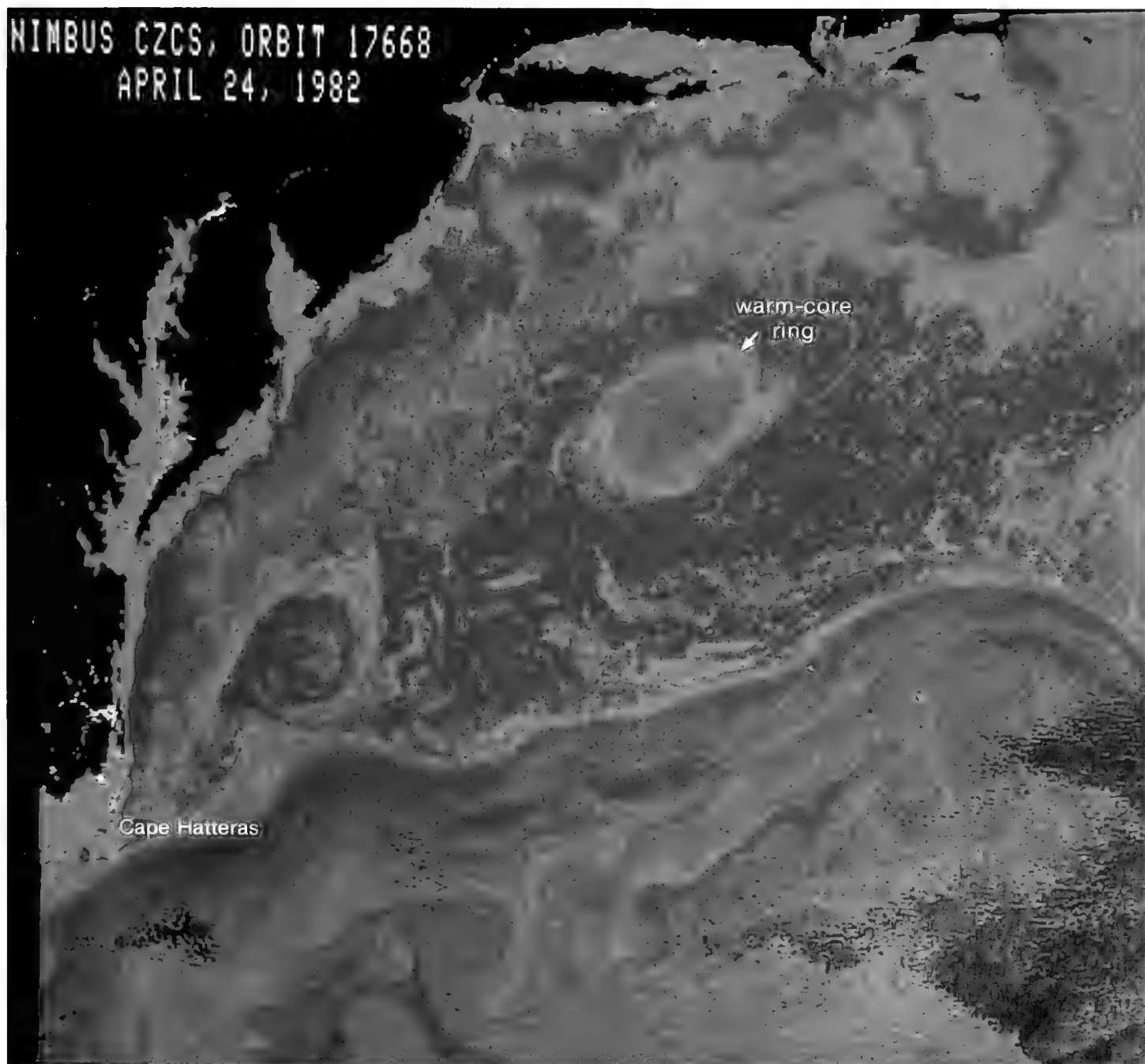
43-1. Nimbus-7. Orbit 17668. 24 April 1982. CZCS False-Color Pigment Image.

3C   Cape Hatteras/Gulf of Maine

Charles S. Yentsch
Bigelow Laboratory of Ocean Sciences
West Boothbay Harbor, Maine

In early spring, highly diverse patterns of phytoplankton distribution are present in the oceanic regions off Cape Hatteras, Cape Cod, and the Gulf of Maine. In terms of seasonal change, this period is the onset of vernal warming—a transition between winter and summer. This climatic transition gives rise to the spring bloom of phytoplankton in the slope waters of the region. This bloom constitutes one of the most important periods of photosynthetic carbon fixation for the ecosystem of this region.

The CZCS pigment image (46-2) shows the high diversity of phytoplankton distribution in the coastal and offshore region from Cape Hatteras to the Gulf of Maine. The region can be subdivided into four areas, based on pigment content, as identified in the locator map (46-1). Area 1 consists of shallow coastal waters (less than 25 m) which extend from Cape Hatteras to Cape Cod and over Nantucket Shoals and Georges Bank. In this area, the pigment concentrations are generally greater than 2 mg m^{-3}. Area 2 consists of deep coastal waters which extend from the edge of the Continental Shelf, circumnavigating Georges Bank, and into the eastern regions of the Gulf of Maine. Pigment concentrations in this area range from 0.2 to 0.5 mg m^{-3}. These are generally lower than the values found on either side of this area. Area 3 encompasses all slope and basin waters greater than 100 m deep, with the seaward limit being the cold wall of the Gulf Stream. It is in this area where the largest diversity in pigment concentration occurs: ignoring the intrusive features, the pigment content ranges from 0.5 mg m^{-3} to values in excess of 2 mg m^{-3}. Area 4 is characterized by the most prominent feature observed in the image: the frontal cold north wall of the Gulf Stream. This strong frontal feature extends from Cape Hatteras meandering eastward to the waters of the open North Atlantic.

Some of the Gulf Stream meanders form eddies which are large rotating cells of water composed of Gulf Stream, Sargasso Sea, and slope water. A warm-core ring, seen in Area 3, is a good example. This is an anticyclonic eddy consisting of a central core of Gulf Stream or Sargasso Sea water surrounded by slope water. A cold-core ring (cyclonic eddy) is also seen in the lower part of the image. This ring was spawned from an encirclement of coastal water by Sargasso Sea or Gulf Stream water. The difference in the pigment content of the water masses, which compose the eddies, allows them to be identified by ocean color. The four pigment-content areas are clearly observed in the enlargement (47-1).

The high diversity of phytoplankton distribution can be explained in terms of variation in the growth of phytoplankton, which is regulated by light and the vertical mixing in the water columns. The amount of vertical mixing regulates the mean light intensity reaching phytoplankton which, in turn, controls their growth. A simple rule of thumb is that water columns which are deep and well-stirred, which is the case of those in Area 2, will promote less phytoplankton growth than those where the mixing depth is retarded by the shoalness of the bottom, which is the case in Area 1. The energy for stirring of these water columns can come from water movements by tides or from other sources across the bottom and/or wind blowing across the surface of these waters. In shallow waters, the tidal components may be the most important during this period. Area 3 differs from Areas 1 and 2 in that the bottom depths are greater and hence the frictional forces which stir the column are much less. In Area 3, the surface layers become more buoyant than the underlying waters because of an increase in solar radiation coinciding with a decrease in surface wind mixing. The combination of these events promotes an intense growth of phytoplankton activity. Area 3 is scarred by water mass intrusions from the coast and Gulf Stream. The fluid motions associated with these intrusions tend to inhibit or destroy buoyancy which essentially retards the onset of the phytoplankton blooms.

46-1. Locator Map for 46-2 and 47-1.

46-2. Nimbus-7. Orbit 2701. 7 May 1979. CZCS Pigment Image.

47-1. Enlarged View. Nimbus-7 Orbit 2701. 7 May 1979. CZCS Pigment Image

47

3D   Cape Hatteras/Sargasso Sea

Charles S. Yentsch

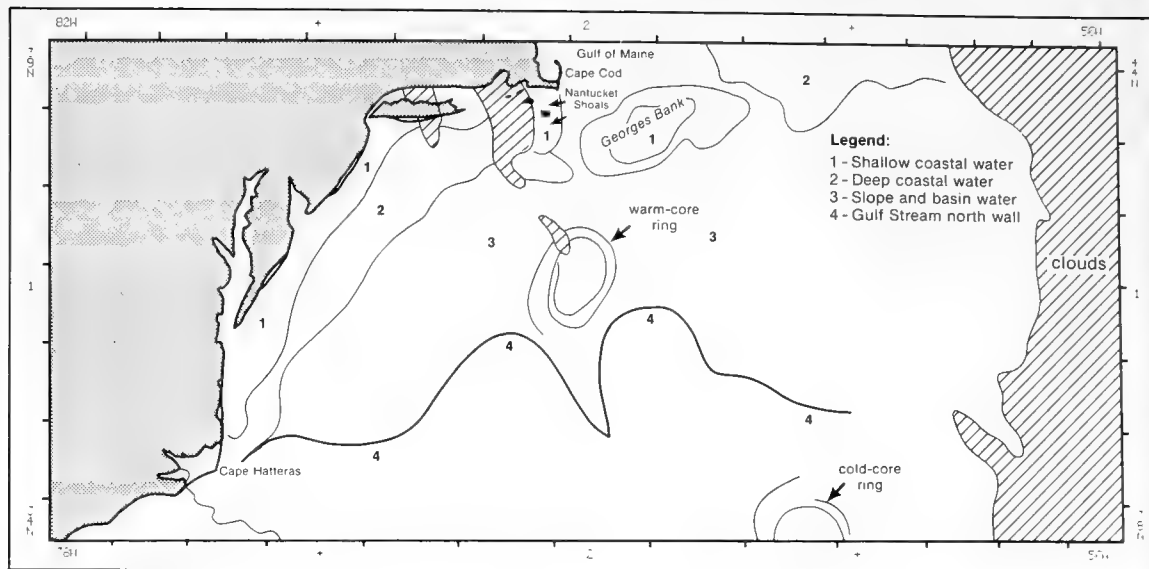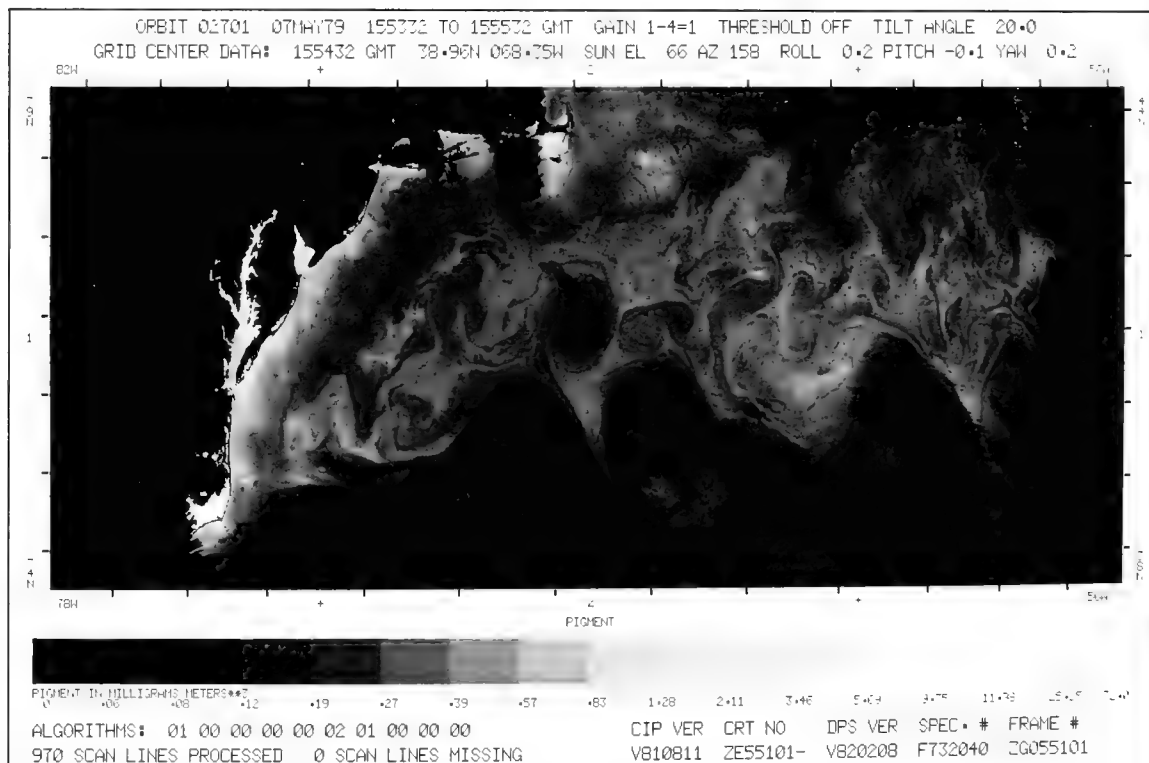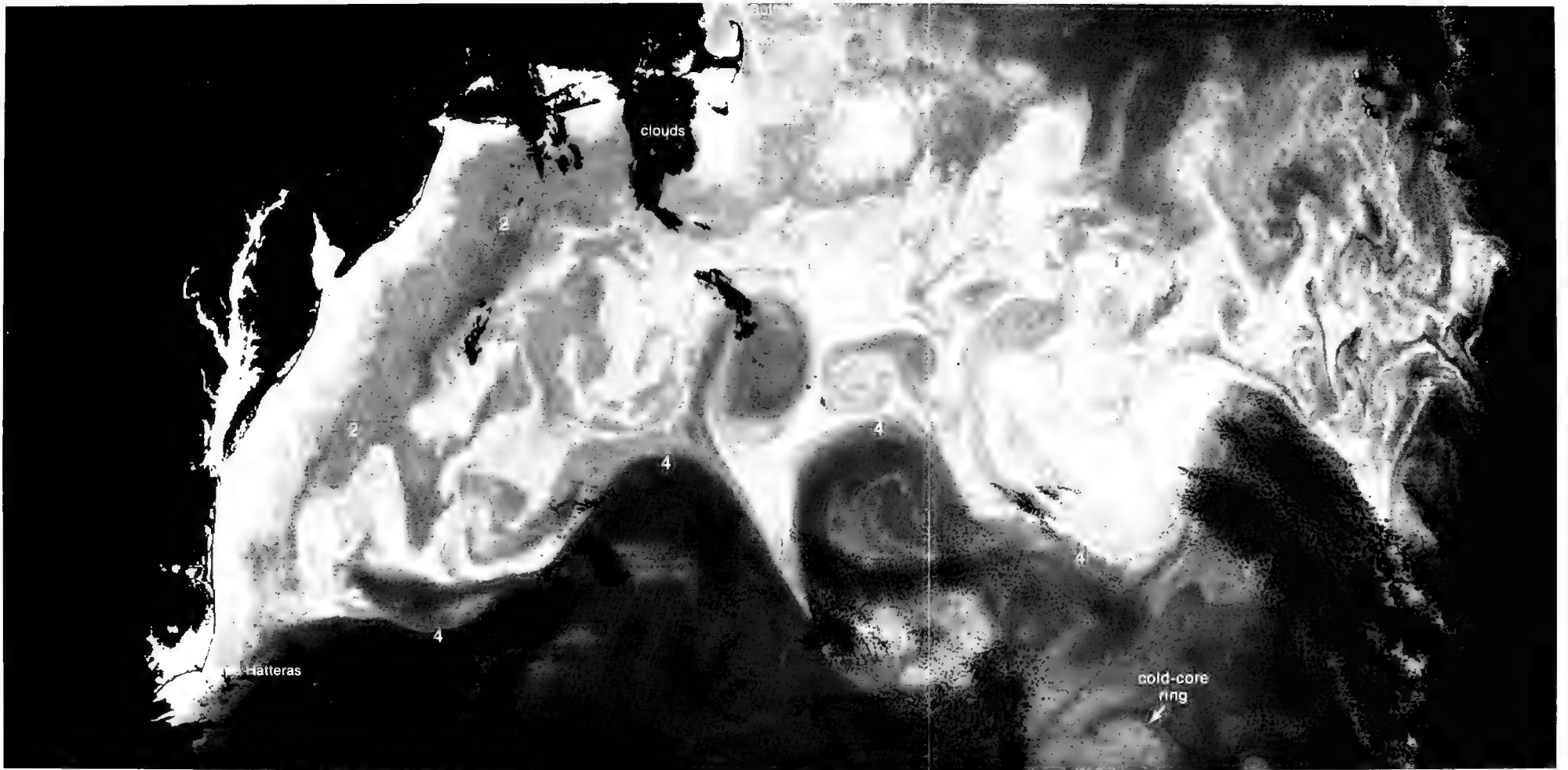Bigelow Laboratory of Ocean Sciences
West Boothbay Harbor, Maine

The density fields of large ocean currents such as the Gulf Stream are baroclinic analogues of upwelling and represent the largest and perhaps most important mechanism in the world's ocean for the vertical transport of nutrients. The conceptual model (49-1) illustrates this mechanism. When the earth's rotation (C_f) is considered as balancing the pressure gradient (P_g), there is a secondary cross-stream flow—that is an aegeostrophic flow—associated with the horizontal advection of the current. This cross-stream flow is transported along lines of equal density from the Sargasso Sea into the slope waters off New England. This flow transports nutrients such as nitrogen and is the reason the slope waters are more heavily populated with phytoplankton than the Gulf Stream proper.
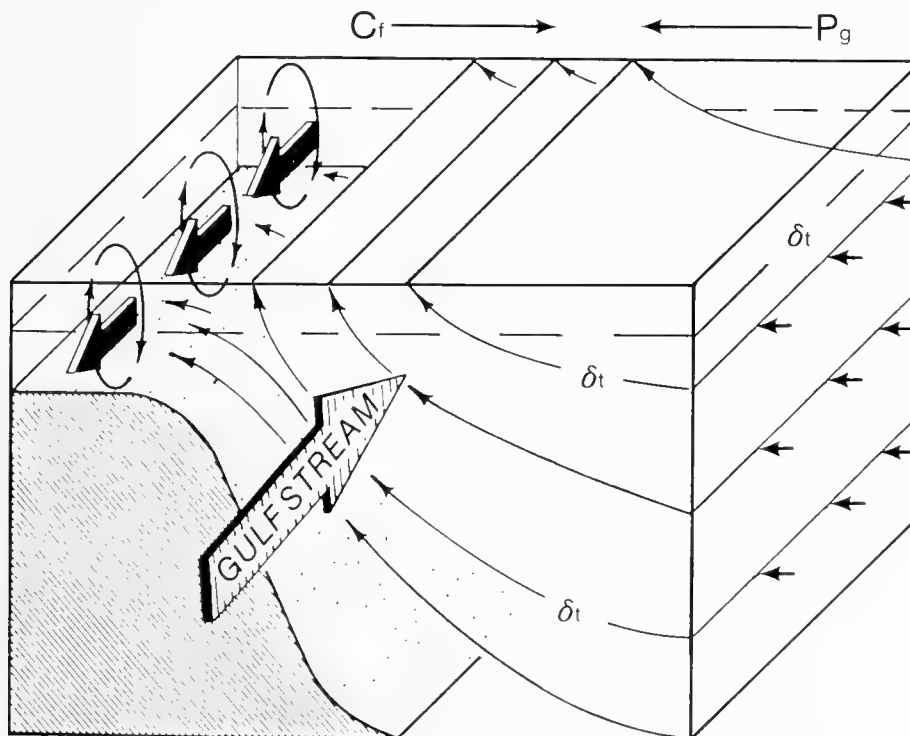
49-1. Conceptual Model of Vertical Transport of Nutrients.

The Gulf Stream—A Distinct Ocean Color Front
May 1979

The CZCS pigment image on 3 May (51-1) shows the Gulf Stream System off the U.S. East Coast. Attention is directed to the very sharp distinction in ocean color of the slope waters (light tones) from that of the main body of the Gulf Stream (dark tones). This distinction in ocean color is due to augmentation of phytoplankton growth associated with the geostrophic flow of the Gulf Stream proper (49-1).

As discussed before, the density fields of large ocean currents such as the Gulf Stream are baroclinic analogues of upwelling and represent the largest and perhaps the most important mechanism for vertical transport of nutrients in the oceans. The CZCS pigment image shows how easily Gulf Stream meanders and eddies (warm-core rings) can be located through the use of remote sensing of ocean color by earth-orbiting satellites.

ORBIT 02646 03MAY79 162242 TO 162442 GMT GAIN 1-4=1 THRESHOLD OFF TILT ANGLE 20·0
GRID CENTER DATA: 162342 GMT 37·65N 075·27W SUN EL 67 AZ 159 ROLL 0·1 PITCH −0·1 YAW 0·3

warm-core
ring

Gulf Stream Meander

Cape Hatteras
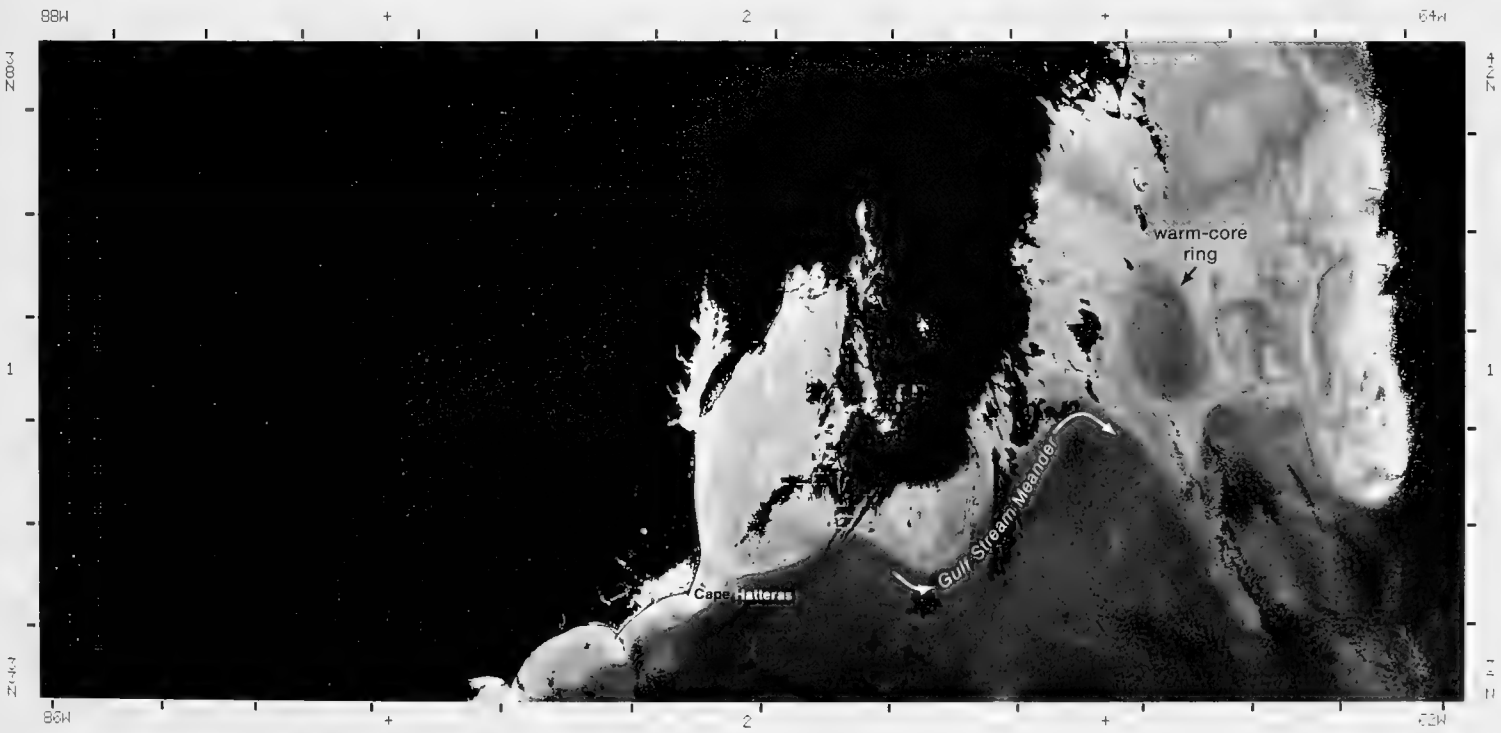
PIGMENT

PIGMENT IN MILLIGRAMS/METERS**3
0   ·06   ·08   ·12   ·19   ·27   ·39   ·57   ·83   1·28   2·11   3·46   5·69   9·75   11·93   15·25   71·0

ALGORITHMS: 01 00 00 00 00 02 01 00 00 00   CIP VER CRT NO DPS VER SPEC· # FRAME #
970 SCAN LINES PROCESSED   0 SCAN LINES MISSING   V   ZE205981 V820401 F732040 ZG205981

51-1. Nimbus-7. Orbit 2646. 3 May 1979. CZCS Pigment Image.

51

3E   New England Seamount Chain

James F. R. Gower
Institute of Ocean Sciences
Sidney, B.C., Canada

Besides mapping the distribution of phytoplankton pigments in the surface layer of the ocean, CZCS imagery shows spatial patterns that contain valuable information on water movement and mixing. In the following example, a particularly striking turbulent eddy field is visible in the water north of the Gulf Stream, which appears to be affected by the New England Seamount chain.

Effects of the New England Seamount Chain
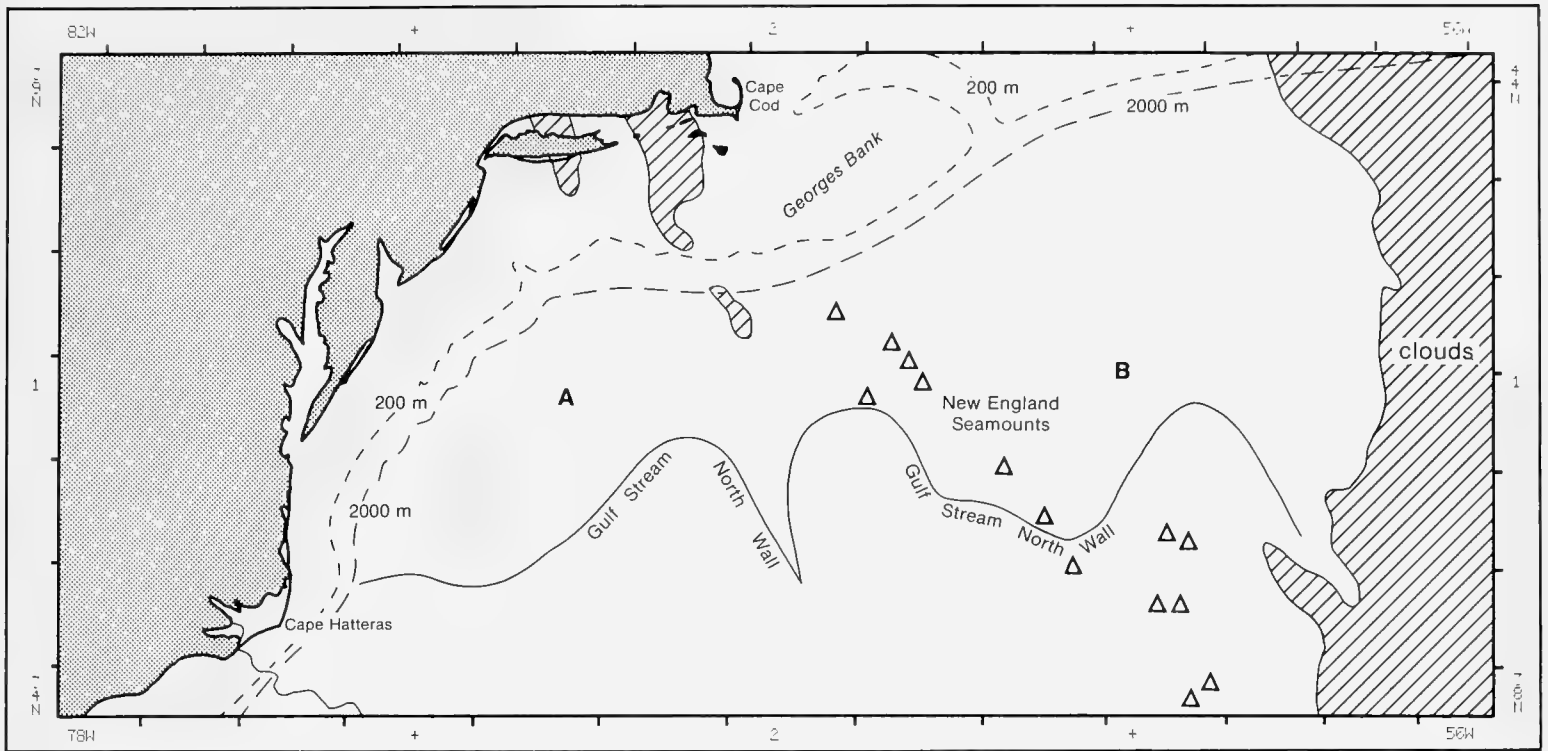## on Gulf Stream Surface Flow
May 1979

The relative levels of the pigment concentrations of the Gulf Stream System have been described by Yentsch (Section 3, page 45) in terms of the different water masses present, and the influence of tidal mixing in shallow areas. In addition, the spatial patterns visible in the CZCS pigment images are also of interest as tracers of the surface flow.

The complex mesoscale eddy field in the water north of the Gulf Stream is well-illustrated in the CZCS pigment image on 7 May (55-2). (Refer to 55-1 for geographical reference purposes.) Such spatial patterns can be quantized in terms of their two-dimensional spatial spectrum (Gower *et al.*, 1981). Any variations in this spectrum, such as those suggested by the increase in high frequency structure on the right side of the pigment image, would be expected to correlate with the changing dynamics of different ocean areas. Such a change is apparent between Area A to the west and Area B to the east. The mean flow is from west to east at $0.5–1.0$ m s^{-1}. The chain of New England Seamounts (plotted as triangles) crosses the image where this change in structure is observed. The seamounts extend up from the bottom (5,000 m) to depths of between 1,000 and 2,000 m, and therefore intercept the Gulf Stream which flows in the top 2,500 m of the ocean. Richardson (1981) has reported the effect of these seamounts on the surface flow as traced by buoy tracks. He observed meanders and small-scale (20 km) eddies, near and extending eastward from individual seamounts. The CZCS pigment image illustrates this effect more fully, with several instances of smaller eddies near the seamounts, and a generally more disorganized flow to the east.

The Gulf Stream is the major source of warm water for the North Atlantic and has a strong influence on North American and European climates, as well as on the Atlantic fisheries. New data on large-scale distortion of the flow and the resulting mixing of the water, such as are provided by CZCS pigment images, can make an important contribution to our understanding of the global climate and food resources.

References
Gower, J. F. R., K. L. Denman, and R. J. Holyer, 1981: Phytoplankton patchiness indicates the fluctuation spectrum of mesoscale turbulence. *Nature*, **288**, 157–159.
Richardson, P. L., 1981: Gulf Stream trajectories measured with free-drifting buoys. *J. Phys. Oceanogr.*, **11**, 999–1010.

55-1. Locator Map for 55-2.

ORBIT 02701 07MAY79 155332 TO 155532 GMT GAIN 1-4=1 THRESHOLD OFF TILT ANGLE 20·0
GRID CENTER DATA: 155432 GMT 38·96N 068·35W SUN EL 66 AZ 158 ROLL 0·2 PITCH −0·1 YAW 0·2

PIGMENT

PIGMENT IN MILLIGRAMS/METERS**3

| 0 | ·06 | ·08 | ·12 | ·19 | ·27 | ·39 | ·57 | ·83 | 1·28 | 2·11 | 3·46 | 5·69 | 9·35 | 11·98 | 25·25 | 72·0 |

ALGORITHMS: 01 00 00 00 00 02 01 00 00 00   CIP VER   CRT NO   DPS VER   SPEC· #   FRAME #
970 SCAN LINES PROCESSED   0 SCAN LINES MISSING   V810811   ZE55101−   V820208   F732040   ZG055101

55-2. Nimbus-7. Orbit 2701. 7 May 1979. CZCS Pigment Image.

3F   New England Coast

Charles S. Yentsch

Bigelow Laboratory of Ocean Sciences
West Boothbay Harbor, Maine

During summer months the stirring of shallow water columns along coastal regions by tides promotes phytoplankton growth which is reflected in the pattern of pigment distribution. The following CZCS images are excellent examples of this phenomenon in the waters off New England, due to the strength of tidal currents and the many large shoals throughout the region.

Enhancement of Phytoplankton Growth by Tidal Mixing
June 1979

Regions of high pigment concentration are strongly correlated with water temperature; that is, pigment concentrations are highest in regions where water temperatures are coolest. On 14 June, such regions of intense tidal mixing on the CZCS pigment image (58-2) and the corresponding false-color CZCS pigment image (59-1) are outlined by sharp ocean color fronts. Inside these frontal boundaries the pigment concentration is greater than 2.0 mg m^{-3}. Outside these fronts, on the warm side, pigment values are less than 0.5 mg m^{-3}. Note that the areas of intense mixing outline the major shoal regions such as Nantucket Shoals and Georges Bank.

The augmentation of phytoplankton growth by tidal stirring is explained as follows: Surface waters, heated by sunlight, become more buoyant than the waters they overlie. This layer of warm water over cold tends to stabilize the water column, thereby isolating the deeper cold water from the warm surface layers. The cold layers contain large concentrations of nutrient fertilizers while the warm surface layers do not. Therefore, isolation of the two layers tends to retard phytoplankton growth. Intense phytoplankton growth occurs when these two layers are actively stirred, such as occurs over the Georges Bank.

The Georges Bank is a shoal region off the New England coast. The energy for stirring the shallow water column over the Georges Bank comes from tidal flow. As these currents move across the bottom, the friction creates turbulent stirring (58-1). Generally speaking, the intensity of the stirring is proportional to the speed of the current and the water depth.

58-1. Schematic of Mixing Process in Shoal Regions.
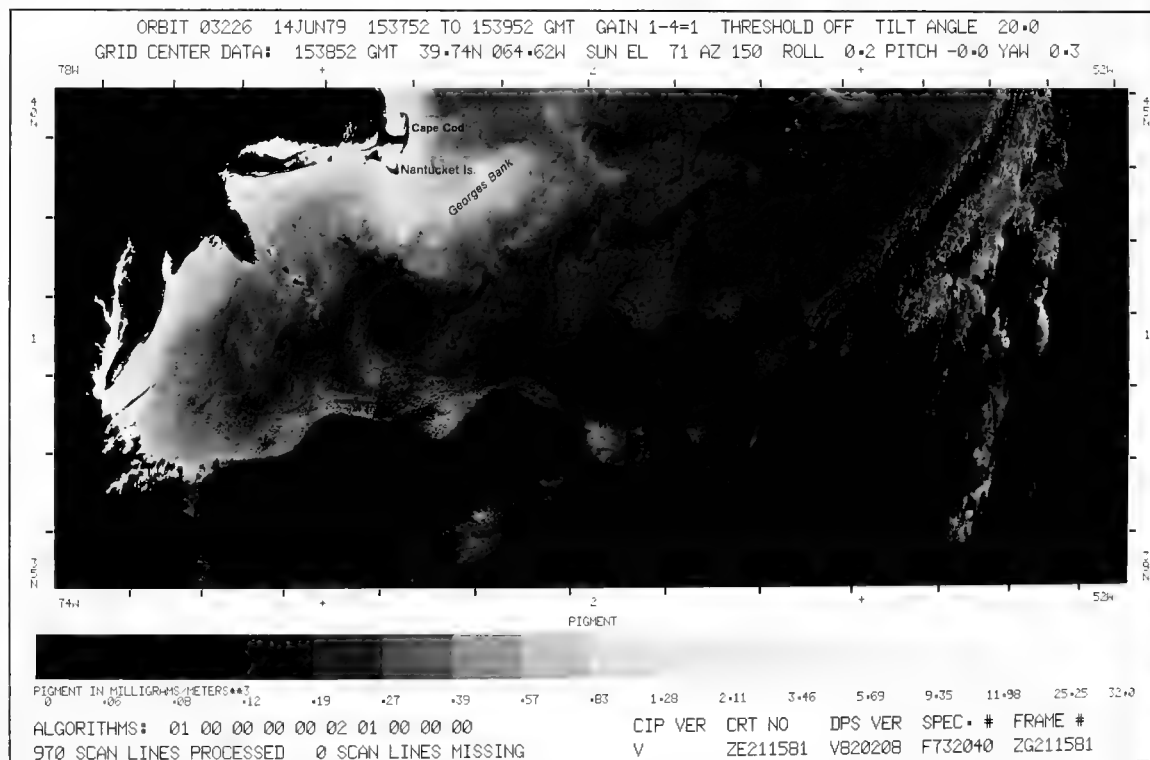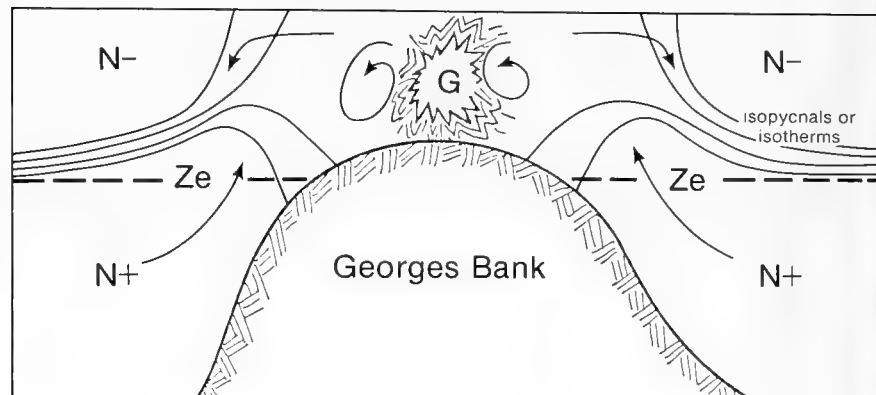
58-2. Nimbus-7. Orbit 3226. 14 June 1979. CZCS Pigment Image.

Cape Co

Nantucket Is

Georges Bank
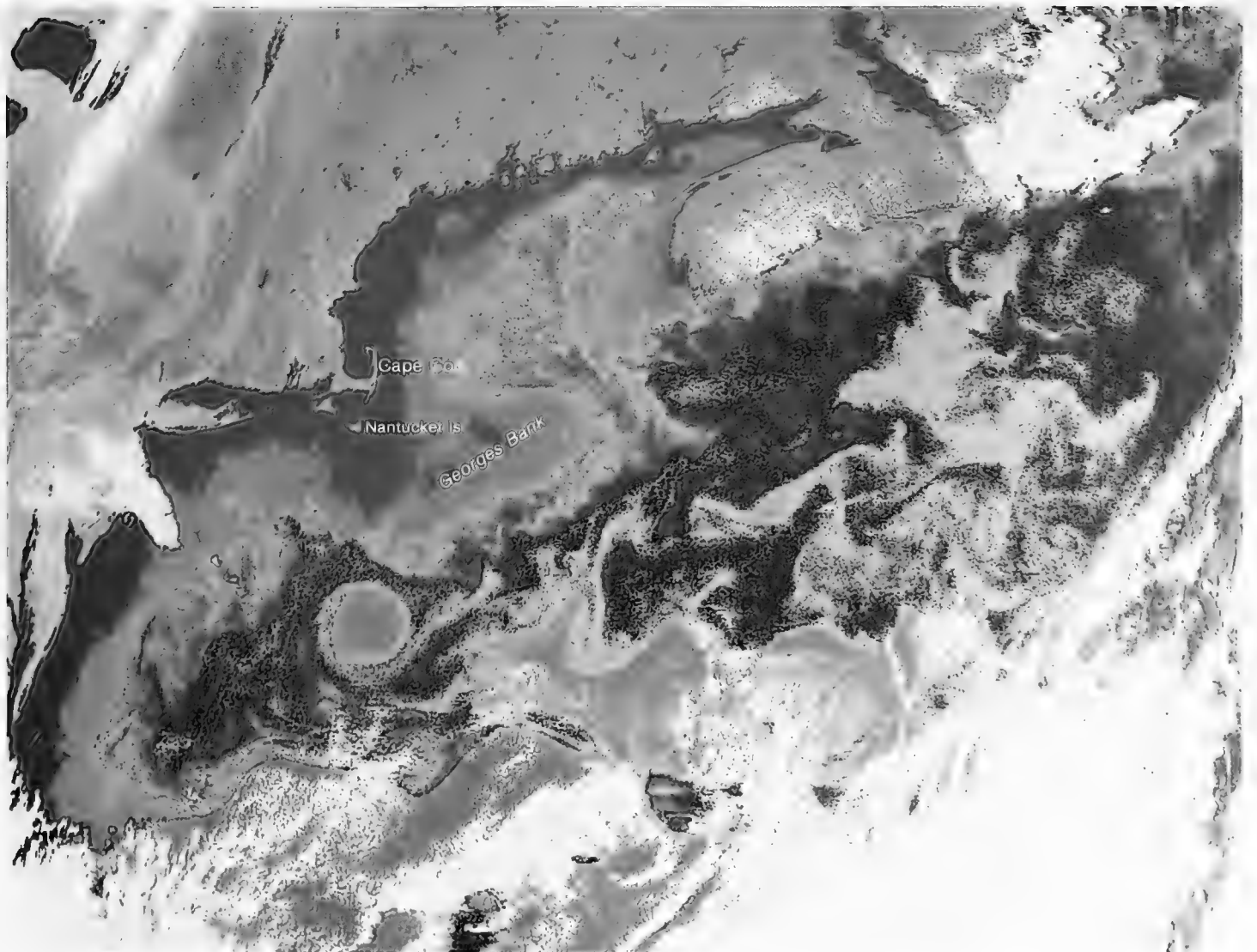
59-1. Nimbus-7. Orbit 3226. 14 June 1979. CZCS False-Color Pigment Image.

Section 4
Gulf of Mexico/Caribbean Sea

4A   Florida West Coast/Central Gulf of Mexico

Charles S. Yentsch

Bigelow Laboratory of Ocean Sciences
West Boothbay Harbor, Maine

An example of phytoplankton growth being augmented by a major ocean current is observed in the CZCS images of Florida and the eastern Gulf of Mexico in this case study. In this region, the thermal Loop Current forms a front which is due to the entry of equatorial water into the eastern Gulf of Mexico through the Straits of Yucatan. The equatorial water penetrates as far north as 27° N, which encompasses most of the eastern Gulf of Mexico.

The Loop Current— Augmentation of Primary Production
March 1979

The CZCS pigment pattern on 15 March (65-2) correlates with the general thermal pattern shown by the CZCS infrared channel (65-1). Warm equatorial waters are associated with low concentrations of phytoplankton pigment (dark tones) and cooler waters are associated with higher levels (light tones) of pigment. This temperature/pigment relationship is reflecting the difference in levels of nutrient enrichment. The increased phytoplankton abundance is due to increased vertical mixing which arises from the flow of the Loop Current and from constraints placed on that current by the shape of the Florida peninsula and its continental shelf (64-1). The dynamic topography on the eastern side of the gulf demonstrates that the mean flow is augmented in the region of the Florida escarpment. Associated with this increase in flow is the imbalance between the Coriolis and pressure forces which create the isopycnal flow, causing enrichment of the waters adjacent to the Florida peninsula by deep nutrient-rich water.

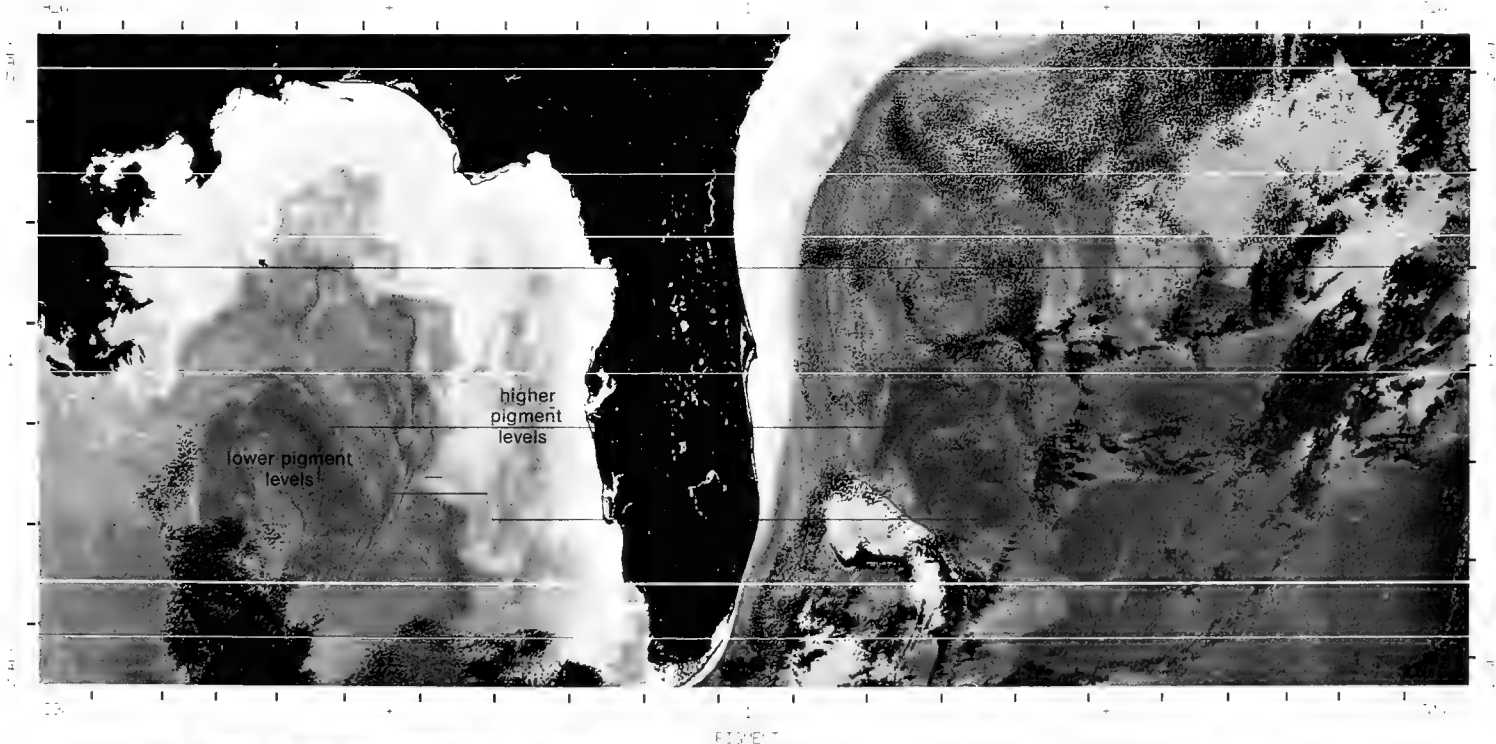64-1. Gulf of Mexico Continental Shelf and Loop Current Velocity Profile.
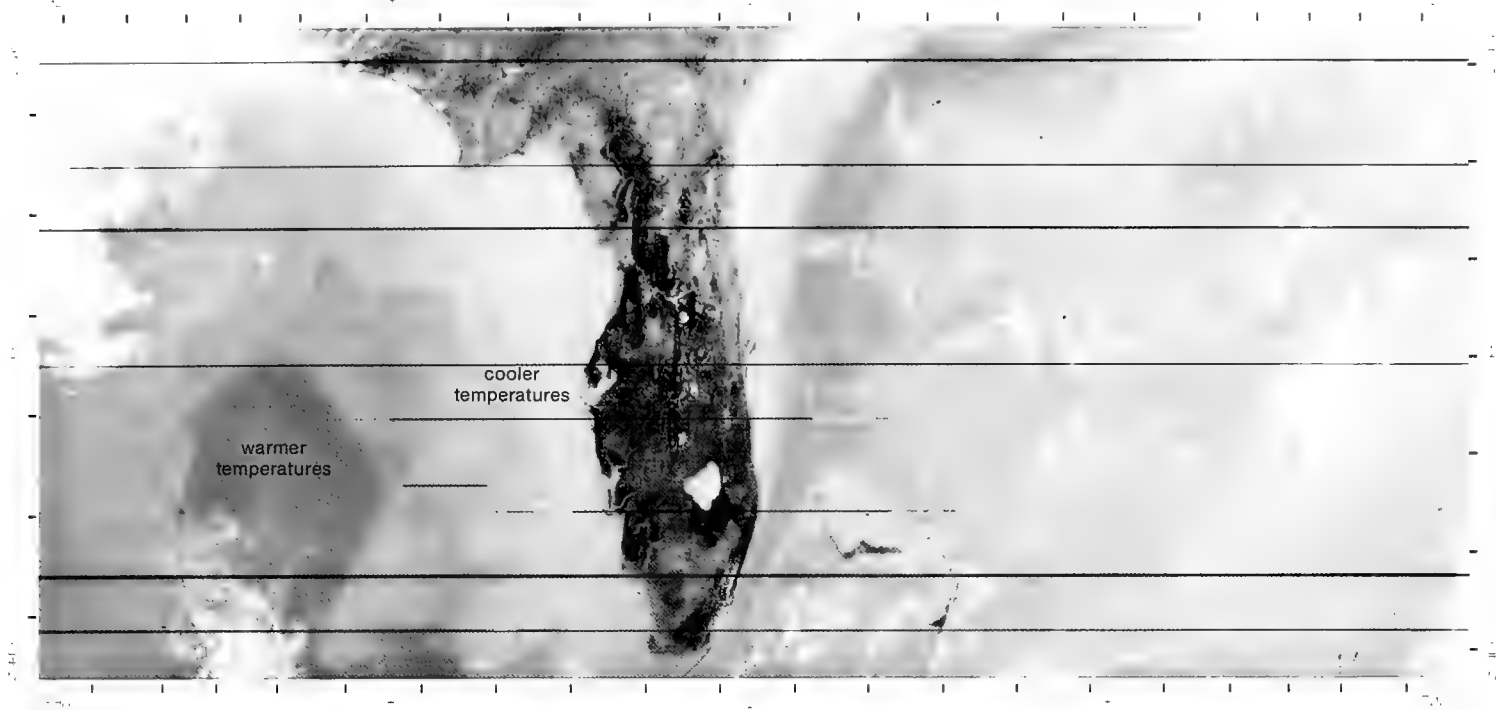
65-1. Nimbus-7. Orbit 1969. 15 March 1979. CZCS Infrared Image.

65-2. Nimbus-7. Orbit 1969. 15 March 1979. CZCS Pigment Image.

65

4B   Gulf of Mexico/Cuba

Sayed Z. El-Sayed
Takashi Ichiye
and
Charles C. Trees
Department of Oceanography
Texas A&M University
College Station, Texas

The Gulf of Mexico is a semi-enclosed basin with inflow through the Yucatan Channel and outflow through the Florida Straits. The most prominent single physical feature of the gulf is the Loop Current. The Loop Current's path and extent of intrusion into the gulf are highly time-dependent, with apparent annual cycles (Leipper, 1970) and significant variability in the year-to-year pattern (Maul, 1977). Mesoscale eddies (rings), which are the second major physical feature in the Gulf of Mexico, are pinched off the Loop Current and drift westward.

The total pigment concentrations (chlorophyll a + phaeopigment) in the Gulf of Mexico exhibit marked contrast between inshore and offshore waters; the offshore waters were characterized by Bogdanov *et al.* (1968), and El-Sayed (1972), as being highly oligotrophic as compared to the more productive neritic regions.

The CZCS pigment image on 3 October (68-2) shows a portion of the Loop Current between two cloud banks in the eastern gulf, with total pigment concentrations in the Loop Current of less than 0.06 mg m⁻³. The circulation patterns in the western gulf are characterized by the presence of mesoscale eddies (68-1, Inset A). The belt of relatively clear water in this region seems to be the boundary of a cyclonic eddy which was also observed during the cruise of the R/V *Gyre* (80 G-1) in April 1980 (Brooks and Eble, 1982). An enlarged view of this area (69-1) shows more distinctly the relatively higher pigmented (chlorophyll) water mass occupying the central area of the cyclonic eddy which is caused by the convergence of the surface waters in the eddy. In the western Gulf of Mexico (68-2) the width of the coastal front, judging from the high pigment concentrations, is narrower than that found off the Yucatan Peninsula. A major contribution to the increase in predicted pigment off the Yucatan Peninsula is caused by suspended sediment and not phytoplankton.

In the Caribbean Sea, some interesting circulation patterns are observed just south of the western tip of Cuba (68-2; and 68-1, Inset B). In the enlarged view of this area (69-2) a cyclonic eddy is observed between the tip of Cuba and Islas de Pinos. This eddy is formed by a countercurrent along the northern coast of Cuba. Such a countercurrent is not often observed, but was inferred from the geostrophic current pattern (Ichiye *et al.*, 1973). This countercurrent entrains coastal waters southward and forms a 40-km eddy. Associated with this eddy are turbulent structures which are also observed south of the eddy.

The CZCS pigment image on 8 October (70-2) in the northern Gulf of Mexico shows the northward intrusion of the Loop Current to within approximately 60 km of the Mississippi Delta (70-1). The intrusion of clear water extends westward to about 92° W (71-1) and represents the farthest westward penetration of the Loop Current recorded in the literature. There is a narrowing of the Loop Current around 85° W which suggests that an eddy could be spinning off at some future time. Leipper (1970) and Whitaker (1971) found that the maximum intrusion of the Loop Current occurred in October, whereas Robinson (1973) and Maul (1977) observed this maximum several months earlier. These results emphasize the temporal and spatial variabilities of the Loop Current.

As the Loop Current passes south of the Mississippi Delta, it entrains coastal waters some 100–150 km out into the Gulf of Mexico. The western edge of the Loop Current generates a cyclonic eddy of coastal waters and entrains this water some 50 km southward.

In the western gulf, coastal waters with high pigment concentrations are transported offshore just east of Brownsville, Texas. This entrainment is caused by two eddies: a northern cyclonic eddy located around 27° N, 94° W, and a southern anticyclonic eddy located at 26° N, 94° W. Brooks and Legeckis (1982) observed the same features in 1980 using satellite-derived surface temperatures.

Around 26° N, 92° W there is entrainment of coastal waters into the gulf (70-1, stippled area). This transport was observed by El-Sayed and Trees (1980), with total pigment concentrations around 0.39 mg m⁻³, which agrees well with that predicted from the CZCS images.
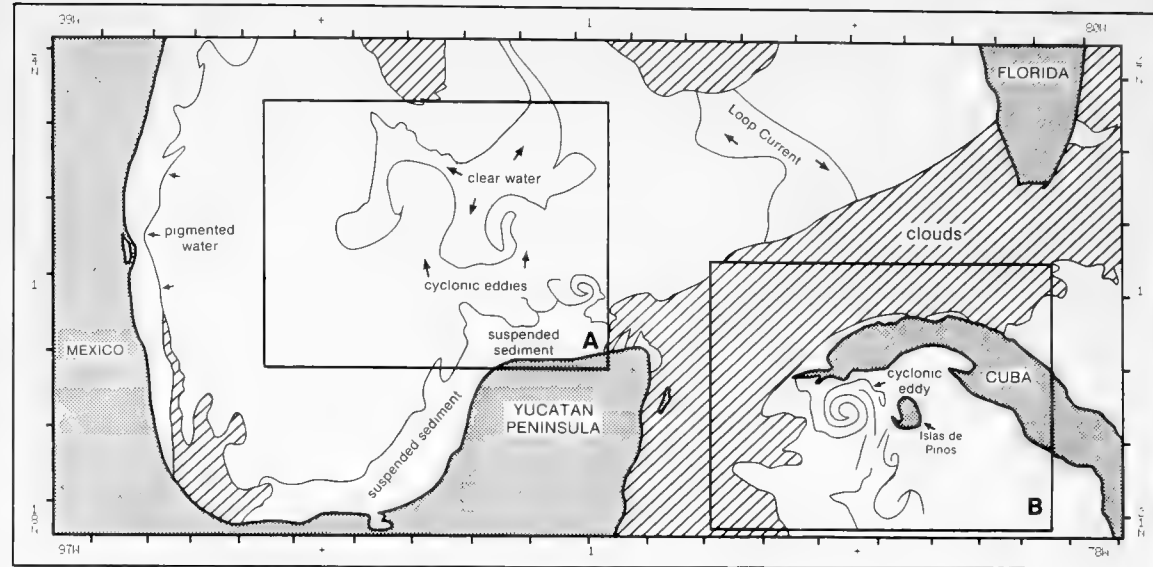
68-1. Locator Map for 68-2, 69-1, and 69-2.
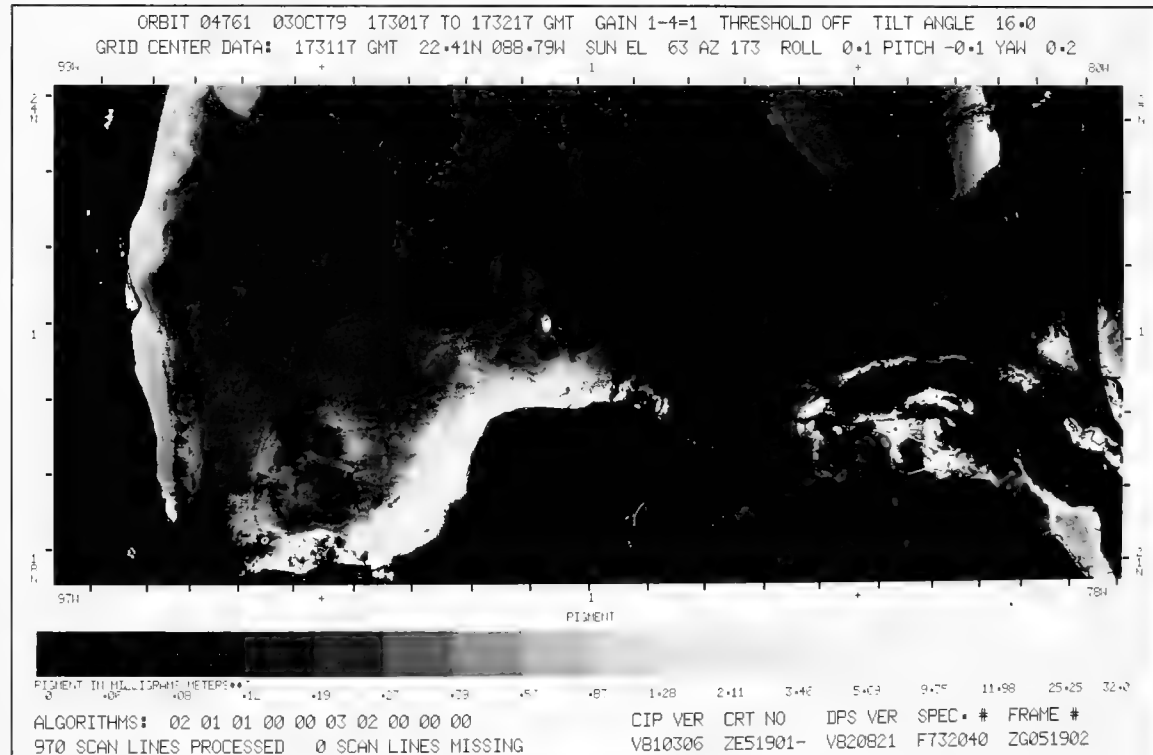
68-2. Nimbus-7. Orbit 4761. 3 October 1979. CZCS Pigment Image.

69-1. Enlarged View of Inset A. Nimbus-7. Orbit 4761. 3 October 1979. CZCS Pigment Image.

69-2. Enlarged View of Inset B. Nimbus-7. Orbit 4761. 3 October 1979. CZCS Pigment Image.

69

70-1. Locator Map for 70-2 and 71-1.

70-2. Nimbus-7. Orbit 4830. 8 October 1979. CZCS Pigment Image.

References

Bogdanov, D. V., V. Sokolov, and W. S. Khromov, 1968: Regions of high biological productivity in the Gulf of Mexico and Caribbean Sea. *Oceanology*, **8**, 371–381.

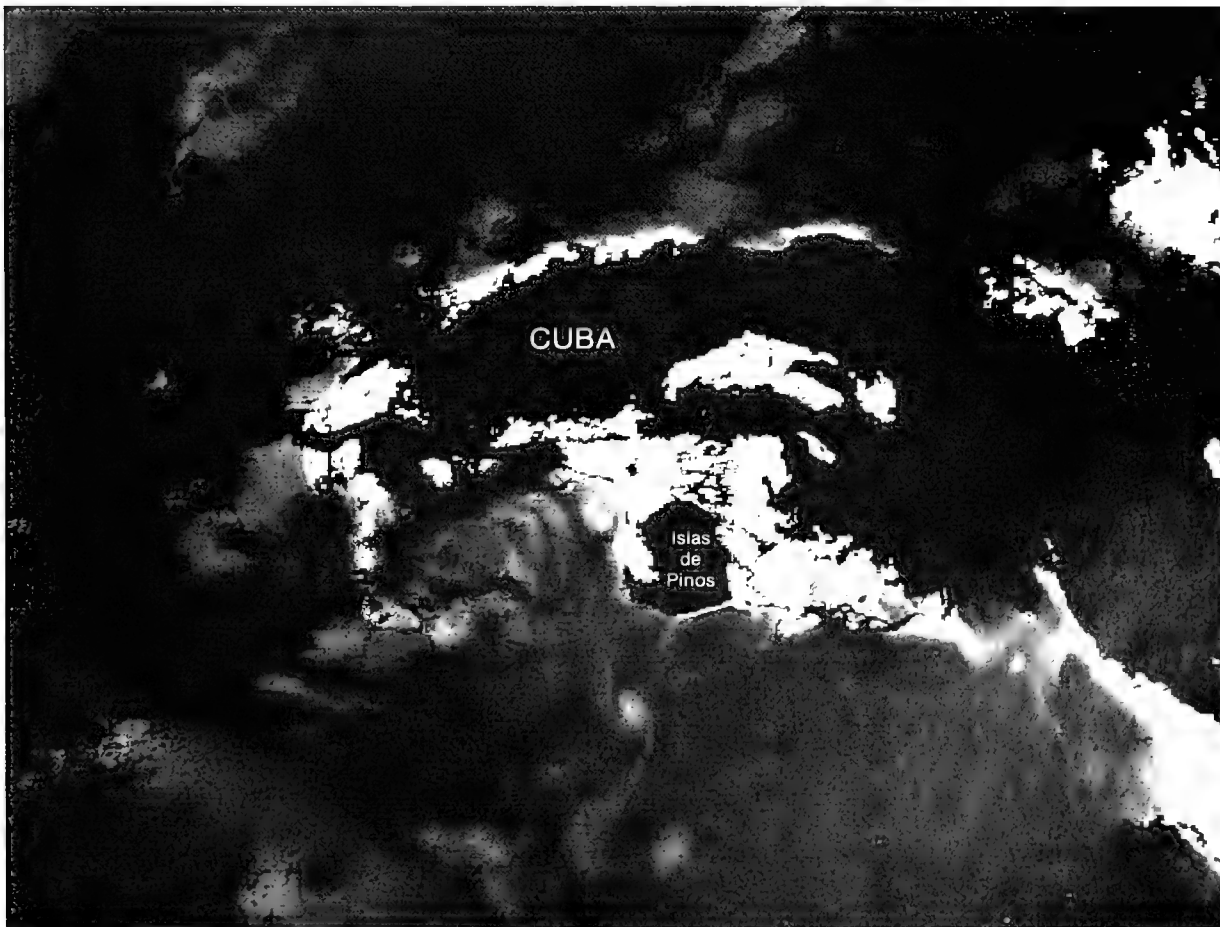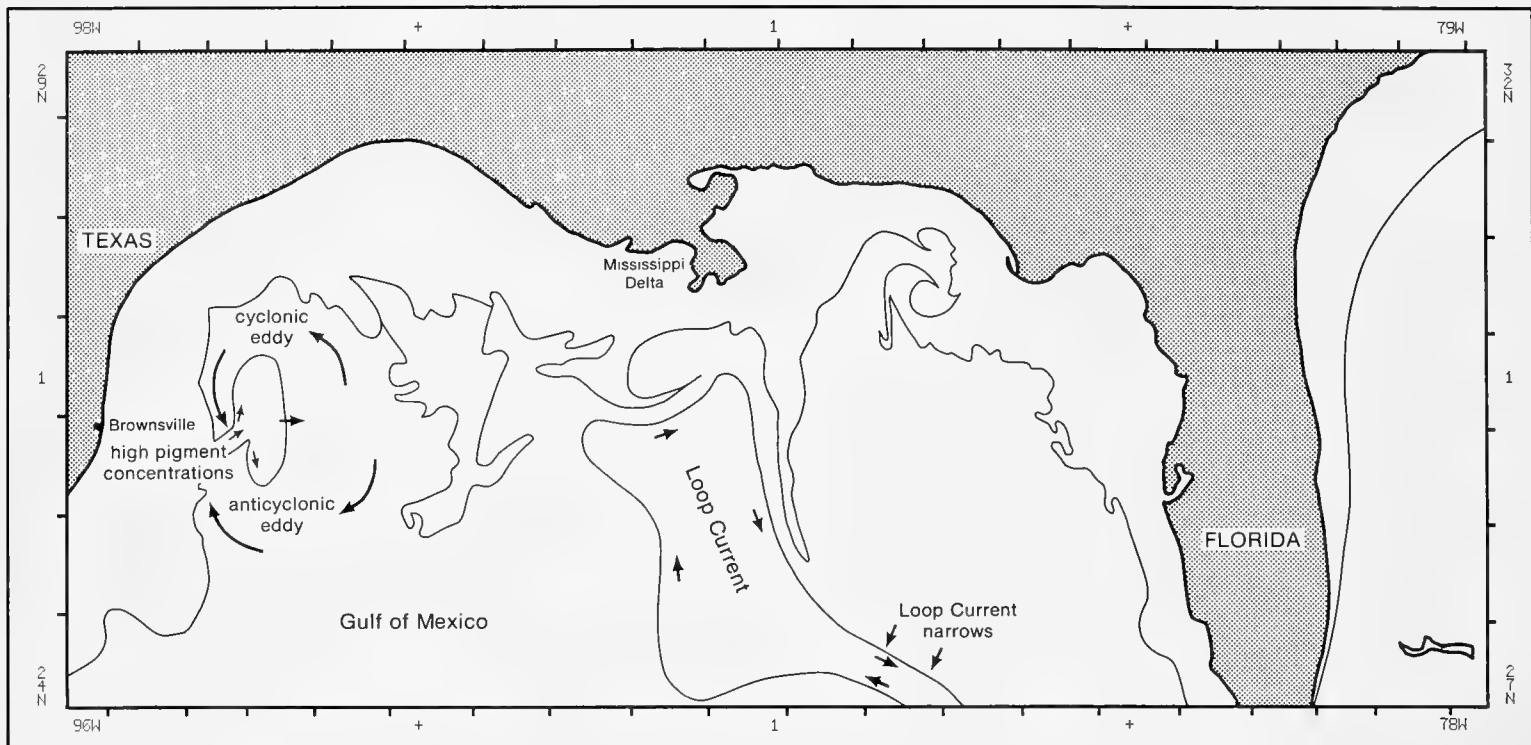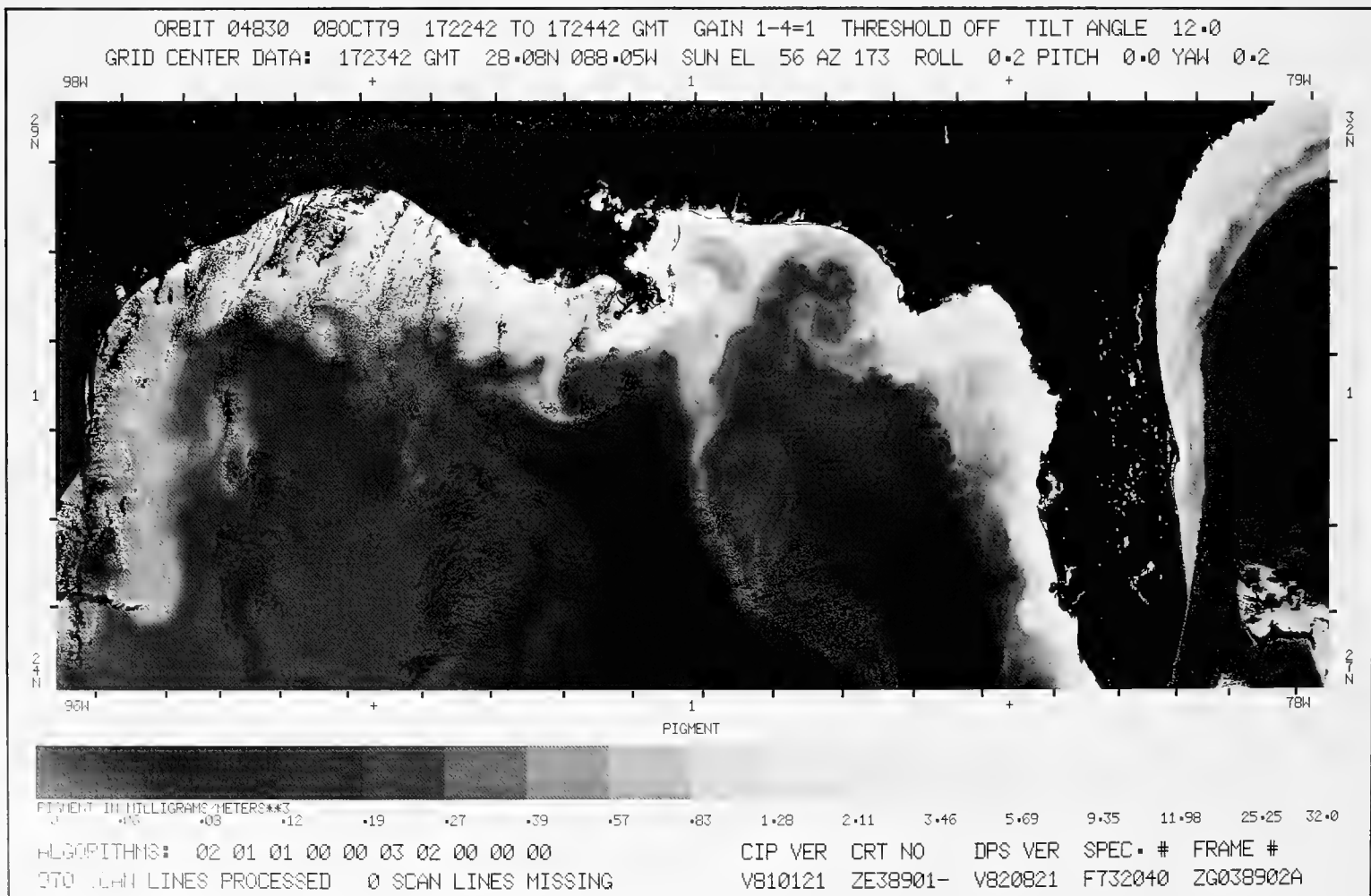Brooks, D. A., and M. C. Eble, 1982: Hydrographic observations in the western Gulf of Mexico. Texas A&M University, Dept. of Oceanography, Ref. 82-2-T, 174 pp.

Brooks, D. A., and R. V. Legeckis, 1982: A ship and satellite view of hydrographic features in the western Gulf of Mexico. *J. Geophys. Res.*, **87(C5)**, 4195–4206.

El-Sayed, S. Z., 1972: Primary productivity and standing crop of phytoplankton. In *Chemistry, Primary Productivity, and Benthic Marine Algae of the Gulf of Mexico, Serial Atlas of the Marine Environment*, Folio 22, edited by V. C. Bushnell, American Geographical Society, 8-13.

El-Sayed, S. Z., and C. C. Trees, 1980: Ecological studies of phytoplankton in the Gulf of Mexico during NOAA/NMFS *Oregon II* Cruise. Texas A&M University, Dept. of Oceanography, Ref. 80-8-T, 53 pp.

Ichiye, T., H.-H. Kuo, and M. Carnes, 1973: Assessment of currents of hydrography of the eastern Gulf of Mexico. Texas A&M University, Dept. of Oceanography, Ref. 601, 2.10-2.29, 5.10-5.15, and 6.1-6.7.

Leipper, D. F., 1970: A sequence of current patterns in the Gulf of Mexico. *J. Geophys. Res.*, **75**, 637–657.

Maul, G. A., 1977: The annual cycle of the Gulf Loop Current Part 1: Observations during a one-year time series. *J. Marine Res.*, **35(1)**, 29–47.

Robinson, M. K., 1973: Atlas of monthly mean sea surface and subsurface temperature and depth of the top of the thermocline, Gulf of Mexico and Caribbean Sea. Scripps Institution of Oceanography, La Jolla, Calif., Ref. 73-8, 105 pp.

Whitaker, R. E., 1971: Seasonal variations of steric and recorded sea level of the Gulf of Mexico. M.S. Thesis, Texas A&M University, Dept. of Oceanography, College Station, Texas, 109 pp.
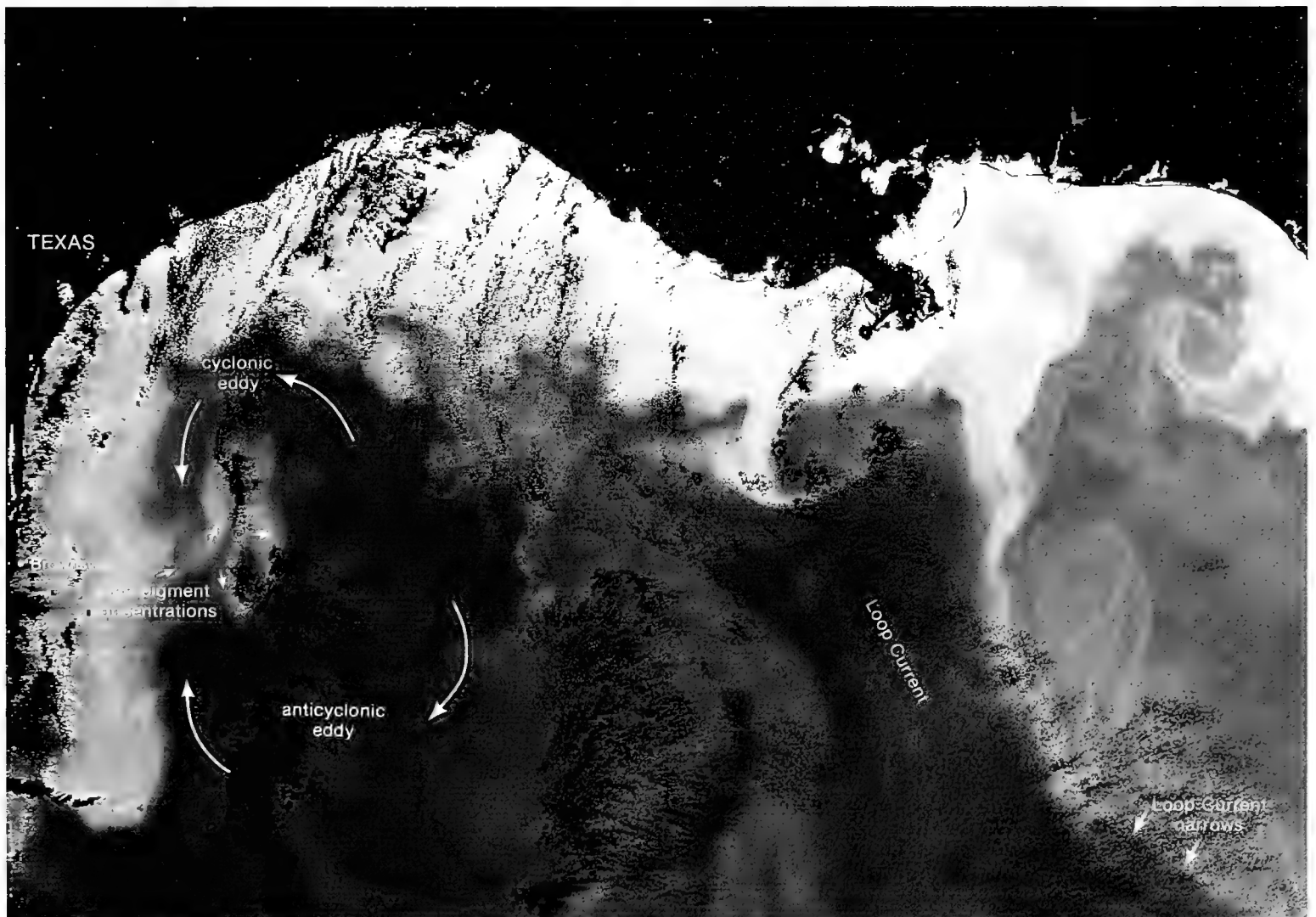
71-1. Enlarged View. Nimbus-7. Orbit 4830. 8 October 1979. CZCS Pigment Image.

Section 5
Western European Basin

5A Celtic Sea/Bay of Biscay

Patrick M. Holligan
Marine Biological Association
Plymouth, United Kingdom
and
Michel Viollier
Station d'Océanologie et de Biologie Marine
Roscoff, France

Each year during the early summer, extensive patches of water giving high reflectance of visible light are observed along the outer shelf margin between 45° and 60° N. Observations taken at sea in 1982 established that these are caused by coccolithophores; phytoplankton with external plates or coccoliths of calcite, which become dominant after the main spring diatom bloom has declined. These organisms, particularly the widespread temperate species *Emiliania huxleyi*, are of particular importance in the biogenic sedimentation of carbon (as calcite) in the oceans. The reflectance of light by the coccoliths must be taken into account in the development of accurate atmospheric correction and chlorophyll algorithms for the processing of remotely sensed ocean color data.

Phytoplankton (Coccolithophores)
June 1979

Frontal boundaries between water masses with distinct hydrographic properties and plankton communities (Pingree *et al.*, 1982) are seen on CZCS images on 19 June (76-1) as regions with relatively high diffuse attenuation coefficients (upper image) and pigment values (lower image). The shelf break frontal system (**SBF**, 77-1), which follows the 200-m isobath, represents the eastern extent of surface mesoscale eddies characteristic of the deep waters of the Bay of Biscay. On the shelf between southwestern England and northwestern France, the tidal front (**TF**) marks the transition from seasonally stratified and relatively warm water in the Celtic Sea to tidally mixed water in the English Channel. The coccolithophore populations appear on the Channel 3 image (77-2, Subsurface Radiance) as areas of high reflectance in outer shelf waters.

The coccolithophores give maximum reflectance in Channel 1 (blue) and, relative to clear offshore and turbid coastal waters, significant reflectance in Channel 4 (red; Holligan *et al.*, 1983). The latter property affects the atmospheric corrections so that appropriate adjustments should be made for water-leaving radiance by correlation with Channels 1–3, or the Channel 4 radiance values for pixels adjacent to the bloom used. These channels are in reference to Level 1 images, which are not shown in this publication.

The influence of coccolith reflectance on the chlorophyll algorithm is more difficult to define, as no correlation between coccolith density and pigment concentration is expected for the scene as a whole. This problem is illustrated by the comparison between the Channel 3 image (77-2) and either the diffuse attenuation coefficient or pigment image (76-1). In the coastal, tidally mixed water, for which the levels of suspended material and chlorophyll can be considered proportional, the spatial patterns of high reflectance are positively correlated. By contrast, no such relationship holds for the coccolithophore water.

The maximum chlorophyll a levels observed in the coccolithophore blooms are generally 2–3 mg m^{-3} compared to values of up to 5 mg m^{-3} associated with persistent diatom populations at the shelf break. A more important parameter to derive from the CZCS imagery, however, is coccolith abundance as a measure of calcite-carbon that will be lost to the bottom sediments. The reflectance signal is generated both by living cells and detached coccoliths, and preliminary calibration values suggest that typical maximum reflectance values correspond to about 1 gm m^{-3} CaCO$_3$ in the surface water.

References

Holligan, P. M., M. Viollier, D. S. Harbour, P. Camus, and M. Champagne-Philippe, 1983: Satellite and ship studies of coccolithophore production along a continental shelf edge. *Nature*, **304**, 339-342.

Pingree, R. D., G. T. Mardell, P. M. Holligan, D. K. Griffiths, and J. Smithers, 1982: Celtic Sea and Armorican current structure and the vertical distribution of temperature and chlorophyll. *Continental Shelf Research*, **1**, 99-116.
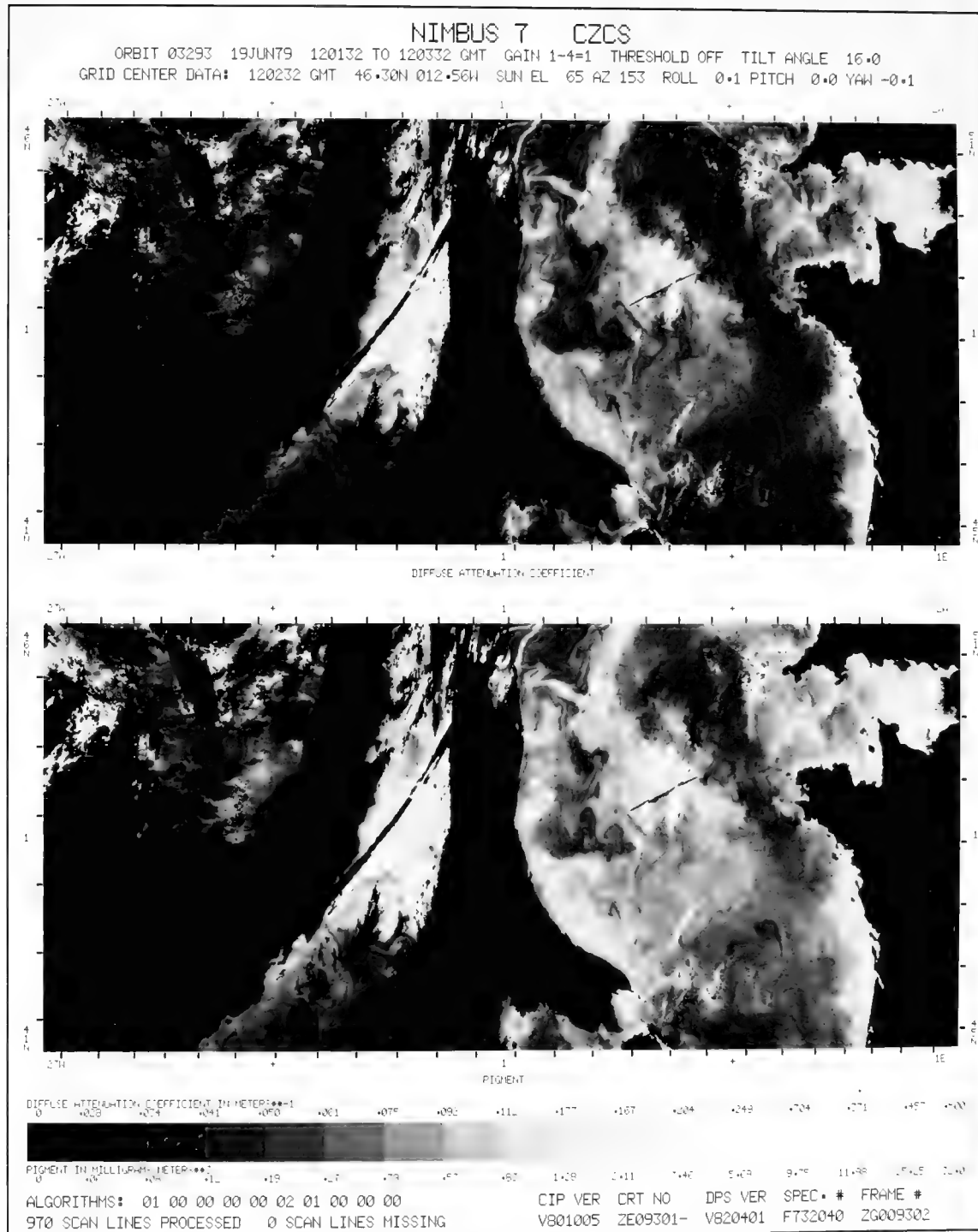
76-1. Nimbus-7. Orbit 3293. 19 June 1979. CZCS Diffuse Attenuation Coefficient (upper) and Pigment (lower) Images.
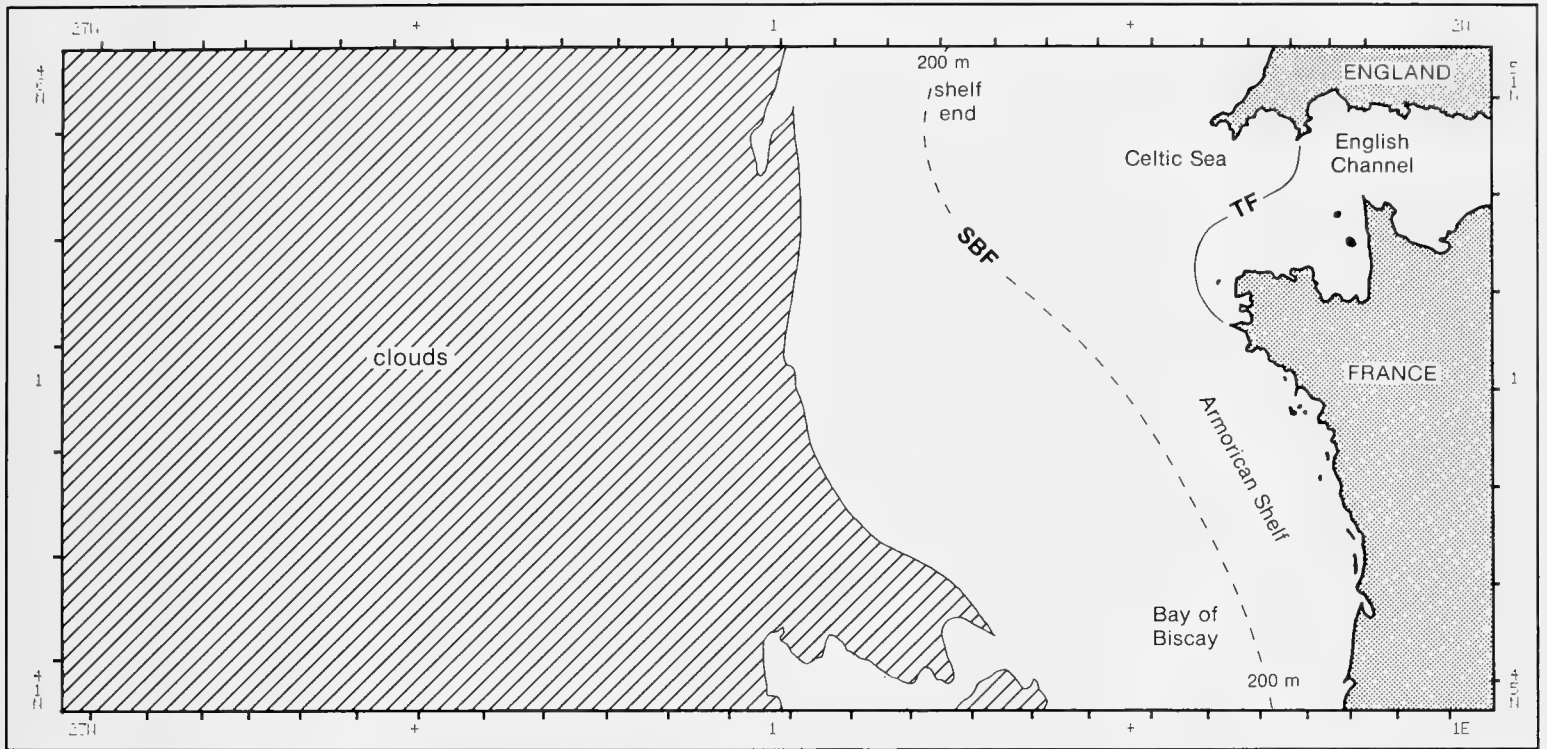
77-1. Locator Map for 76-1 and 77-2.

ORBIT 03293 **JUN79 120132 TO 120332 GMT GAIN 1-4=1 THRESHOLD OFF TILT ANGLE 16·0
GRID CENTER DATA: 120232 GMT 46·30N 012·56W SUN EL 65 AZ 153 ROLL 0·1 PITCH 0·0 YAW -0·1

UPWELLED RADIANCE

CHANNEL 7 ELB:UPFACE RADIANCE   ·09 ·19 ·28 ·38 ·47 ·56 ·66 ·75 ·85 ·94 1·04 1·17 1·22 1·31 1·41 1·50

ALGORITHMS: 01 00 00 00 00 02 01 00 00 00   CIP VER CRT NO   DPS VER SPEC·# FRAME #
970 SCAN LINES PROCESSED   0 SCAN LINES MISSING   V801005 ZE09301- V820401 F732040 ZG009302

77-2. Nimbus-7. Orbit 3293. 19 June 1979. CZCS Upwelled Radiance Image.

Section 6
Atlantic South American Coast

6A   Amazon River

Charles S. Yentsch
Bigelow Laboratory of Ocean Sciences
West Boothbay Harbor, Maine

During the early studies of primary production, the distinguished marine biologist Einer Steeman Nielsen demonstrated a correlation between ocean color (as measured by Forel standards) and photosynthetic carbon fixation. He observed that green waters were most productive, blue waters less so. However, a major deviation from this correlation occurs in the region of the Amazon River outfall.

The Amazon River Outfall
August 1979

The false-color CZCS pigment image on 17 August (83-1) of the ocean region off the Amazon shows changes in water color from yellow near the coast to dark blue offshore, just prior to the onset of the rainy season. This distinct color distribution highlights the Amazon outfall area. In this region, major color change is due to input of river water heavily laden with yellow organic material, and not due to changes in concentration of photosynthetic phytoplankton. The outfall of the Amazon is diverted north by the Guiana Current, but eventually curves out from the coast to the open ocean.
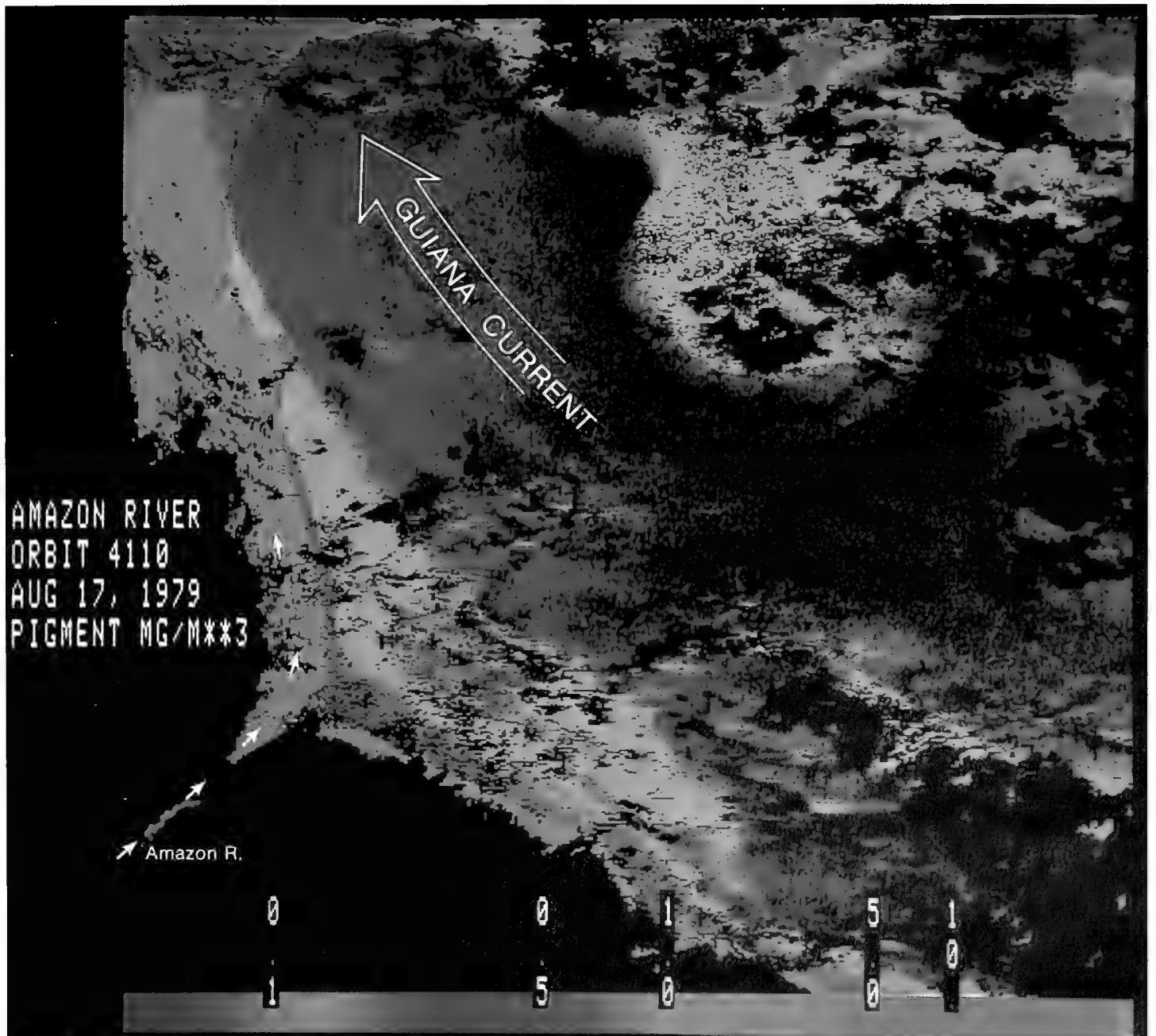
83-1. Nimbus-7. Orbit 4110. 17 August 1979. CZCS False-Color Pigment Image.

Section 7
South Africa

7A   South Africa West Coast

L. Vere Shannon
Sea Fisheries Research Institute
Cape Town, South Africa
and
Frank P. Anderson
National Research Institute for Oceanology
Stellenbosch, South Africa

The Benguela Current region off the west coast of southern Africa, particularly the southern portion of the region, is characterized by intense upwelling driven by specific wind events, well-defined frontal systems, and high concentrations of primary plankton. Because of the pulsed nature of the upwelling, this region is ideal for the study of the initiation, growth, and decay of upwelling events, in contrast to regions further north where upwelling occurs almost continuously. However, because of the high frequency of events, the use of conventional shipboard techniques is impractical. The CZCS with its large spatial coverage, high resolution, and comparatively high repetition frequency is ideal for the study of these upwelling events.

The Benguela Current—Coastal Upwelling February 1979

The false-color CZCS pigment image on 19 February (89-1) shows the distribution of chlorophyll off the west coast of South Africa. The chlorophyll concentrations range from less than 0.1 mg m^{-3} to over 10.0 mg m^{-3}. Clearly shown is the extent of coastal waters with a cool surface layer and chlorophyll concentrations exceeding 0.1 mg m^{-3} separated from the warmer, chlorophyll-poor oceanic water by a well-defined front. The corresponding thermal infrared image (89-2) shows the surface temperature distribution and confirms that the thermal and color fronts coincide. The thermal infrared image temperature range is ±12° C (dark blue) to ±20° C (red).

There are three areas of high chlorophyll concentrations within the coastal waters (89-1). The first area of high chlorophyll, off the Cape Peninsula, is separated from the land by a strip of very cold, freshly upwelled water (89-2) containing comparatively low concentrations of chlorophyll. This cold surface water is forced offshore fairly rapidly by the continued upwelling; and the plankton, needing time to grow, achieves its maximum concentration some distance offshore. Growth is also accelerated by the warming of the surface water as it moves offshore.

The second area of high concentration, off Saldanha Bay, is most likely the result of the same wind event, but because of the less rugged topography along the coast, the upwelling is not as intense and hence chlorophyll has had time to develop alongside the coast without being inhibited by a strong flow of very cold upwelled water, as is the case off the Cape Peninsula.

The third high-chlorophyll area in the north is the southern extremity of the quasi-stationary "straight-coast" upwelling which extends northward along the entire west coast of southern Africa.

Other features of note are the meanders in the front, with a large cyclonic eddy west of Saldanha Bay, probably the result of a breakdown in the front following intensification of the front by a previous upwelling event. Such intensification is evident west of the peninsula where there are signs that the meander in that area could develop into an eddy at some later stage.

North of Cape Columbine, the complex flow regime in the area is clearly illustrated by the chlorophyll concentration patterns which confirm the extreme patchiness of the chlorophyll distribution.

The patch of high chlorophyll in St. Helena Bay could be evidence of a cyclonic eddy entraining high chlorophyll concentrations from the northern extension of the Saldanha Bay upwelling cell, or it could be a result of the input of nutrients from the Berg River which runs into the St. Helena Bay at about the point where the plankton "plume" touches the land.

Both the thermal infrared and the pigment images show very clearly the expected north to northwesterly flow of surface water away from the coast under the influence of the prevailing southeasterly wind that maintains the intense offshore oceanic front during the summer months. Winter imagery available does not show evidence of a continuous, intense oceanic front.

Although the CZCS does not provide data on the vertical distribution of chlorophyll in the water columns, it does provide a major step forward in the study of upwelling regions such as that of the southern Benguela region, and could play a role in fisheries management if imagery was routinely available which could be processed to provide a quantitative assessment of primary production.

CHLOROPHYLL CONCENTRATION
m gm⁻³

■	<1.0
▨	1.0 – 3.0
▨	3.0 – 1.0
▨	1.0 – 3.0
▨	3.0 – 10.0
■	>10.0

Algorithm developed and images produced by
Mr. N. Walters, National Physical Research Laboratory, South Africa.
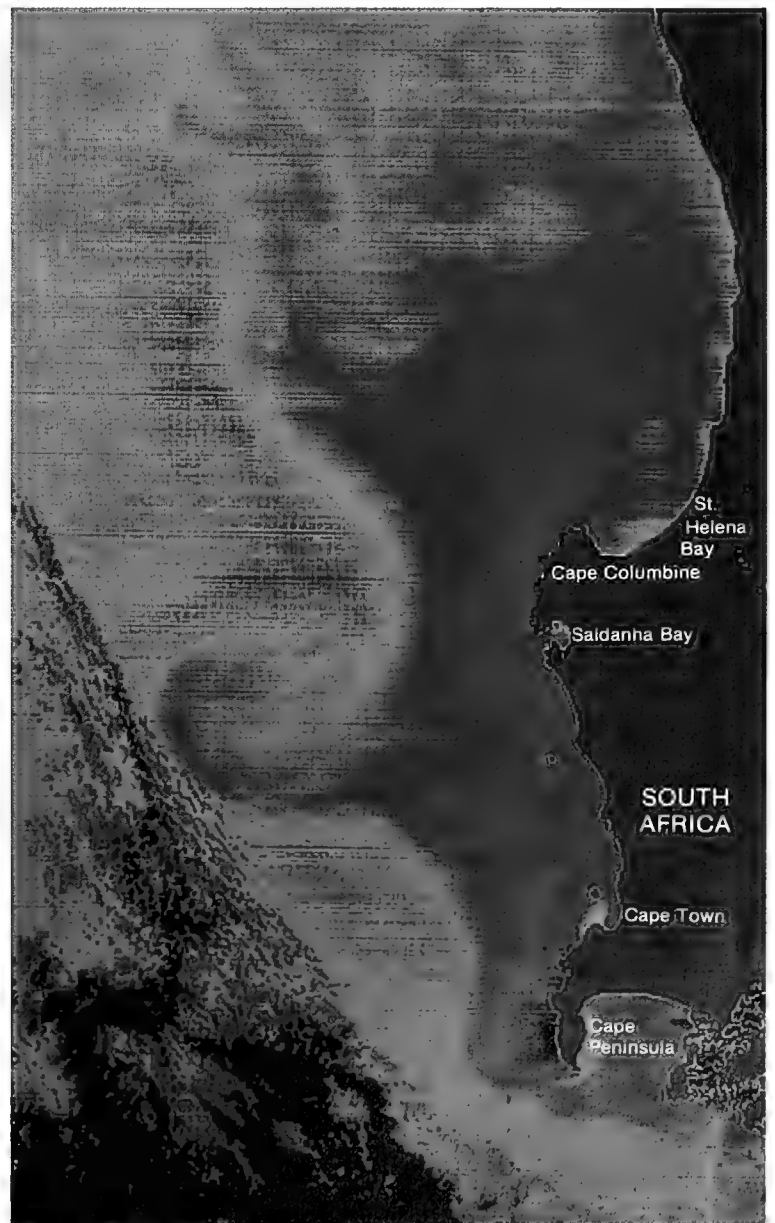
89-1. Nimbus-7. Orbit 1634. 19 February 1979.
CZCS False-Color Pigment Image.

89-2. Nimbus-7. Orbit 1634. 19 February 1979.
CZCS False-Color Infrared Image.

7B   South Africa South Coast

Eckart H. Schumann

Department of Oceanography
University of Port Elizabeth
Port Elizabeth, South Africa

The dominating oceanographic feature along the southern tip of Africa is the Agulhas Current. This current flows poleward along the eastern edge of the Agulhas Bank, paralleling the southern coast of South Africa, and turns into the West Wind Drift of the Circumpolar Current. It is a warm-water current, generally very low in nutrients in the surface waters. Large eddies are a common feature on the northern front of the current, and a cold-eddy can be enclosed within the bight of such a meander. Upwelling also takes place along the inshore frontal region, and may be an important source of nutrients for the whole bank area.

The Agulhas Current—Surface Temperature, Eddies, Water Content
June 1979

The false-color CZCS pigment images (93-1 and 93-2) cover the area from the Breede River in the west to Cape Seal in the east, and extend about 200 km offshore. Off Cape Seal the Agulhas Bank shelf width is about 80 km, widening rapidly westward to about 270 km off Cape Infanta (not shown, west of Breede River).

The relative difference in surface temperature makes the Agulhas Current very easy to identify in thermal infrared images (93-1). The image shows the main flow of the current in the bottom right hand corner. An eddy with a scale of 100 to 200 km is observed inshore of this flow, enclosing a cold core. There is an indication of an increase in total suspended solids (TSS), perhaps due to the upwelling known to be associated with such a cold core.

The temperature gradients across the frontal areas are considerable, with changes of 3 to 4° C taking place over a few pixels. The structure within the eddy itself is also apparent, while smaller scale features can be seen developing on the northern front. This may be part of the "energy-cascade" to smaller scale processes, and a means whereby the Agulhas Current surface waters can penetrate onto the shallower bank regions.

The thermal infrared image does not show whether there is a countercurrent associated with the sheared-off tongue of Agulhas Current water. However, if it is assumed that the main source of TSS is in the coastal rivers, then this image tends to indicate total movement toward the southwest. This would occur by a process of entrainment.

Cooler surface water is shown on the wider reaches of the bank, with the pronged temperature structure apparently correlating with the pattern of TSS. With the limited sea surface temperature gradients in this area, it is not possible to use these for determining circulation patterns.

On the other hand, it is known that the Breede River, and probably also the Gourits River, were flowing strongly after general rains in their catchments prior to the image being taken. Other minor contributions would also have come from smaller rivers along the coast. The resultant sediment distribution tends to lie in a band less than 20 km wide all along the coast, giving an indication that alongshore currents dominated the flow structures.

It is probably the wind that is the primary driving force in these inshore regions, with westerlies generally dominant in winter when the image was taken. An eastward coastal jet would result, though the change in coastline near the Gourits River may affect this flow. Offshore there is a tongue of TSS apparently progressing further east.

In such an analysis, TSS can be used as a tracer, although to be really useful a series of such images separated by periods of a day or so could provide information on the development of current systems. It is also acknowledged that TSS, whether they be organic or inorganic, play a very important part in chemical and biological processes operating in the shelf areas. A knowledge of the distribution of different TSS (confirmed by sea truth data), their origin and eventual fate would therefore be invaluable in the determination of trophic pathways. Such information would be important to the fishing industry.

The actual distribution of sediment deposited in such a shelf region could also be investigated with the TSS images. In this area it is known that there is a mud and sediment band parallel to the coast and fairly close inshore, which tends to tie in with the conclusions reached earlier.

93-1. Nimbus-7. Orbit 3251.
16 June 1979. CZCS False-Color
Infrared Image.

93-2. Nimbus-7. Orbit 3251.
16 June 1979. CZCS False-Color
Suspended-Solids Image.

Section 8
Antarctica

8A Drake Passage/Western Scotia Sea

Sayed Z. El-Sayed

and

Eileen E. Hofmann

Department of Oceanography
Texas A&M University
College Station, Texas

In recent years, several countries have shown increasing interest in exploiting the Southern Ocean's living resources. If the harvest of these resources is to be properly managed, we first need an accurate assessment of the biological productivity in the Southern Ocean. Without adequate synoptic data, it is difficult to arrive at realistic estimates of phytoplankton abundance and to develop models of phytoplankton dynamics which will successfully predict trophic interactions. Although a great deal of useful information has been obtained on the Southern Ocean's standing crop and primary production during the past 25 years, these estimates are based largely on point sources (i.e., stations) and were taken onboard oceanographic ships at different seasons and often in different years (El-Sayed, 1967). As a result, overall estimates reflect broad temporal and spatial variability in the phytoplankton standing crop and primary production.

For large and difficult-to-explore areas such as the Southern Ocean, the CZCS, combined with ground-truth data, makes it possible to arrive at an accurate estimate of phytoplankton biomass and possibly of primary productivity. The following case study documents efforts to obtain such estimates with the CZCS.

The Polar Front/Cold-Core Rings—
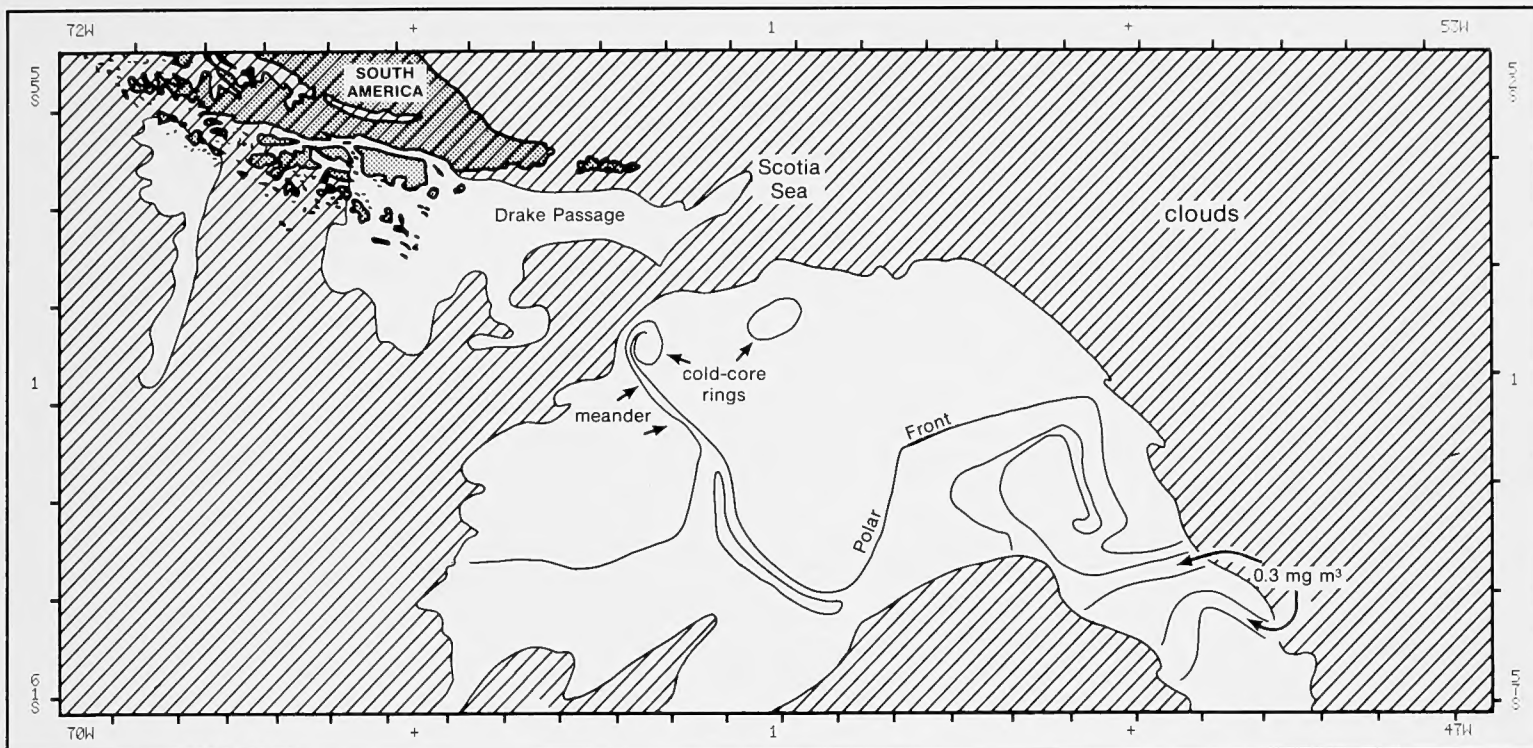# Effects on Abundance and Distribution of Phytoplankton
January 1979

The dramatic CZCS pigment image of the central Drake Passage and western Scotia Sea taken on 6 January (99-2) and the corresponding locator map (99-1) show the extensive geographical variability of near-surface distributions of phytoplankton pigments in these icy waters. This is in sharp contrast to the relatively smooth pattern of pigment distribution obtained from shipboard observations made in this region. The image shows generally low pigment values in the polar front region (0.05 mg chl m^{-3}). However, there is, within the polar front, a region of relatively high pigment concentration squeezed between bands of low pigment concentration. Pigment values north of the polar front are also generally low, but isolated regions of concentrations in excess of 0.1 mg chl m^{-3} are observed. The highest pigment values occur to the south of the polar front. The reasons for these enhanced concentrations are unknown. The general pattern and values of the pigments shown in the image are in agreement with shipboard observations made in this region of the Southern Ocean (El-Sayed et al., 1964; El-Sayed, 1967).

The meandering nature of the polar front is apparent in the CZCS image. Also apparent are cold-core rings which form from meanders in the polar front (Joyce and Patterson, 1977; Joyce et al., 1981; Peterson et al., 1982; Hofmann et al., 1984). Like their counterparts in the Gulf Stream and Agulhas Current, these rings retain their physical and probably biological characteristics for long periods. Peterson et al. (1982) suggest that these rings are an important component of the heat and salt budgets of the Southern Ocean. It has been shown that within Gulf Stream cold-core rings, the structure of the planktonic community is conserved (Wiebe et al., 1976). Furthermore, Wiebe and Boyd (1978) suggest that these cold-core rings are capable of transporting zooplankton communities a long distance from their usual habitat. Similarly, cold-core rings in the Southern Ocean may also transport biological and chemical properties across the Antarctic Circumpolar Current.
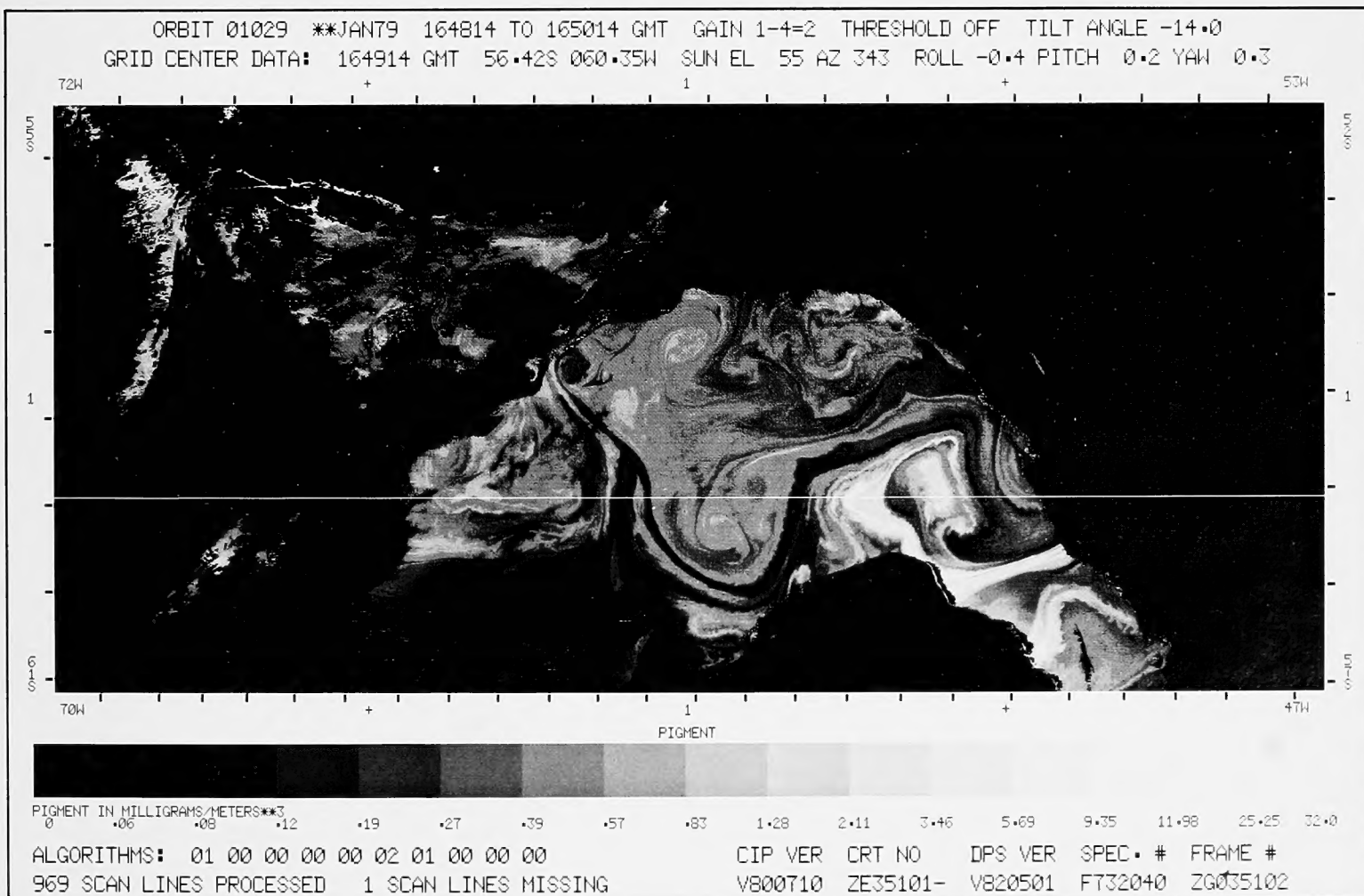
It is unfortunate that this region of the Southern Ocean is often covered by clouds. This makes it difficult to obtain a sequence of CZCS images from which the time development of phytoplankton blooms and water movement can be studied. However, the available images do provide synoptic observations in a region in which logistical constraints make a comprehensive field study difficult.

References

El-Sayed, S. Z., 1967: On the productivity of the Southwest Atlantic Ocean and the waters west of the Antarctic Peninsula, Antarctic Research Series. In *Biology of the Antarctic Seas III*, **11**, edited by Waldo Schmitt and George Llano, American Geophysical Union, Washington, D.C., 15–47.

———, 1972: Primary productivity and standing crop of phytoplankton. In *Chemistry, Primary Productivity, and Benthic Marine Algae of the Gulf of Mexico, Serial Atlas of the Marine Environment*, Folio 22, edited by V. C. Bushnell, American Geographical Society, 8–13.

El-Sayed, S. Z., E. F. Mandelli, and Y. Sugimura, 1964: Primary organic production in the Drake Passage and Bransfield Strait. In *Biology of the Antarctic Seas I*, **1**, edited by M. O. Lee, American Geophysical Union, Washington, D.C., 1–110.

Hofmann, E., T. Whitworth III, and D. Nowlin, Jr., 1984: Mesoscale flow variability at Drake Passage. *J. Geophys. Res.*, submitted.

Joyce, T. M., and S. L. Patterson, 1977: Cyclonic ring formation at the polar front in Drake Passage. *Nature*, **265**, 131–133.

Joyce, T. M., S. L. Patterson, and R. C. Millard, Jr., 1981: Anatomy of a cyclonic ring in Drake Passage. *Deep-Sea Res.*, **28**, 1265–1289.

Peterson, R. G., W. D. Nowlin, Jr., and T. Whitworth III, 1982: Generation and evolution of a cyclonic ring at Drake Passage in early 1979. *J. Phys. Oceanogr.*, **12**, 712–719.

Wiebe, P. H., and S. H. Boyd, 1978: Limits of Nematoscelis megalops in the Northwestern Atlantic in relation to Gulf Stream and cold-core rings. I. Horizontal and vertical distributors. *J. Marine Res.*, **36**, 119–142.

Wiebe, P. H., E. M. Halburt, E. J. Carpenter, A. E. Jahn, G. P. Knapp III, S. H. Boyd, P. B. Ortner, and J. L. Cox, 1976: Gulf Stream cold-core rings: Large-scale interaction sites for open ocean plankton communities. *Deep-Sea Res.*, **23**, 695–710.

72W + 1 + 53W

SOUTH
AMERICA

Drake Passage

Scotia
Sea

clouds

cold-core
rings

meander

Front

Polar

0.3 mg m³

70W + 1 + 47W

99-1. Locator Map for 99-2.

ORBIT 01029 **JAN79 164814 TO 165014 GMT GAIN 1-4=2 THRESHOLD OFF TILT ANGLE −14·0
GRID CENTER DATA: 164914 GMT 56·42S 060·35W SUN EL 55 AZ 343 ROLL −0·4 PITCH 0·2 YAW 0·3

PIGMENT

PIGMENT IN MILLIGRAMS/METERS**3
0   ·06   ·08   ·12   ·19   ·27   ·39   ·57   ·83   1·28   2·11   3·46   5·69   9·35   11·98   25·25   32·0

ALGORITHMS: 01 00 00 00 00 02 01 00 00 00   CIP VER   CRT NO   DPS VER   SPEC· #   FRAME #
969 SCAN LINES PROCESSED   1 SCAN LINES MISSING   V800710   ZE35101−   V820501   F732040   ZG035102

99-2. Nimbus-7. Orbit 1029. 6 January 1979. CZCS Pigment Image.